Characterization of a 6 DOF Haptic Device for Mixed-Reality Temporal Bone Surgery Simulation

by

Milad Khazraee

A Thesis submitted to the Faculty of Graduate Studies of

The University of Manitoba

in partial fulfilment of the requirements of the degree of

MASTER OF SCIENCE

Department of Mechanical and Manufacturing Engineering

University of Manitoba

Winnipeg, Manitoba, Canada

Abstract

The temporal bone is a complicated bone in which diseases can necessitate surgery. Current surgery training methods in this area include human cadaver, physical and virtual models. The objective of this research is to modify a haptic system as a part of a Mixed Reality (MR) temporal bone surgery simulator. The simulator employs a haptic model of soft tissue, which is sufficiently simple not to alter the performance characteristics of the haptic system, overlaid on a physical model of the bone to include advantages of both. A gripper has been developed to retrofit a haptic device with a surgical drill. Device characteristics are explored and modified to compensate for gravity effects of the gripper on the system and to transmit the haptic interaction point to the drill tip, where the soft tissue model's forces should be felt. This developed system should contribute in providing a more realistic surgery simulation.

Acknowledgment

I would like to forward my most sincere appreciation to my advisors, Dr. Nariman Sepehri and Dr. Bertram Unger whose encouragements and supports have made this thesis possible. I feel tremendously fortunate to have such a fabulous opportunity to work with advisors who have both solid theoretical knowledge and experimental expertise which strengthened this project in both aspects.

I also wish to sincerely thank Dr. Jordan Hochman who played an important role in enriching this project by his comments as the temporal bone surgeon of our research group.

No word describes my heartfelt thanks to my family whose support has always been encouraging during my studies.

On this project, I had the opportunity of working with Mr. Ehsan Jalayeri, the Fluid Power and Telerobotics Research Laboratory's support engineer. I would like to thank him for his technical support in preparing experimental test rigs.

I also wish to thank my friends and my peers in the fluid power lab, especially Dr. Kurosh Zareinia and Mr. Yaser Maddahi who made a friendly atmosphere in the lab during my course of study.

Table of Contents

List of Tables

List of Figures

Chapter 1

1. Introduction

1.1. Problem Statement

The temporal bone is complicated and diseases of it may require surgery. The current major training tool for temporal bone surgery is surgical rehearsals on human cadavers. This method has problems such as legal issues and the risk of disease transmission. Other current training methods such as plastic models and Virtual Reality (VR) simulators [1] are not able to provide the realistic vibrations and contact forces or realistic conditions such as blood flow. The objective of this research is to help develop a better simulation tool. This simulation tool should demonstrate that haptic devices can be modified to work in Mixed Reality (MR) environments. Device features should be determined. The haptic device should be equipped and modified to have the capabilities to produce the realistic temporal bone surgery conditions. The simulator should be developed to work in MR condition without exhibiting instability.

The temporal bone is one of the most complex anatomical parts of human body [2]. It is very close to the brain's outer surface and protects and encloses several vital soft tissues such as arteries, veins and facial nerves. A wide range of potential treatments such as removing tumours and cysts, repairing broken bones, restoring hearing, correcting balance disorders [2], and preventing infections may require temporal bone surgery. Therefore, a large number of temporal bone surgeries are performed around the world each year. During this surgery, residents drill the temporal bone, Figure 1, with surgical drills. As a result, trained surgeons in this field are needed. These surgeons should have an astute knowledge of the region's anatomy, experience with anatomy's dissection, and a high level of dexterity to perform a successful surgery [2], otherwise, these surgeries can cause permanent deformity, loss of hearing and potentially death. Therefore, medical residents should be well-trained in this region's anatomy before learning from clinical experiences. Training consists of gaining realistic surgical experience in drilling the bony structure and contacting or penetrating soft tissues inside bony structures [2].

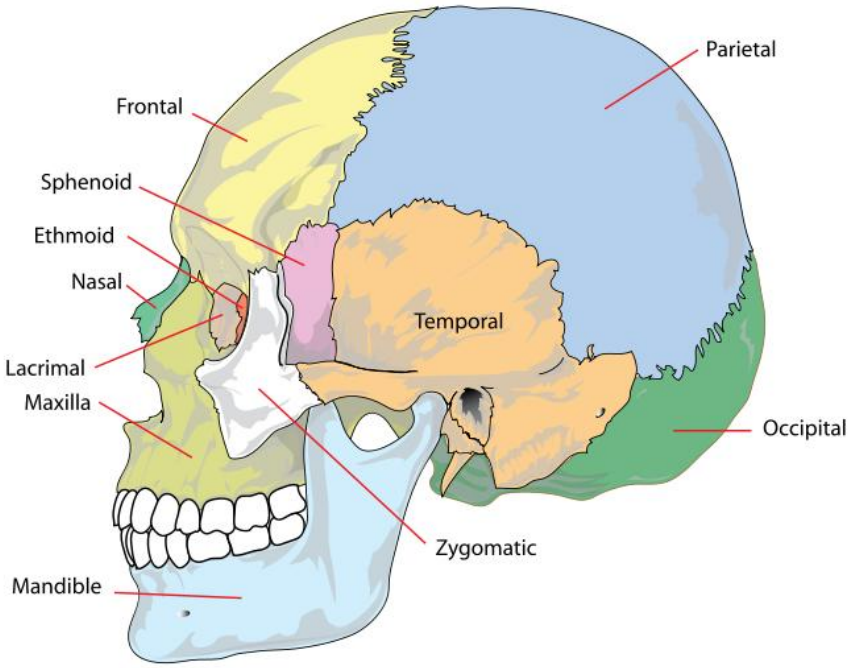

Figure 1: Human skull side bones graphical model, Temporal bone is shown in the centre of the picture

The human cadaver is the primary teaching tool in traditional methods of temporal bone surgery training. This method have significant drawbacks, namely and legal issues, limited number of necessary cadavers, significant costs, difficult access to training material, and risk of diseases transmission [3]. Cadaveric temporal bones are harvested by the trainees. Resident practice surgical techniques by performing simulated procedures on them. Since, they use real human cadavers; they obtain a better sense of the contact forces and surgery conditions by means of their sense of touch which is very important.

Novel teaching methods include the use of simulators. There are several motivators to develop such methods. For example, surgeons and trainees can explore new surgical techniques and use the technology without fear of making mistakes [4]. They can train to manage normal and

abnormal medical conditions. In traditional methods, due to limitations in hours of clinical practice, materials, and cadavers, all trainees could not expose to similar sets of cases [2].

There are different types of simulators, Figure 2. As a simple classification, three types of simulators are potentially useful for temporal bone surgery:

1. Physical Models: They have the closest condition to the cadavers and are mostly designed for practical trainings. Common examples of these models are rapid-prototyped models (Figure 2-a) and plastic models such as "Pettigrew plastic temporal bones", which are broadly considered as alternatives to cadaveric trainings [3]. Pettigrew plastic temporal bone models are made of a "plastic model with colored dyes to highlight the facial nerve, sigmoid sinus and carotid artery. Moreover, adding extra red irrigation fluid simulates bleeding during the drilling" [5]. One of the problems with these kinds of training tools is that they are single use; hence, not cost effective. Conversely, computer based simulators can be used many times.
2. Virtual Reality (VR)[1] Simulators: This type of simulator consists of traditional human-computer interfaces such as a keyboard and a mouse. They provide a graphical interpretation of simulated physical conditions (Figure 2-b). The major problem of this type of simulators is their inability to provide the realistic vibrations and contact forces.
3. Virtual Reality Simulators with Force Feedback (Haptics[2]): This type of simulator has the features of a VR Simulator, but includes the capability of producing tactile information force feedback (Figure 2-c). This capability helps the trainees to feel virtual contact forces through

[1] Computer-simulated environments (More detailed definition in Chapter 2)
[2] Haptic is a technology that interfaces with the user through the sense of touch. (More detailed definition in Chapter 2)

their sense of touch, while performing the simulated surgery. Simultaneously, trainees can see the virtual environment through the provided graphical interface. Although, this type of simulator has many advantages, available haptic devices are unable to adequately produce the high stiffness associated with bone. Therefore, they cannot provide the sufficient realistic sense of tool vibration, which is necessary for the temporal bone surgery training.

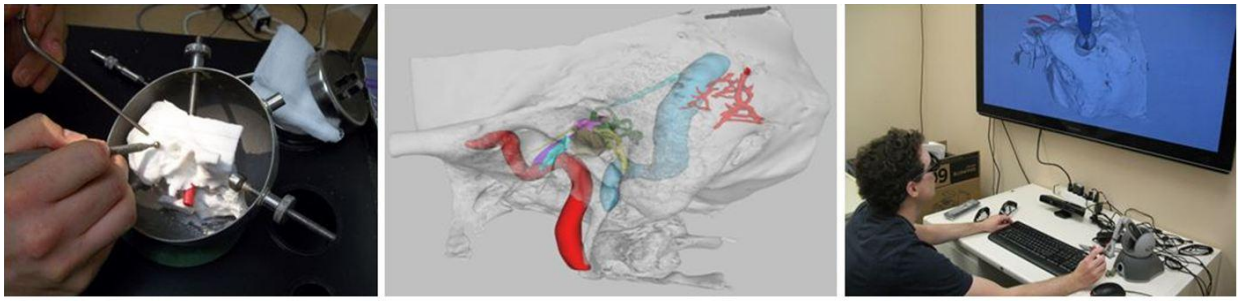

(a) (b) (c)

Figure 2: Three types of current used simulators for temporal bone surgery: a) Rapid-prototyped physical model of bony structure, b) VR simulator with graphical interpretation, c) VR simulator with graphical interpretation and haptics force feedback

In this study, a novel approach of using MR simulators is presented. MR medical simulation is a novel idea that is presented in few researches. In most cases, the MR system graphically mixes real and virtual environment (MR in graphic area) and provides force feedback by means of haptics. In this study, MR is provided in the area of haptics and contact force space. The proposed MR temporal bone surgery simulator in this research consists of combining real and virtual environments' forces.

A prototyped physical model of bone is overlaid with virtual haptic models of soft tissues. Thus, the advantages of each one are included, while their individual limitations are overcome. Surgical training simulators that use haptics have the capability to render the soft tissue

interactions; however, they are unable to adequately produce the forces associated with high stiffness of bony structures. Available prototyped physical models of bony structures provide a realistic sense of vibrational properties, while they can only simulate the bone. These models ignore the embedded or surrounding soft tissue structures as well as bleeding and other surgical dynamics. Difficulties in creating prototyped physical models of soft tissue structures are: (*i*) Existing materials are not appropriate for simulating the soft tissue characteristics, (*ii*) In some areas such as temporal bone, there are variety of soft tissues such as arteries, veins and facial nerves, in different directions, geometries and stiffness. This is a significant challenge to prototype these soft tissues in the enclosed and complicated space in which these tissues reside inside bony parts of the physical models of temporal bone, (*iii*) Modeling of these soft tissues with different geometries and stiffness is not cost effective. Moreover, placing physical models of soft tissues in narrow areas between bony parts is challenging.

The idea of a MR simulator is to use both physical and virtual models simultaneously to simulate the whole anticipated system. Some parts of the system are modeled physically and other parts are modeled virtually. These two models together create the desired simulation environment.

Computed Tomography, a CT scan, and Magnetic Resonance Imaging, MRI, data are used to display patient-specific bony and soft-tissue anatomy in the simulator system. MR approach provides the ability to employ the realism of prototyped physical models, the flexibility of haptic models and the immediacy of graphic models.

1.2. Objectives of this Research

The objectives of the current research are to explore the capabilities of the Quanser HD^2 (High Definition Haptic Device), haptic system, develop the system to work in MR condition, and devise a simple MR model, which is a virtual deformable haptic model of soft tissue associated with physical models of the bone, to test the developed system. The developed model can be overlaid on a rapid-prototyped physical model of the bone structure, Figure 2-a, to generate the MR environment. Current haptic technology cannot adequately produce the high stiffness associated with the bone. By overlaying a physical model of the bone with a virtual haptic simulation of the soft tissues, their individual limitations are overcome. This work aims at:

(i) Choosing a tissue model which is applicable by the haptic device, while satisfying the requirements for realistic temporal bone surgery simulation. Implementing the model by programming the Quanser HD^2 haptic device.

(ii) Prototyping a gripper for equipping the HD^2 haptic device with a surgical drill, and cancelling the gripper's gravity in order to provide more realistic training condition.

(iii) Studying the kinematics of the HD^2 haptic device to transmit the haptic interaction point to the drill tip and to compensate the gripper's gravity effects.

(iv) Understanding the nature of interactions between real and virtual models.

(v) Validating functionality and effectiveness of the developed MR system.

1.3. Scope of this Thesis

In the area of temporal bone surgery training, the available haptic devices and tissue models have been reviewed. Also the conditions and requirements for surgery training should be considered to

determine an appropriate tool which satisfies the training goals and encourages the trainees. Realistic soft tissue models should be chosen such that they are sufficiently simple to be implemented on the available haptic devices. To create the feeling of continuous virtual environment and vibrations, haptic rendering codes should run at least at frequency of 1 kHz [6], which requires tasks with low processing time need in implementing and running of soft tissue models. Reasonable processing power is essential for the workstation to simulate in an almost real-time manner for medical training; while considering the cost effectiveness of the utilized software and hardware for the training purposes. The mentioned factors are considered for choosing an appropriate soft tissue model that can be modified and enhanced in future as well.

The training conditions must be as much as possible close to the real surgery conditions. Hence, several circumstances should be considered to make a realistic simulation environment. The considered conditions for this study are:

- The real surgical drill which is used in the temporal bone surgeries must be used. In this research, a gripper is developed to equip the HD^2 haptic device with Medtronic surgical drill (Figure 3). This helps the trainees to train with the identical tools they will use during the real surgery. The gripper has to be resistant to the dynamic forces and vibrations and sufficiently light to avoid changing in the dynamics of the system.

Figure 3: Medtronic surgical drill. HD^2 haptic device is equipped with this surgical drill, to train the trainees with the identical tools they will use during the real surgery

- In the real surgery, soft tissues contact with the drill tip and apply the forces to that point. In the simulator, the modeled forces of the soft tissue are produced by the haptic device in the HD^2 interaction point which is located at the center of the handle. These forces should be felt in the drill tip. Hence, the applied forces in the HD^2 interaction point should be transmitted to the drill tip, simulator interaction point. The gripper should attach the drill to the haptic device in a manner that trainee senses the anticipated forces and torques while holding the surgical drill during the simulated surgery. Any kind of offset, extra forces or torques, or different degrees of freedom in comparison with the real surgery may cause misleading training. During a real surgery, surgeons just feel the gravity effects of the drill and its attachments such as electricity wire and irrigation tubing. The designed simulator should have enough haptic transparency, so the gravity effects of the gripper and handle excluding the drill, should be cancelled as much as possible.

In order to position the haptic interaction point at the drill tip and compensate the gripper's gravity effects, the characteristics of the system are determined to address the necessary modifications. The effects of adding the drill and gripper, haptic device's limitations, and the modifications in the haptic device kinematics, dynamics, control, and applied forces and torques should be considered.

Next, the functionality of the simulator should be studied. The effect of drill vibrations and contact forces on the stability and capabilities of the haptic device during the drilling procedure of physical models of the bone should be examined. The simulator should demonstrate operations in normal conditions with gross stability, appears stable, and should not exhibit instabilities such as continuous oscillations or large amplitude vibrations under expected operating conditions. Functionality in the interaction between real and virtual models should be evaluated and reported, and suggestions for increasing the stability should be provided.

1.4. Thesis Outline

In Chapter 2, a literature review along with some definitions is provided. The idea of MR is explained. Haptics and its specifications for interaction with humans are reviewed, and examples of using simulator for temporal bone surgery training are provided. Different types of soft tissue models are reviewed and the implemented soft tissue model is introduced.

Chapter 3 describes the experimental setup used in this research. Relevant information about Quanser HD^2 haptic device is provided and steps for developing the surgical drill gripper is explained.

The theoretical works related to transmission of the haptic interaction point to the drill tip, compensating the gripper's gravity effects, and the system's background program and algorithm architecture are described in Chapter 4.

Chapter 5 is devoted to experiments and their results. By means of these tests the effectiveness, performance, gross stability and functionality of the developed simulator are evaluated.

Contributions of this research, along with suggestions for future work related to the developed simulator are provided in Chapter 6.

Chapter 2

2. Background and Definitions

2.1. Virtual Reality and Mixed Reality

2.1.1. History and Definition

Paul Milgram and Fumio Kishino defined MR as “Anywhere between the extreme of the Reality-Virtuality (RV) Continuum” [7]. The simulator developed in this study is a MR that uses both real and virtual environments. In this work application, MR can be defined as merging of real and virtual worlds to produce new environments and visualizations, where physical and digital objects co-exist and interact in real-time. Milgram and Colquhoun [8] defined the RV continuum as a continuum of real-to-virtual environments, which consists of completely real through to completely virtual environments; intermediate environments such as Augmented Reality (AR) and Augmented Virtuality (AV) are shown in (Figure 4).

Figure 4: (MR). A continuum of real-to-virtual environments, which consists of completely real through to completely virtual environments; intermediates such as (AR) and (AV) lie between. [9]

Each part of MR can be defined separately:

Real objects are defined as "Any objects that have an actual objective existence. In order for a real object to be viewed, it can either be observed directly or it can be sampled and then resynthesized via some display devices." [7]. The features of the real object such as geometry, surface condition, and hardness can be modeled by the haptic device. Operator can see the object in its surrounding environment through the provided graphic interface and feel the modeled features of the object while moving the device's interaction point aground the modeled object.

Virtual objects are defined as "Objects that exist in essence or effect, but not formally or actually. In order for a virtual object to be viewed, it must be simulated, since in essence it does not exist." [7] .Virtual environment can have the properties of the real world. Moreover, virtual environments can go beyond the limitation of physical reality and disregard typical physical laws such as time, material properties, gravity, and mechanics [7].

AR is the part of the RV continuum that is "Adjacent to, but excluding, the real environment extreme" [8]. In AR, the display of a real environment is augmented by means of virtual (computer graphic) objects [7]. The surrounding environment is real and AR creates a local

virtuality. Users can observe the real world, with overlaid and compounded virtual objects. AR complements reality but does not totally replace it [10] [11] [12].

On the contrary, AV is the part of RV continuum that is "Adjacent to, but excluding, the virtual environment end" [8]. In AV, real objects are supplemented with virtual objects; hence, the surrounding environment is virtual.

Compared to aforementioned environments, MR "covers essentially the entire breadth of the RV continuum, but excludes the end points" [8]. The applications of AR are similar to the MR and in some applications they are considered almost the same. MR simulation technology provides the users advantages of using both the real and virtual components of their system [8]. In most applications, definition of MR is about graphically mixing the real and virtual environments. In this research, a more narrow definition of MR is used. MR is provided in the area of haptics and contact force space. Both real and virtual forces are co-exist and interact in real-time to provide a new environment with contact forces of physical and virtual models.

2.1.2. Applications

MR and AR are used in a wide range of applications [10] [11] [12]. Some of the most popular areas are:

- Personal information systems such as personal assistance, advertisement, navigation, touring.
- Industrial applications such as maintenance and repair, assembly, design, and manufacturing.

In these applications there are a number of procedures that use the haptic interface, especially in the training process of assembly. For instance, [13] presented a system to prepare operators for manipulation and assembly tasks. Operator works with a haptic workstation by the mean of his

hands to provide the feeling of the assembly task. In this application, the assembly process of a MR table is simulated. The MR table consists of both virtual and real parts.

The use of MR has also been considered in [14]. They proposed a virtual assembly instructor based on MR; however, the system is limited to real object manipulation. Another example of interaction with real objects while providing haptic feedback is presented in [15]. Due to the ability of the user to feel the haptic textures of objects, which they could not feel with their real hands, it is considered an augmented haptic system.

An approach for hand interaction with virtual objects is described in [16]. In this approach, to provide better visualization of hand posture, video of the hands is overlaid on the virtual world, which makes it a MR system. However, in this system the user can only manipulate virtual objects. Kotranza [17] investigated the performance of a two-handed interface for conducting MR engineering assembly. It was shown that using two hands to perform an assembly task in MR did not improve the performance comparing to one hand. However, using two hands allows the participants to complete the task in an approach similar to the real-world assembly.

- Military applications such as simulation of combat, reconnaissance, navigation, and targeting of aircrafts.
- Commercial applications such as sports broadcasting (to enhance sporting events and insert or replace advertisements in a scene [10], [12], [18]; Figure 5), entertainment, and gaming. There are varieties of examples in the gaming applications, such as RV-Border Guards game, [12] [19]; and Aqua-Gauntlet which is a multiplayer MR game. The guns used in Aqua-Gauntlet incorporate vibrating motors, which gives players the feel of a mechanical shock when they shoot invaders [20].

Figure 5: AR in live sports broadcasting: In football [10]**,** [12]**,** [18]**. Graphical highlighted line is added to the real world in football broadcasting to make a graphical AR which helps the viewer's determine the correct judgment.**

- Education and training, such as collaboration in office spaces or annotation [12].
- Academic applications in research fields such as medicine, visualization, and robot path planning.

Almost all of the aforementioned systems and applications are very different from this research. In these systems, MR is about graphically mixing real and virtual environments (MR is used in graphic area) and providing force feedback by means of haptics. For instance in the Aqua-Gauntlet game, forces that are applied to the player, provides the feel of a mechanical shock, but there is not any MR force feedback in the cases player contact with one of the real objects of the game. In this thesis, MR is provided in the area of haptics and contact force world.

(a) (b)

Figure 6: Aqua-Gauntlet, a multiplayer MR game [13]**: (a) Without augmentation, and (b) With see-through augmentation. The invaders are modeled virtually, and players can shoot them by means of the provided guns. The guns of the Aqua-Gauntlet incorporate vibrating motors, which give the players feel of a mechanical shock when they shoot invaders.**

2.2. Haptics and Haptic Technology

Haptics is defined as "The sense of touch", which originated from the ancient Greek word "haptikos" [21]. Moreover, haptics has its scientific definition in at least three different fields. It has a history of 150 years in the field of medical research on human touch perception. In the area of computer science, haptics is defined as using tele-operation robots to provide a sense of touch using calculated forces. In engineering, haptics commonly refers to the case where the sense of touch is associated with applying force. Any kind of tool that involves applying force through the sense of touch can be considered as primary haptics; hence, the first guidance tools such as rulers can be defined as the inception of haptics in the engineering [21].

Haptic Technology or haptics, refers to the interaction of technology with users by means of tactile force feedback, which is applying force, vibration or motion to provide a sense of touch

[22]. Human's tactile sensations are related to the interaction of neuroreceptors in the skin with electricity, temperature, surface conditions, and applied forces.

The users can feel and touch virtual objects with their hands, or interact with virtual and remote environment by means of a haptic interface. The interface has the capability to generate and apply forces against human's neuroreceptors in skin, especially in hands [6].

There are different methods for learning and training. Interaction with an environment while perceiving it is one of the best methods for learning and training. Touch is a key interaction method. Children start to play and learn about their surrounding environment through their tactile sensations from their early childhood. The ability to train and perform in different fields such as art (musical performance, painting, sculpting) and sport (gymnastics) depends on physical interactions [6]. Touch or haptics is a two directional interaction; energy is exchanged between the hands and the object when they push against each other [6]. Haptic devices can replace real objects with virtual objects to help the operators to gain experience through virtual objects. This can be performed before training with a real object. This method is essential in the case that a lack of experience may cause dangerous situations for the operator, for example working with hazardous substances or objects, such as a part of human body which needs a surgery.

The use of mechanical devices for haptic interactions has existed since the 1940s, when the danger of working with nuclear materials required the development of remote manipulation [23]. Later, in the 1960s, virtual objects were first touched by means of a computer-controlled haptic interface. In the 1990s, virtual reality became a distinct area of research. Obviously, making images linked to haptics, improves human interaction with a computer. By means of keyboards and mice, users have very limited interaction with computer. Instrumented gloves add more

features but with less precision. The use of haptic devices increased the range of potential interactions. As an example, the Phantom™ (Sensible - www.Sensable.com) haptic device provides the advantage of touching virtual objects with the head of a stylus [6].

Haptic technologies have been used in broad range of applications such as medical robotics and telesurgery, [24] [25] [26] [27] [28] [29], mobile robots [30] [31] [32] [33], operations on hazardous materials [23] or in dangerous and rough environment [34], tele-operation [34], and training [13] [15]. Moreover, this technology is applied in various complexity levels. Haptic devices are commonly used in scenarios with simple geometrical virtual objects [35] [36] [37], or complex 6 degrees of freedom scenarios [38].

The haptic device acts as a human interface with an interaction system that consists of three major parts: haptic device, computer interface, and the operator. Haptic device and computer interfaces should have the capability to interact practically with the operator based on human abilities. Haptic images are composed of both tactile and kinesthetic information; however, it is not essential for this information to perfectly replicate reality since it must merely match the abilities and limitations of the human sensation system. For instance, the update rate of graphics loop is generally much less than that of the haptic loop. According to the limitations of human vision, 25 to 30 frames per second is a sufficient rate for graphic images. However, in order to simulate a continuous tactile system, the update rate should not be less than 1 kHz [6]. Human fingertips' kinesthetic resolution is about 1 mm for position sense, "with an ability to discriminate differences of about 10 percent for velocity and 20 percent for acceleration" [6]. "The maximum controllable force exerted through the fingers is 50 to 100 [N]" [6]. These are the minimal mandatory capabilities for a haptic interaction. Hence, the implemented virtual environment should be sufficiently simple to be implemented on the available haptic devices,

with reasonable processing power according to workstations, and cost effective utilized software and hardware designed for the application.

2.3. Tissue Models

Cadavers and animals are used for surgical training purposes; however, surgical simulators are designed to replace them. The models used in such simulations have to be as "physically based" as possible, to avoid misleading training [39]. "Physically based" means that the models are based on: sufficient representations of the geometry of the organ, appropriate materials which accurately follow the specifications of the tissue behavior, and appropriate rules for boundary conditions. The most difficult issues in "Physically based" modeling of soft tissues are: highly nonlinear force displacement, enormous deformations, and viscous behavior of soft tissues.

A realistic appearance of the simulated environment needs real-time simulation. Therefore, a visual update rate of at least around 30 Hz and a haptic update rate of at least 1 kHz are essential. Accurate simulation of tool-tissue mechanics requires extremely high processing power [39]. Because real objects do not oscillate indefinitely, damping must be added for a more realistic simulation [40].

Modeling of the geometry, materials, kinematics, and dynamic properties of the desired virtual environment is necessary for creating a feeling of the virtual objects. The interaction forces with the object are modeled and implemented through the haptic device. The utilized models and real-time constraints must be considered in developing the algorithms. Generating smooth transitions and distinct sensations requires sufficiently high update rates and efficient rendering algorithms [6].

There is always a trade-off between the fidelity and complexity of the models. In general, an increase in the complexity of the model results in higher costs and more time required for the computation of the forces. Therefore, the choice of model and rendering methods is critical in surgical training simulators [6].

Finite Element Modeling (FEM) is a very common method, which is used in [39] and [41]. In [39], a model that uses simple quadrilateral elements is presented. This model is a physically based one that is suitable for simulating the nonlinear force-displacement behavior of biological tissues, and real-time rendering of interactions between surgical tools and soft tissues for surgical simulations.

In [42]and [43] deformable models have been presented. In many of these studies, deformable models are based on a fixed space discretization rate, which means that the workspace is divided into blocks of equal size and shape. Conversely, an adaptive technique is utilized in more advanced deformable models. In the adaptive technique, different levels of resolution are used for different parts in order to simulate relevant levels of detail in each part. For instance, in [44] with the purpose of modeling deformable bodies in real-time; an adaptive technique is used to reduce the overall complexity.

2.3.1. Applied Virtual Soft Tissue Models

As mentioned above, there is always a trade-off between the computing time and complexity of the models. In medical applications, real-time rendering is an essential criterion. Moreover, this factor plays an important role in training with simulators, due to the fact that trainee should feel the virtual environment in the correct position and time. Hence, the chosen model should be sufficiently non-complex to minimize its effects on the performance of the simulator.

Most of finite element models use complex and time-consuming force computations. Even in adaptive FEMs in which the computational load is decreased in some areas, computing time and real-time simulation should be considered. In a few projects, soft tissue is modeled by linear equations. For instance, in [44], an estimation model is developed based on fitting a polynomial to the recorded experimental data. Endoscope insertion in a tube-like soft tissue is simulated and the force and displacement data during simulation is recorded by means of a designed device. Development of a soft tissue model is considered for calculation of insertion forces during haptic simulation feedback [44]. Since this model is sufficiently simple and provides an acceptable computing time, it has been chosen for modeling the virtual soft tissues in this research. The main goal of this research is to develop a MR system which has the satisfactory conditions to be used in a simulating temporal bone surgery simulator. In this first development of the system, soft tissue models should be sufficiently non-complex to have the least influence on the performance of the system, while in future developments, more complex models with variable geometry and material features and non-linear force profiles will be considered.

In [44] a "least squares" approach is used to fit the recorded forces' data to polynomials. The forces are presented in the general model of:

$$F(x, \dot{x}) = F_c + K(x) \cdot x + B(\dot{x}) \cdot \dot{x} \quad \textbf{1}$$

In this equation, F_c presents coulomb friction, $K(x)$ presents the spring effects, and $B(\dot{x})$ presents the damping and viscosity effect. Based on the fact that it is a tube-like soft tissue model, the forces are estimated in one direction (1D force model). Also, force model is a function of both the displacement(x), and the velocity$(\dot{x})$.

The general first order polynomial is shown in 2 :

$$F(x, \dot{x}) = a_0 + a_1 \cdot x + a_2 \cdot \dot{x}$$

2

Two sets of coefficients are determined for insertion equation 3 and retraction equation 4 of the endoscope in [44]. The coefficients values and desired insertion depth should result the force values that are applicable by the haptic device (Table 1, page 33).

$$F(x, \dot{x})_{in} = 0.1055 + 0.02 \cdot x + 0.001 \cdot \dot{x}\,; \quad [K(x) = 0.02;\ B(\dot{x}) = 0.001]$$

3

$$F(x, \dot{x})_{out} = 0.0732 + 0.0196 \cdot x + 0.0117 \cdot \dot{x}; \quad [K(x) = 0.0196;\ B(\dot{x}) = 0.0117]$$

4

The soft tissue model used for the developed simulator in this research is based on the proposed model in [44]. x values are in millimetres since the $K(x)$ is in N/mm; hence, recorded values of displacement (which are provided in meters by the device's sensors) are multiplied by 1000 and then used in these equations. $\dot{x}$ values are in m/s since $B(\dot{x})$ is in N.s/m. There are merely a few differences between the model which is used in this study and the model presented in [48]. These differences are based on the conditions of simulation and haptic device limitations. In the proposed model in [44], two sets of coefficients are determined for insertion (going inside, $F(x, \dot{x})_{in}$) and retraction (coming back, $F(x, \dot{x})_{out}$) of the tube-like soft tissue. In the implemented model in this study similar conditions are considered, while the value of spring constant is considered 0.015 N/mm instead of 0.2 N/mm for insertion forces. In the insertion procedure of the simulator, forces of soft tissue model and gripper gravity compensation program (section 4.1)

are all in the same direction, upward. Therefore, these two forces are added in this condition and the resulted forces, which must be applied by the device, will be more than the limitations of the device, Table 1 (page 33). In order to avoid this condition, the insertion spring force is decreased by considering 0.015 N/mm instead of 0.2 N/mm for the insertion spring constant. Conversely, in the retraction movement, tissue model forces are downward, resisting to the upward movement of drill tip, but the gripper gravity compensation program forces are upward. These two forces are subtracted in this condition and the resulted forces will be in the applicable force range of haptic device.

2.4. Temporal Bone Surgery Simulators

Training is a vital issue in medicine, and it is essential for better health care. The human cadaver was an important teaching tool in traditional methods; however, these methods have drawbacks. There are many rules and legal issues about using cadavers in training and debates about their moral and technical limitations. These limitations have always motivated scientists for other methods. There are several alternative methods for theoretical and practical training in medicine, especially in temporal bone surgery [5], which is the main goal of this research.

Regarding theories and conceptual understanding in temporal bone surgical training, there are several anatomy text books with different levels of details. Three-dimensional models and interactive atlases are published to increase the quality of this method of training [1].

Plastic models are another method for training in temporal bone surgery, which is mostly designed for practical training. A common example for these plastic models is "Pettigrew plastic temporal bones", which are broadly considered as an alternative to cadaveric trainings [3]. These

plastic bones are made of a “plastic model with colored dyes to highlight the facial nerve, sigmoid sinus and carotid artery. Moreover, adding extra red irrigation fluid, simulates bleeding during the drilling” [5].

The remaining alternative methods are surgical training simulators, which are based on the interaction of a haptic interface with the virtual environment. For better training of young surgeons, the interaction should become as realistic as possible. Realistic experience necessitates the haptic device represent small mass and inertia, negligible friction, and high stiffness. In addition, sufficient degrees of freedom, gravity compensation, and overall robustness should be supported. An appropriate and accurate model that describes the tissue behavior is essential for a realistic interaction [44].

Modern surgical training simulators can be effective for training novice surgeons [44]. These simulators provide a good level of realistic experience during training, while they are cost effective as the initial cost is distributed among trainees. They have the capability to evaluate trainees’ performance during training, and provide basic experiences for the trainees in a highly fast and accurate manner.

In most cases, three subsystems are connected together to form the surgical virtual reality simulators: “The force feedback haptic mechanism, the visualization subsystem, and the control subsystem” [44].

Many researchers such as [44], [5], and [1] suggest and verify the use of temporal bone simulators for training of the junior trainees; however, clinical experience is always considered as the key factor in the last stages of training.

The first three-dimensional temporal bone simulator with a haptic interface was proposed in 1997 by Kuppersmith et al. [45]. Afterwards, a number of researches focused on the temporal bone simulator with haptic interface; however, most of them focused on modeling the bony structures and simulating bone dissection with haptic rendering:

Understanding of the anatomy was the major objective of the early systems such as [46]. Subsequently, more research focused on the realistic simulation of the visual and haptic interactions. The Ohio virtual temporal bone dissection simulator [47] [48] [49], and the VOXEL-MAN^{TM} system [50] and [51] are examples of these works. In [3], a physically-based contact model is implemented by two PHANTOM^{TM} haptic devices and visual feedback by a binocular display.

In [52] a bone dissection (bone cutting burr) simulator, which provides haptic and visual renderings, is presented. They considered haptic force calculation, the bone erosion process, and the resulting debris. "The bone erosion is implemented by decreasing the density of the areas that are in contact with the burr, according to the predicted local mass flows." [52].

Networked haptic learning environments are presented in [53]. Networked virtual environments emphasize communication between an instructor and a student. In addition, the haptic interface as a simulation component is associated with the communication components.

Surgical training simulators that use haptics have the capability to render the soft tissue interactions; however, they are unable to adequately produce the forces associated with high stiffness of bony structures. Within haptic rendering of soft tissues and physically prototyped modeling of the bony structures, the proposed MR simulator in this study has the capability to employ the realism of prototyped physical models, and the flexibility of soft tissue haptic

models. Research on MR medical simulation is novel and to the best of author's knowledge there is little in the literature regarding medical MR haptic interfaces.

Chapter 3

3. Experimental Setup

The MR temporal bone surgery-training simulator developed for this research uses the Quanser HD^2 haptic device. A real surgical drill used in the temporal bone surgeries must be employed. This allows the trainees to become skillful with the same tools which they will use during real surgery. Hence, a gripper is designed to equip the HD^2 haptic device with the surgical drill. The gripper should be resistant to the dynamic forces and vibrations from drilling and operator's hand, while sufficiently light to avoid significant changes in the dynamics of the system.

3.1. Quanser High Definition Haptic Device

3.1.1. General Description

As seen in Figure 7, the HD^2 consists of a double two-link planar arm layout, and by utilizing two universal joints (U-joints), the arms are placed parallel to a rod, which makes the end-effector of the device. Two capstan-drive DC motors, located at the base of the arm, use a

parallel mechanism to actuate each of the two-link planar arms, moreover, to achieve a third degree of freedom (pitch), another DC motor is mounted at the waist of each two-link planar arms. In addition, two sets of adjustable brass counterbalances are set on each arm, one on the waist of the arm and other on the one of the two motors at each base to minimize equivalent weight over the HD^2 entire workspace as seen in Figure 8. Furthermore, the robot is made up of lightweight materials.

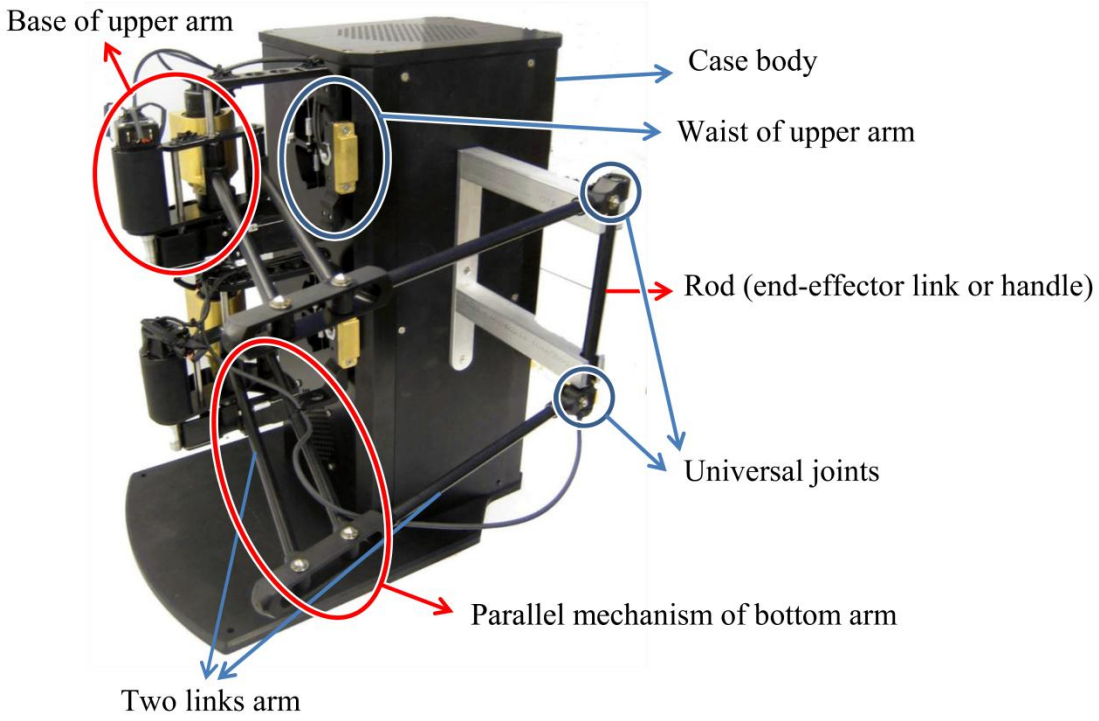

Figure 7: Different parts of the HD^2: The waist and base of upper arm, parallel mechanism and other link of the bottom arm, universal joints, and rod (which shall be known as handle or end-effector link too) are shown.

In addition to parallel mechanisms and capstan drive actuators, six built-in high-performance linear current amplifiers are employed. Consequently, the HD^2 provides the user with stiffness coefficients as high as 20,000 N/m. The gain of each amplifier and current sensor are set to 0.415 A/V and 0.5 V/A respectively [54].

The HD^2 utilizes six custom-made "Faulhaber Coreless DC Motors (3863V006)", depicted in Figure 8. M1 and M2 are the top shoulder motors, M3 and M4 are the bottom shoulder motors, and M5 and M6 are the top and bottom base motors, respectively. Also, a digital switch input is provided by a user push pedal, which is used for switching applications.

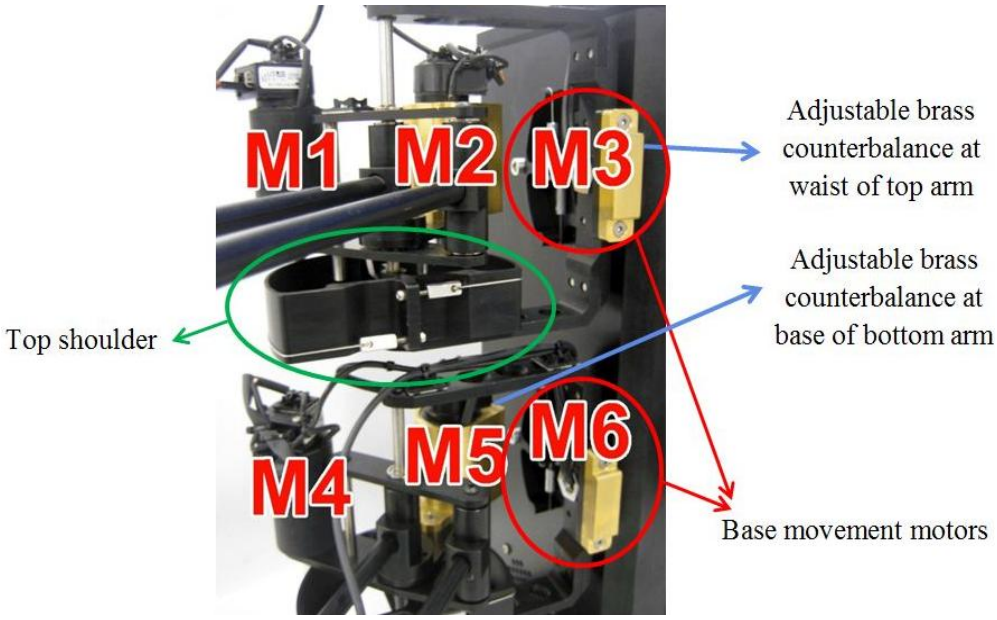

Figure 8: Motor positions and referenced numbers in HD^2. The position of each motor and its assigned number is shown. M1 and M2 are the top shoulder motors, M4 and M5 are the bottom shoulder motors and M3 and M6 are the top and bottom base motors, respectively. Two sets of adjustable brass counterbalances, which are set on each arm, one on the base of the arm and other on the one of the two motors at each shoulder, are shown.

The motion of the operator can be tracked in six degrees of freedom (three translational motions in Cartesian coordinates and three angular motions as roll, pitch and yaw) by utilizing seven high-resolution optical encoders. As shown in Figure 9, "When directly facing the HD^2's front side, moving the end-effector to the left corresponds to a movement along the positive X axis, moving the end-effector towards yourself corresponds to a movement along the positive Y axis, and moving the end-effector up corresponds to a movement along the positive Z axis. Rotations about each of these axes are denoted by θx (Roll), θy (Pitch) and θz (Yaw), respectively." [54].

According to Figure 9, the HD^2 default base coordinate system is fixed at a virtual point almost in the middle of the space between M3 and M6 motors, near the case body of the robot. Therefore, when the robot is in its home position and handle is placed in the jig, the position of the HD^2 interaction point, which is placed in the centre of the handle, is: X= -21.83 cm, Y= 20.85 cm, and Z = 1.11 cm.

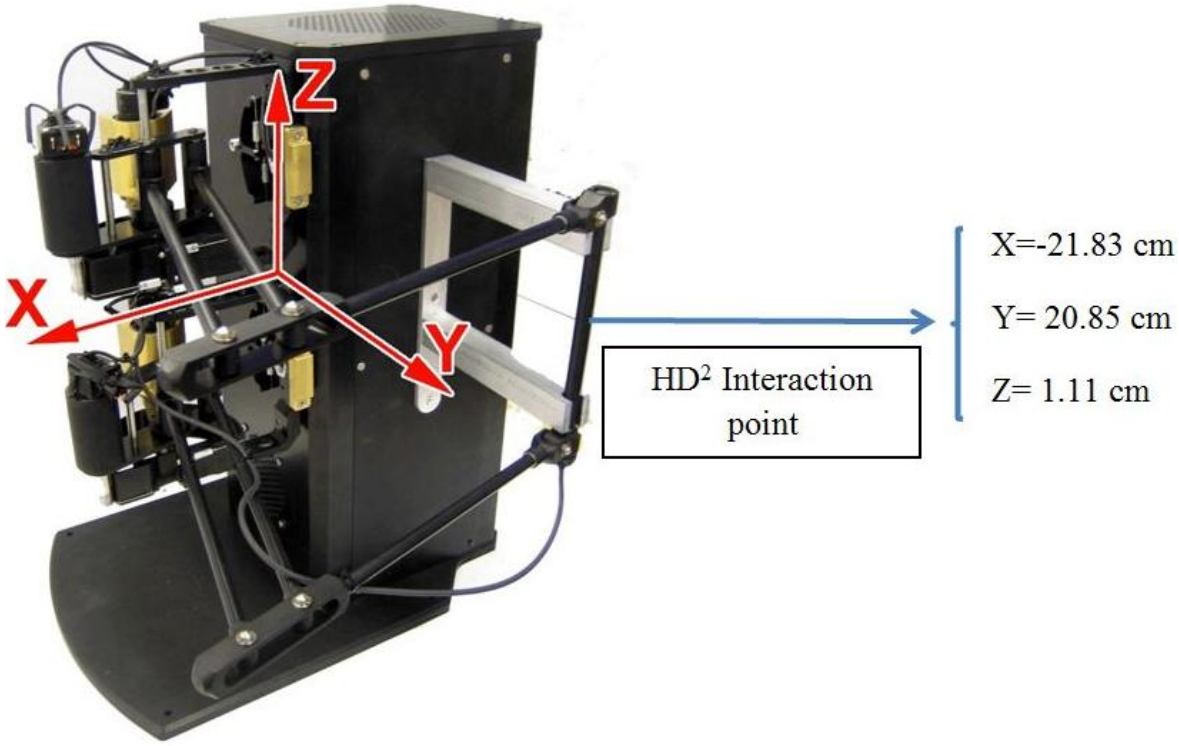

Figure 9: HD^2 in the home position with the default fixed base Cartesian coordinate systems. The position of HD^2 interaction point, when the robot is in its home position, is determined based on the fixed base Cartesian coordinate systems.

The HD^2 has two types of safety features: vibration, and high velocity safety thresholds. They are chosen by the manufacturing company (Quanser), preventing device damage.

The number of sign changes in the velocity of each degree of freedom, introduced as vibration, is monitored by the vibration safety feature over windows of 1.9 seconds. If this feature is enabled, a threshold is set which defines the number of allowed back and forth vibrations in any direction.

If this threshold is passed, the safety switch is triggered and the driver is stopped. This threshold is set to 40 by default. Note that the operator can completely disable the safety feature or change the threshold.

The velocity of each degree of freedom is monitored by the high velocity safety feature, which triggers a high velocity switch and stops the driver in any of the following cases:

- The device end-effector reaches a velocity of 1 m/s or more for at least 0.08 seconds in the X, Y or Z directions.
- The device end-effector reaches an angular velocity of 1.5 rad/s or more for at least 0.2 seconds in the Roll or Pitch directions, yaw does not get monitored.

With motor arm length of 28 cm, forearm length of 29 cm, and end-effector arm (handle) length of 17.5 cm, the HD^2 has a sufficient workspace for different applications such as temporal bone surgery simulation. According to the surgeon's recommendations for human temporal bone surgery, a workspace of 20×20×20 cm will be an ideal space; since, most of the surgeon’s hand movements can be considered as wrist-related movements. The end-effector can move along the X axis from -0.520 to +0.520 m, along the Y axis from 0.200 to 0.555 m, and along the Z axis from -0.275 to +0.275 m. The handle can rotate about the X axis (roll) and Y axis (pitch) from -90 to +90 degrees. The handle rotation about its Z axis (yaw) can be continuous.

The force and torque specifications of the HD^2 are listed in Table 1. The HD^2 is shown to have sufficient force and torque output for generating substantial forces for continuous operations and the capability to apply even larger values for a short period of time (peak output).

	Fx [N]	Fy [N]	Fz [N]	Roll-Torque [N.m]	Pitch-Torque [N.m]	Yaw-Torque [N.m]
Maximum Continuous Output At the Operating Position	10.48	10.48	7.67	0.948	0.948	0.948
Peak Output At the Operating Position	19.71	19.71	13.94	1.72	1.72	1.72

Table 1: Force and torque specifications of the HD^2 for comparison with experimental test results. Calculated required forces and torques should be less than the Maximum Continuous Output at the Operating Position. Also, transient forces and torques should be less than the Peak Output values, which are the forces and torques values that haptic device can apply for just very short period of time.

3.1.2. The Position Control Scheme

HD^2 has the capability of acting in two different control modes: force control and position control. Force control operates in an open loop manner, where the controller sends an output signal to the motors to apply the desired torques computed by the running program. Position control is done in a closed loop manner. The controller uses the encoders' signals as the feedback for the three transitional motions in Cartesian space and two rotational motions, Roll and Pitch. The implemented controller does not control yaw-rotation, but there are possibilities to develop the controller to control the yaw-rotation.

Figure 10 shows that the HD^2 uses a Proportional-plus-Velocity (PV) controller. The PV controller compares the position and velocity of the interaction point, as a three dimensional vector, with the desired Cartesian coordinate positions (X, Y, Z) and velocities to calculate the required forces (Fx, Fy, Fz) for achieving the desired position. It also compares the desired

angular roll and pitch positions and velocities with the measured ones to calculate the required torques roll-torque and pitch-torque as well [54].

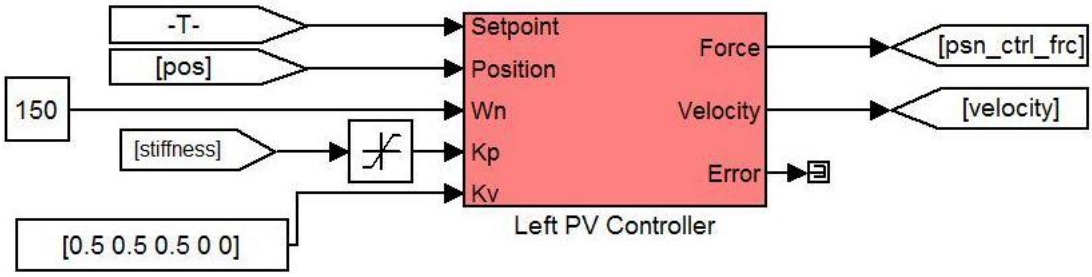

Figure 10: HD^2 position controller's Simulink diagram. The inputs of the controller are position set point, measured position, filter frequency, and both controller gains. The outputs and the value of needed forces and torques and also the value of filtered velocity are shown.

The stiffness block shown in the Figure 10 provides the controller with the data of desired user stiffness in the five controlled degree of freedoms, including three Cartesian coordinate positions and roll and pitch. This stiffness is applied as the Kp factor in the proportional part of the controller. The saturation block limits these values to be within (-2500, + 2500) N/m for X, Y and Z and within (-4, + 4) Nm/rad for roll and pitch. The default values are set to +1500 N/m for X, Y and Z and +2 Nm/rad for roll and pitch [54]. The stiffness values can be changed by the operator in the driver program or the application program. The block which goes to Kv, determines the values of proportional velocity error part of the controller. Kv is equal to 0.5 for three Cartesian coordinate positions, and zero for two angular positions; which means there is not any velocity control for rotations by default. W_n input determines the frequency of the filter used in the controller, Figure 12. This value is 150 [Hz] by default. T block determines the set point value, which is the position of the HD^2 interaction point when the system is put in hold mode (position controller is turned on). The Pos block provides the current measured position values of the HD^2 interaction point. The Psn_ctrl_frc, gets the calculated forces and torques

values as the output of the PV controller and provides these values for other parts of the Simulink driver program. Also, the velocity block is fed with the values of filtered velocity and provides these values for other parts of the Simulink driver program.

Details of HD^2 position controller's Simulink diagram are shown in Figure 11. Difference between desired (set point values) and measured values of position is considered as the proportional error. The value of proportional error is multiplied by the Kp values and then subtracted from the value of the filtered velocity multiplied by Kv, to calculate the values of required forces and torques, Fx, Fy, Fz, roll-torque and pitch-torque. The values of filtered velocity are provided by the filter block which uses the current position, constant value of z, equal to 1 for this case, and the chosen value of W_n, frequency of the filter, in order to calculate the values of filtered position, out, and filtered velocity, out_dot.

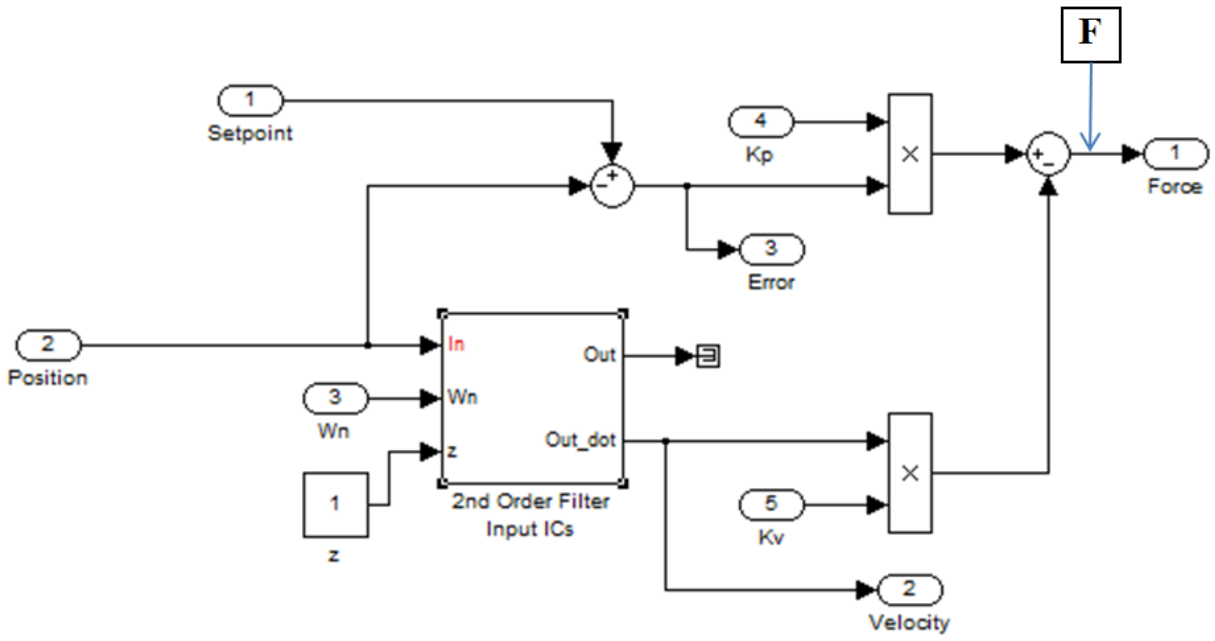

Figure 11: Details of HD^2 position controller's Simulink diagram

Details of the implemented filter are shown in Figure 12. According to the fact that 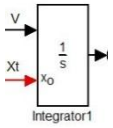

is an integral block with initial value of x_t, and input value of filtered velocity; the output of this block is $x_t{}^f$ which is the filtered position. The input value of the whole block diagram is equal to x_t, current measured position, (block 

).

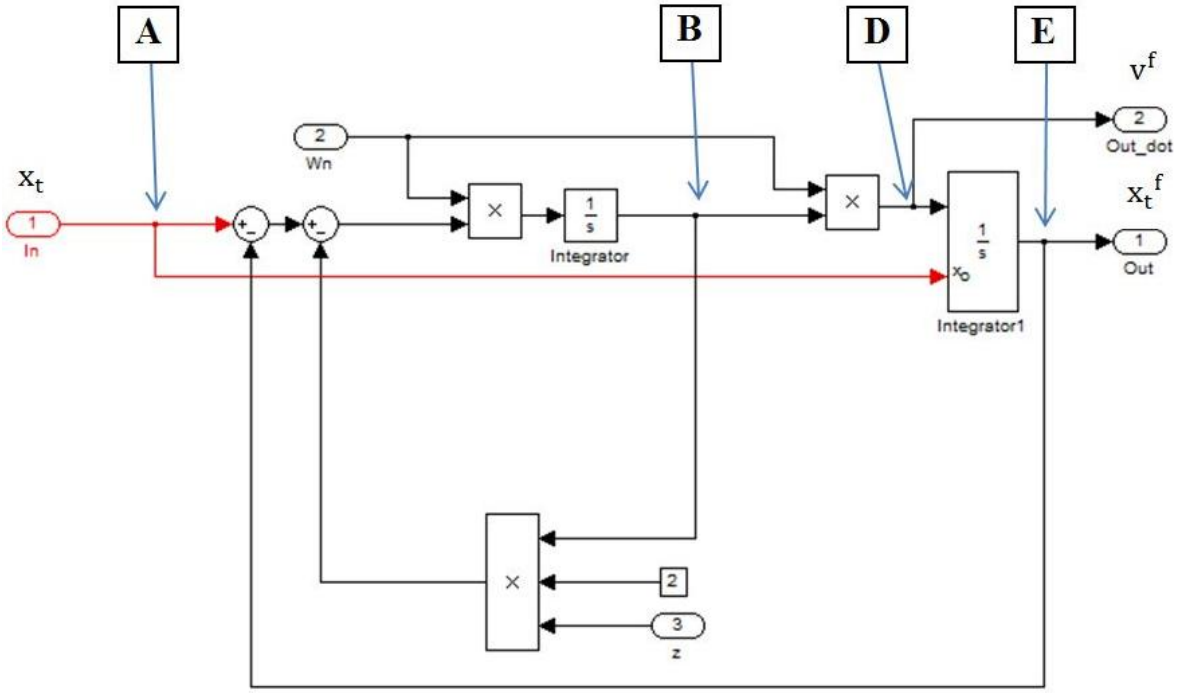

Figure 12: Details of the implemented second order filter in the HD^2 position controller's Simulink diagram

Moving from point A to B:

$$[(x_t - x_t{}^f) - 2b] \cdot \omega_n \cdot \frac{1}{s} = b \qquad (5)$$

b is the value of the signal in point B, and $\Delta x = (x_t - x_t{}^f)$. To find the value of b:

$$[\Delta x - 2b] \cdot \frac{\omega_n}{s} = b \Rightarrow \Delta x \cdot \frac{\omega_n}{s} = \left(1 + \frac{2\omega_n}{s}\right) \cdot b \Rightarrow b = \frac{\frac{\omega_n}{s}}{1 + \frac{2\omega_n}{s}} \cdot \Delta x = \frac{\omega_n}{s + 2\omega_n} \cdot \Delta x$$

6

Moving from point B to D (d is the value of the signal in point D):

$$b \cdot \omega_n = d \Rightarrow \Delta x \cdot \frac{{\omega_n}^2}{s+2\omega_n} = d$$

7

Moving from D to E (value of the signal in point E is equal to the output of whole block diagram and is given to  block. This value is ${x_t}^f$:

$$d \cdot \frac{1}{s} = e \Rightarrow \left(\Delta x \cdot \frac{{\omega_n}^2}{s + 2\omega_n}\right) \cdot \frac{1}{s} = {x_t}^f$$

8

As $\Delta x = (x_t - {x_t}^f)$:

$$(x_t - {x_t}^f)\left(\frac{{\omega_n}^2}{s^2 + 2\omega_n s}\right) = {x_t}^f \Rightarrow x_t\left(\frac{{\omega_n}^2}{s^2 + 2\omega_n s}\right) = {x_t}^f\left(1 + \frac{{\omega_n}^2}{s^2 + 2\omega_n s}\right) \Rightarrow$$

$$x_t\left(\frac{{\omega_n}^2}{s^2 + 2\omega_n s}\right) = {x_t}^f\left(\frac{s^2 + 2\omega_n s + {\omega_n}^2}{s^2 + 2\omega_n s}\right) \Rightarrow \frac{\text{output}}{\text{input}} = \frac{{x_t}^f}{x_t} = \frac{{\omega_n}^2}{s^2 + 2\omega_n s + {\omega_n}^2}$$

9

Hence, transfer function of whole system is $\frac{{\omega_n}^2}{s^2+2\omega_n s+{\omega_n}^2}$ which is a second order transform function. Since both the output and input are positions, the whole block diagram in figure 3 acts as a second order filter:

$$x_t{}^f = \frac{{\omega_n}^2}{s^2 + 2\omega_n s + {\omega_n}^2} x_t$$

10

Based on Figure 11, the out signal of the second order filter is not used in the block diagram of this figure. Instead the value of out_dot signal, which is the value of the signal in point D of Figure 12, is used in the block diagram of Figure 11.

The out signal value of second order filter (Figure 12) is position; hence, the out_dot signal value, which is the output value before integral block, is velocity. Thus, the value of d is equal to the filtered velocity (v^f).

$$d = v^f$$

11

According to the value of the signal in point D ($d = \Delta x \cdot \frac{{\omega_n}^2}{s+2\omega_n}$):

$$v^f = \left(\frac{{\omega_n}^2}{s+2\omega_n}\right) \cdot (x_t - x_t{}^f)$$

12

The value of signal in point F (Figure 11) is equal to:

$$f = k_p(error) - k_v(out\_dot) = k_p(error) - k_v \cdot (v^f)$$

13

In which "error" is equal to $(x_{set\ point} - x_{measured})$. Controller command force can be calculated as $f = k_p(error) - k_v v$ which is a PV controller command force. The output force of control schema is equal to $k_p(\text{position error}) - k_v(\text{filtered velocity})$. According to the fact that the control does not have any integral control term, the system has small position error in generating the forces needed for compensating the gravity effects of the handle, arms and other attachments.

3.2. Description of Surgical Drill Gripper

A real surgical drill, the Medtronic surgical drill, will be used in the simulated temporal bone surgeries. Hence, the HD^2 haptic device is equipped with a designed gripper to develop the simulator. Designed gripper is made of aluminum, which is a lightweight, cost effective, and is readily available with acceptable mechanical strength.

Moreover, the gripper attaches the drill to the haptic device in such a way that the trainee feels the expected forces and torques while holding the surgical drill during the simulated surgery. Any offset, extra forces or torques, or different degrees of freedom compared to the real surgery will mislead the trainee. According to the HD^2 kinematic and force specification, the surgical drill should be attached to the handle such that both have same axis of rotation (see Figure 14). Hence, the gripper is designed to place the drill along with the handle, outside of the HD^2 double two-link planar arms. The gripper consists of four parts, these parts and their duties are explained in Figure 13. Handle model design is similar to the original HD^2 handle. The difference is that the model part has a longer length than in the component with a smaller diameter. This

component is rigidly fixed between the parts that connect to the handle. In the same manner, the surgical drill is held and rigidly fixed to the gripper. Therefore, surgical drill is connected to the handle and the haptic device. A Solid-Works model of the assembled gripper, handle and surgical drill is shown in Figure 13. Also, equipped simulator and the position of the trainees' hand during the training are shown in Figure 14.

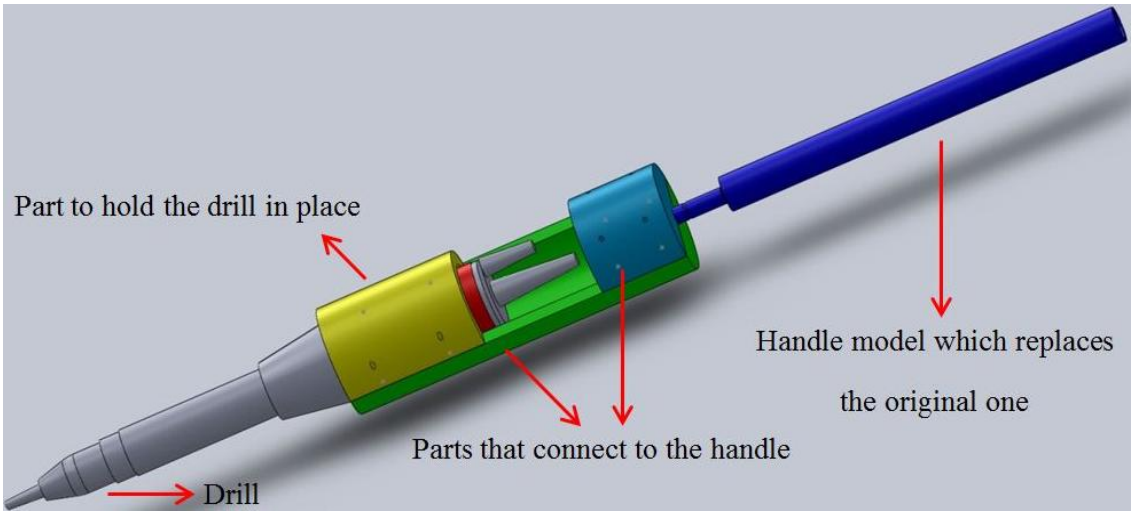

Figure 13: Solid-Works model of the assembled gripper, handle model and surgical drill. The four parts of gripper and their duties are explained

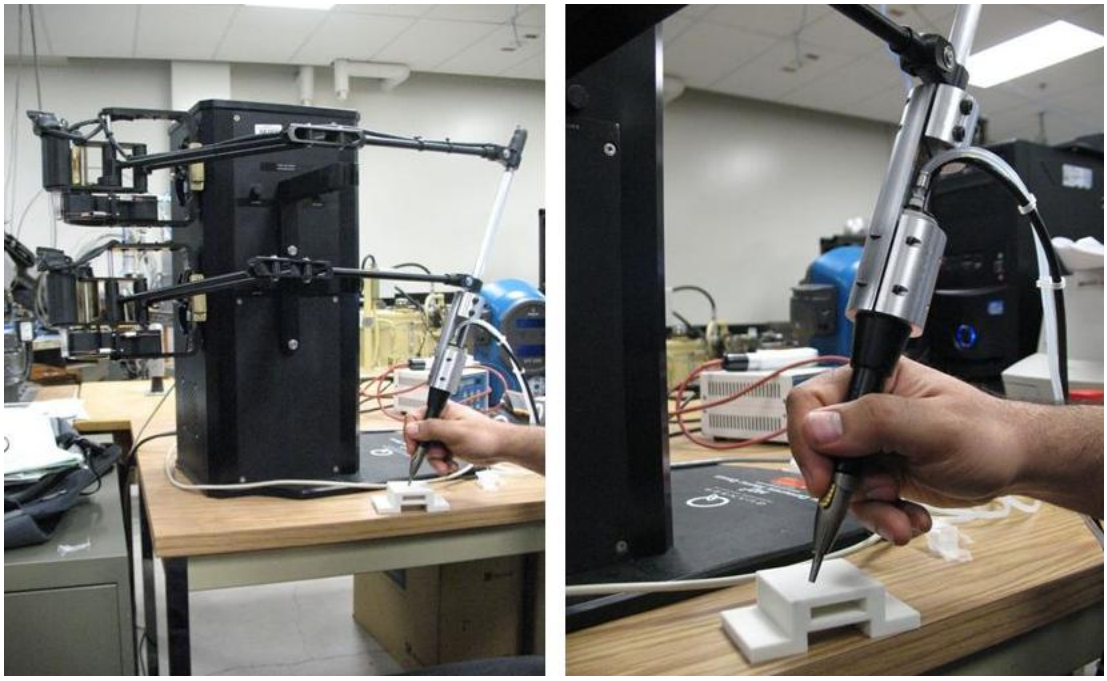

Figure 14: The equipped simulator: assembled gripper, handle, surgical drill, and the position of the trainees' hand during the training are shown. Surgical drill should be attached to the handle such that both have same axis of rotation in order to trainee feels the expected (realistic) forces and torques while holding the surgical drill during the simulated surgery.

Chapter 4

4. Developing Haptic Models for a Mixed Reality Simulator

4.1. Transmitting Soft Tissue Contact Forces

In surgery training simulators, conditions must be as close as possible to real surgery conditions. Hence, several scenarios should be considered to make a realistic simulation environment. The HD^2 is designed for an environment in which the operator holds its handle and the haptic device applies the modeled forces and torques through the HD^2 interaction point (centre of the handle). In the real surgery however, soft tissue will have contact with the drill tip and apply forces and torques to that point.

In the developed simulator, the modeled forces of the soft tissue are produced by the haptic device at the HD^2 interaction point, centre of the handle or h point, but these forces should be felt in the drill tip, simulator interaction point or d point in Figure 15. A part of this project is to implement the modeled forces and torques of the soft tissue at the drill tip.. Hence, the applied

forces in the center of the HD^2 handle, which is haptic interaction point, h, should be transmitted to the drill tip, d, that is the simulator interaction point. The forces which are transmitting to the drill tip can be any kind of force such as gravity compensation. They are not just limited to the soft tissue model forces.

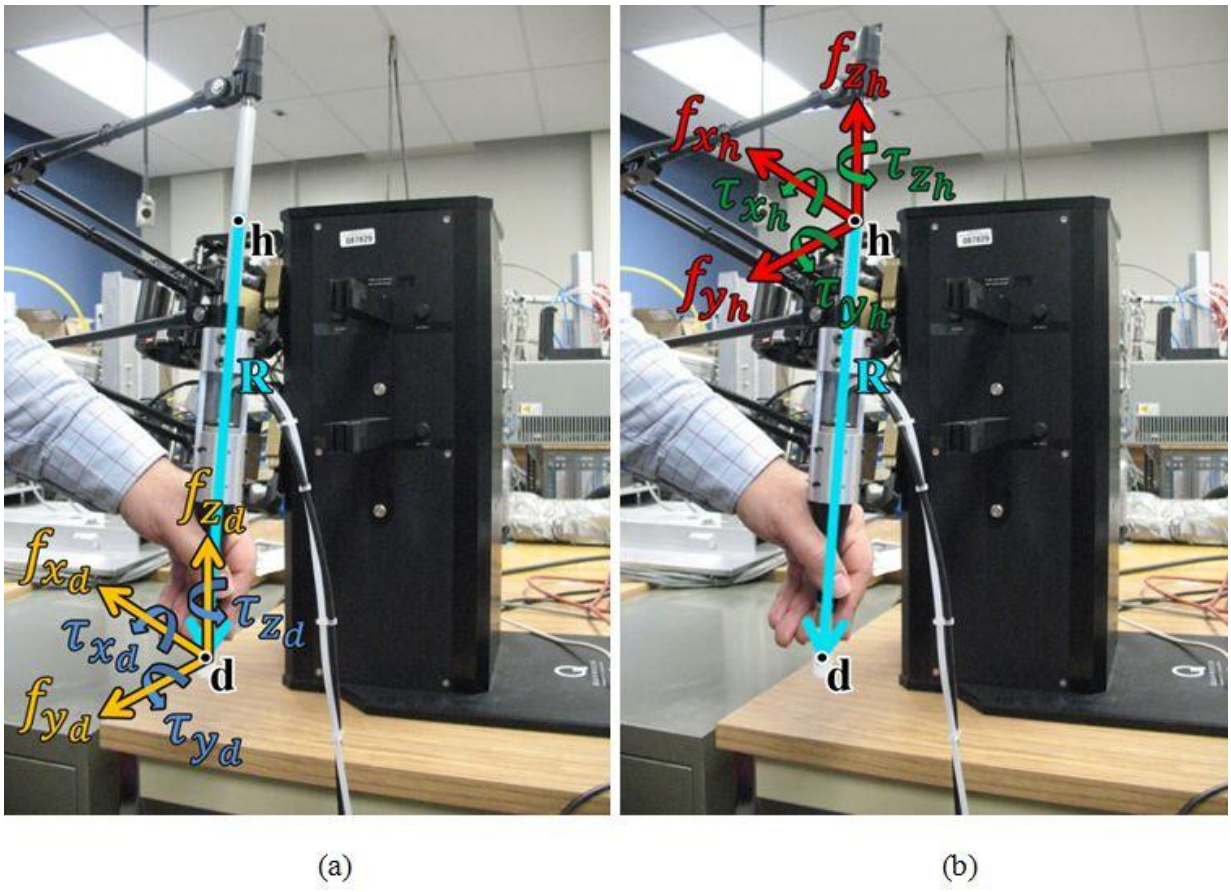

Figure 15: Forces and torques in: a) Drill tip, which is simulator interaction point or d point. These are the forces and torques calculated by the soft tissue models. They should be felt in the drill tip. b) HD^2 interaction point, which is center of the handle or h point. These are the forces and torques that can be applied by the haptic device in the HD^2 interaction point. They should be transmitted to the drill tip to produce the needed forces and torques in the drill tip.

4.1.1. Applied Forces

The handle, the gripper, and the surgical drill are rigidly fixed together. Therefore, the system between HD^2 interaction point and simulator interaction point, which should be refered to as "interaction points' trasmission system", is considered as a rigid body without any joints. Thus, the forces at the HD^2 interaction point ($\overrightarrow{F_h}$), which are the applied forces by the haptic device, are the same as the forces at simulator interaction point ($\overrightarrow{F_d}$), which are defined by soft tissue models. This is considered as general force equation :

$$\overrightarrow{F_h} = \overrightarrow{F_d} \rightarrow \begin{cases} f_{x_h} = f_{x_d} \\ f_{y_h} = f_{y_d} \\ f_{z_h} = f_{z_d} \end{cases} \quad \textbf{14}$$

4.1.2. Applied Torques

The aforementioned force transmission needs certain torques ($\overrightarrow{T_t}$) to be applied by the robot. According to dynamics, if any forces transmit in any direction not parallel to their axis, certain torques will be created; however, in transmitting torques no extra forces or torques will be added. Moreover, the implemented model in the drill tip includes both forces and torques. The torques of the soft tissue models ($\overrightarrow{T_d}$) are produced by the device's applied torques ($\overrightarrow{T_h}$) in the HD^2 interaction point too. However, because the "interaction points' trasmission system" is rigid there is no need for any extra force or torque to transmit the soft tissue torques to the drill tip. Therefore the torque equation is formulated as:

$$\overrightarrow{T_h} = \overrightarrow{T_t} + \overrightarrow{T_d}$$

15

In this equation, $\overrightarrow{T_h}$ is the applied torque by the robot in the centre of the handle (h point), $\overrightarrow{T_d}$ is the torque of the soft tissue models, and $\overrightarrow{T_t}$ is the torque required for transmitting the tissue model forces (Figure 16). $\overrightarrow{T_t}$ is equal to:

$$\overrightarrow{T_t} = \vec{R} \times \overrightarrow{F_d}$$

16

$\vec{R}$ is the distance vector from the HD^2 interaction point, h, to simulator interaction point, d, that is drill tip position.

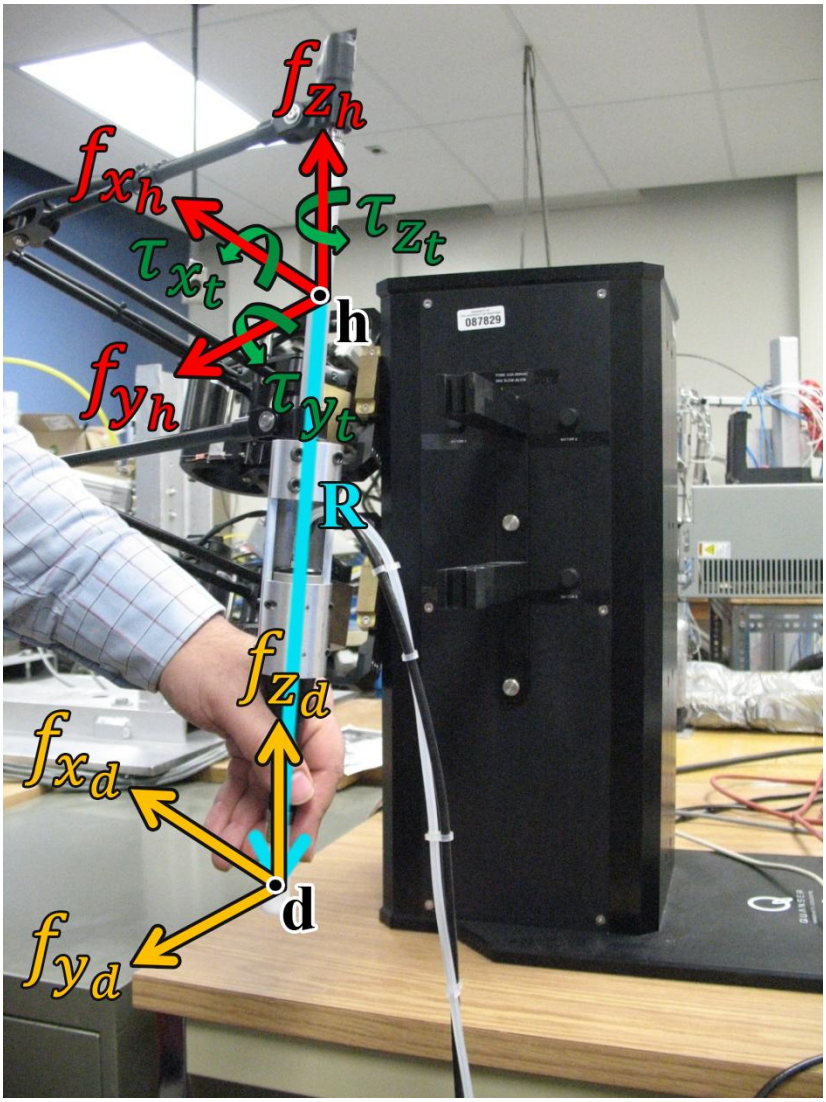

Figure 16: Transmitting the applied forces in the h point, centre of the handle or HD[2] interaction point, to d point that is simulator interaction point or drill tip. For this transmission certain torques ($\overrightarrow{T_t}$) should be applied by the haptic device.

Combining equations 15 and 16; torque equation can be defined as:

$$\overrightarrow{T_h} = \vec{R} \times \overrightarrow{F_d} + \overrightarrow{T_d}$$

17

In this equation, $\overrightarrow{F_d}$ and $\overrightarrow{T_d}$ are known vectors which are defined by soft tissue models. In order to find the $\overrightarrow{T_h}$ vector , its terms can be determined along local Cartesian coordinate frame in point h Figure 17. The local Cartesian coordinate frames are the base Cartesian coordinate frame in different origins, at point d or point h. Hence Cartesian terms of each force or torque vector, not the positions' vectors, are the same according to these local Cartesian coordinate frames or base Cartesian coordinate frame.

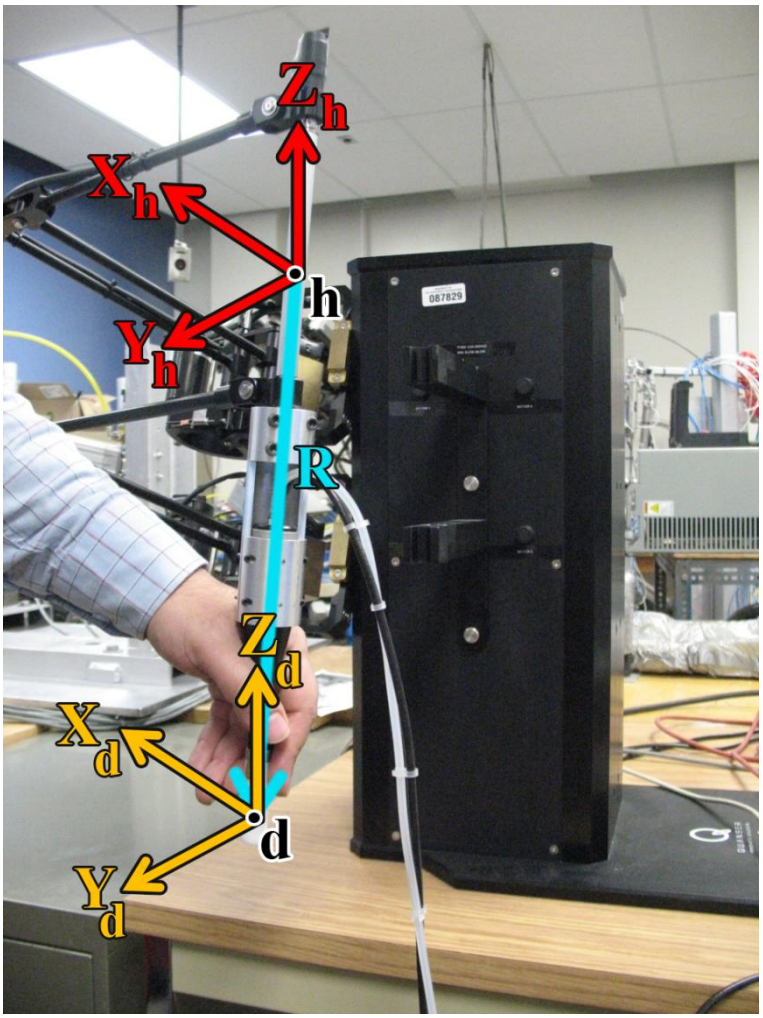

Figure 17: local Cartesian coordinate frames in point h and point d. The local Cartesian coordinate frames are the base Cartesian coordinate frame in different origins, point d or point h. Cartesian terms of each force or torque vector, not the positions' vectors, are the same according to these local Cartesian coordinate frames or base Cartesian coordinate frame.

The $\overrightarrow{T_h}$ vector's terms along local Cartesian coordinate frame in point h are determined as follows:

According to cross product in vector space:

$$\overrightarrow{T_t} = \vec{R} \times \overrightarrow{F_d} \rightarrow \begin{bmatrix} \tau_{x_t} \\ \tau_{y_t} \\ \tau_{z_t} \end{bmatrix} = \begin{bmatrix} r_x \\ r_y \\ r_z \end{bmatrix} \times \begin{bmatrix} f_{x_d} \\ f_{y_d} \\ f_{z_d} \end{bmatrix} \rightarrow \begin{cases} \boldsymbol{\tau_{x_t}} = r_y \cdot f_{z_d} - r_z \cdot f_{y_d} \\ \boldsymbol{\tau_{y_t}} = -(r_x \cdot f_{z_d} - r_z \cdot f_{x_d}) \\ \boldsymbol{\tau_{z_t}} = r_x \cdot f_{y_d} - r_y \cdot f_{x_d} \end{cases}$$

18

According to equations 17, 18, and $\overrightarrow{T_d} = \begin{bmatrix} \tau_{x_d} \\ \tau_{y_d} \\ \tau_{z_d} \end{bmatrix}$:

$$\overrightarrow{T_h} = \vec{R} \times \overrightarrow{F_d} + \overrightarrow{T_d} \rightarrow \begin{cases} \boldsymbol{\tau_{x_h}} = r_y \cdot f_{z_d} - r_z \cdot f_{y_d} + \tau_{x_d} \\ \boldsymbol{\tau_{y_h}} = -(r_x \cdot f_{z_d} - r_z \cdot f_{x_d}) + \tau_{y_d} \\ \boldsymbol{\tau_{z_h}} = r_x \cdot f_{y_d} - r_y \cdot f_{x_d} + \tau_{z_d} \end{cases}$$

19

In this equations, $\tau_{x_d}, \tau_{y_d}, \tau_{z_d}$, f_{x_d}, f_{y_d}, and f_{z_d} are defined by soft tissue models. τ_{x_h}, τ_{y_h}, and τ_{z_h} are parameters calculated based on $\tau_{x_d}, \tau_{y_d}, \tau_{z_d}, r_x, r_y, r_z, f_{x_d}, f_{y_d}$, and f_{z_d}; and applied by the haptic device.

As mentioned before, $\vec{R}$ is the distance vector from the HD[2] interaction point, h, to simulator interaction point, d, the drill tip position. This vector's terms within the Cartesian coordinate system are determined as follows:

When the robot is in its home position, $\vec{R}$ is defined as:

$$\vec{R}_{\text{Home Position}} = \begin{bmatrix} 0 \\ 0 \\ -r \\ 1 \end{bmatrix} \quad \textbf{20}$$

Because $\vec{R}$ connects two point of a rigid body, any position of $\vec{R}$ ($\vec{R}_{\text{General}}$), which is defined based on the local Cartesian coordinate frame at the HD^2 interaction point, h, can be determined by rotating $\vec{R}_{\text{Home Position}}$ around three Cartesian coordinates (Figure 17). Based on the robot specifications, rotation about the local X axis is considered as roll movement, θ_{Roll}, rotation about the local Y axis is considered as pitch movement, θ_{Pitch}, and rotation about the local Z axis is considered as yaw movement, θ_{Yaw}. Hence the rotation equations are:

$$\text{Rot}(x, \theta_{\text{Roll}}) = \begin{bmatrix} 1 & 0 & 0 & 0 \\ 0 & \sin\theta_r & -\sin\theta_r & 0 \\ 0 & \sin\theta_r & \cos\theta_r & 0 \\ 0 & 0 & 0 & 1 \end{bmatrix}; \quad \theta_r = \theta_{\text{Roll}} \quad \textbf{21}$$

$$\text{Rot}(y, \theta_{\text{Pitch}}) = \begin{bmatrix} \cos\theta_p & 0 & \sin\theta_p & 0 \\ 0 & 1 & 0 & 0 \\ -\sin\theta_p & 0 & \cos\theta_p & 0 \\ 0 & 0 & 0 & 1 \end{bmatrix}; \quad \theta_p = \theta_{\text{Pitch}} \quad \textbf{22}$$

$$\text{Rot}(z, \theta_{\text{Yaw}}) = \begin{bmatrix} \cos\theta_w & -\sin\theta_w & 0 & 0 \\ \sin\theta_w & \cos\theta_w & 0 & 0 \\ 0 & 0 & 1 & 0 \\ 0 & 0 & 0 & 1 \end{bmatrix}; \quad \theta_w = \theta_{\text{Yaw}} \quad \textbf{23}$$

Therefore, $\vec{R}$ generally can be defined as:

$$\vec{R}_{General} = Rot(x, \theta_{Roll}) \times Rot(y, \theta_{Pitch}) \times Rot(z, \theta_{Yaw}) \times \vec{R}_{Home\ Position} \quad \textbf{24}$$

$$\vec{R} = \begin{bmatrix} -r \cdot \sin\theta_p \\ r \cdot \cos\theta_p \cdot \sin\theta_r \\ -r \cdot \cos\theta_p \cdot \sin\theta_r \\ 1 \end{bmatrix} \rightarrow \begin{cases} \mathbf{r_x} = -r \cdot \sin\theta_p \\ \mathbf{r_y} = r \cdot \cos\theta_p \cdot \sin\theta_r \\ \mathbf{r_z} = -r \cdot \cos\theta_p \cdot \cos\theta_r \end{cases} \quad \textbf{25}$$

In these equations, the constant value of "r" is equal to the distance between HD^2 interaction point, h, and simulator interaction point, which is d or the drill tip position. Substituting r_x, r_y, and r_z from equation 25 in equation 19, the general torque equation, which is the torque to be applied by the haptic device, results in (Figure 18):

$$\overrightarrow{T_h} = \begin{bmatrix} \tau_{x_h} \\ \tau_{y_h} \\ \tau_{z_h} \end{bmatrix}; \begin{cases} \boldsymbol{\tau_{x_h}} = (r\ \cos\theta_p \sin\theta_r) f_{z_d} + (r\ \cos\theta_p \cos\theta_r) f_{y_d} + \tau_{x_d} \\ \boldsymbol{\tau_{y_h}} = (r\ \sin\theta_p) f_{z_d} - (r\ \cos\theta_p \cos\theta_r) f_{x_d} + \tau_{y_d} \\ \boldsymbol{\tau_{z_h}} = (r\ \sin\theta_p) f_{z_d} - (r\ \cos\theta_p \cos\theta_r) f_{x_d} + \tau_{z_d} \end{cases} \quad \textbf{26}$$

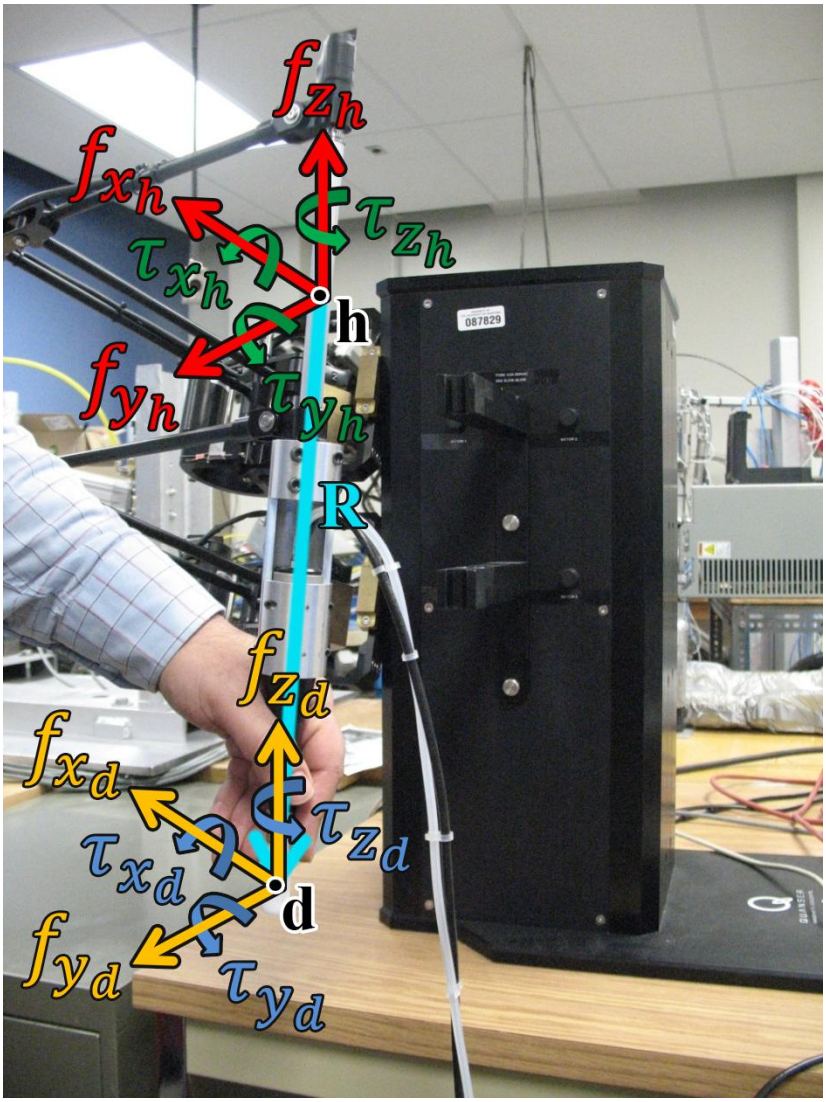

Figure 18: Forces and torques of "interaction points' transmission system". Forces and torques in the point d are the forces and torques calculated by the virtual soft tissue models and should be felt in the drill tip. These forces and torques are produced by the applied forces in the h point, centre of the handle or HD[2] interaction point.

The results of force and torque equations are used to create the "force trasmission" program (see Appendix A). This program is used to calculate the device's forces and torques which are required to produce the feeling of the soft tissue model's forces and torques in the drill tip.

4.2. Compensating the Gripper's Gravity Effects

During a real surgery, surgeons feel just the weight of the drill and the attachments such as the wires and the irrigation tubing. The designed simulator should have the same condition, so the gravity effects of the gripper and handle, excluding the drill, should be cancelled as much as possible.

In order to achieve this goal, certain forces and torques should be applied by the haptic device to cancel these gravity effects. These forces and torques should keep the system from falling when the drill is removed. In this condition, the surgical drill is separated from the gripper and removed from the system. When significant external forces, such as trainees' hand forces and not the system's weight, move the system, simulator without the drill, to a new position and then release it, the system should hold its new position until another significant external force changes the gripper's position.

The gripper's weight is about 90 gr in the Z direction, which needs a less than 1 N force to overcome the weight; however, in experiments 1 N force is not enough to cancel the weight effects. This is because the gravity effects of other parts of the haptic device such as handle and arms are not considered. Therefore, several tests are performed to determine the suitable force and torques for compensating the gripper's gravity effects. In these tests, the new system, which is the simulator without drill but with the gripper, is moved to different areas of its workspace and then the position controller is activated to hold the new position. These tests are similar to test 1-1 which is described in more detail in Chapter 5. The applied forces and torques of the device are recorded and same forces and torques (Fz = 2.25 N, pitch-torque = 0.1 Nm, and roll-torque = 0.02 Nm) are programmed in the gripper gravity compensation program. These constant

values compensate the gravity effects of the gripper in whole workspace and in different configurations.

When the developed simulator is operating, the gripper gravity compensation program is activated and cancels the gravity of the system excluding the drill. Two sets of experiments in section 5.3 and 5.4 verify the effectiveness and performance of the "gripper gravity compensation" program. Impacts of this program on other parts of the system and whole simulator performance are studied in those experiments.

4.3. System's Program Architecture

According to Figure 19, the developed simulator has a specialized haptic programming loop. In the locating interaction part, sensor data are received by means of the device driver, yielding the local position of the interaction point. In the collision detection part, measured position of the haptic interaction point is compared with a model of the virtual world. For instance, it must be determined whether or not the interaction point, which is the drill tip, is in the virtual soft tissue area or not.

In the computing desired forces and torques part, the desired forces and torques which are applied by the device to create the feeling of the desired virtual environment, are calculated. This part consists of several subparts. First, according to the position of the interaction point, relevant forces and torques of the virtual soft tissue model are calculated. Information about the position of the interaction point is provided to the virtual soft tissue model, by means of locating interaction part. Afterwards, based on the force transmission program, the soft tissue model forces and torques which are applied by the haptic device are calculated. These forces and

torques values are added to the forces and torques of the gripper gravity compensation program, to compute the total forces and torques which are applied by the device.

In the next step, which is robot specifications and limitations, calculated total values are compared with the maximum applicable values of the robotic haptic device. If these values are more than the maximum applicable values, the operator will receive an error message, while the device applies the maximum applicable values instead of total calculated values. In the output force and torques part, force commands are converted to actuator commands. These forces are applied to the real environment and impacts on the position of the simulator in this environment that will be measured in the locate interaction part again.

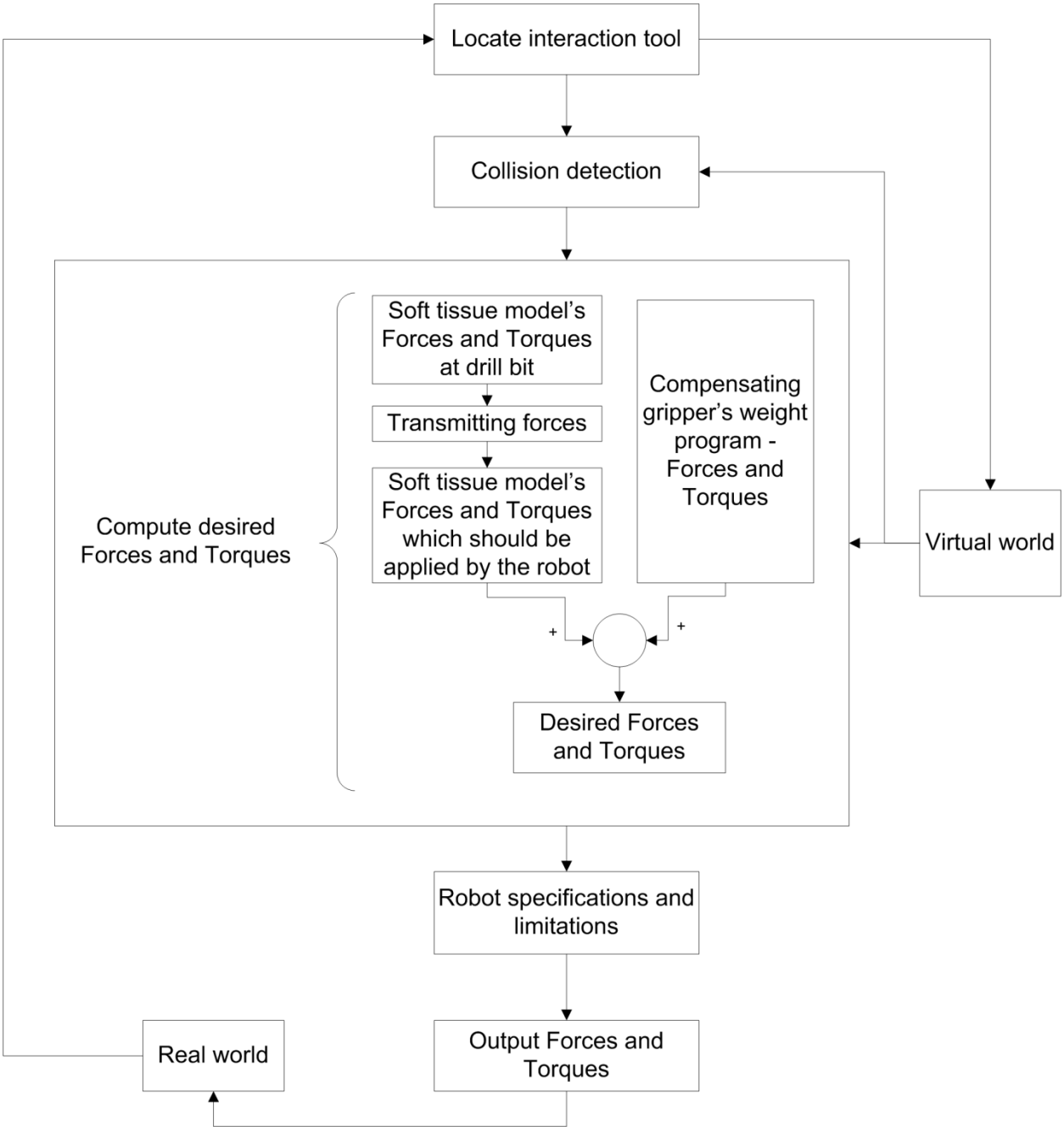

Figure 19: Haptic programming loop

Chapter 5

5. Results and Verification

5.1. Introduction

In this chapter, the performed experiments that were designed to determine the effectiveness and performance of the developed simulator are explained. The theoretical works which have been done for compensating the gripper's gravity and simulating the virtual soft tissue are implemented. The stability of the developed simulator is studied in different conditions. The most critical factors of the training conditions for the simulator are drill vibration, contact forces of drilling the prototyped physical model of bony structures, and interaction between real and virtual models.

In the tests mentioned, critical factors are considered. In each test, first the description of the conditions of the test is provided, and then the reasons for performing the test are explained, such as studying the effects of the gripper's gravity or virtual soft tissue.

In all the tests, the simulator must appear stable and the required forces and torques be less than the device's maximum continuous applicable forces and torques, based on force and torque specifications in Table 1. Transient forces and torques can be more than the maximum continuous applicable values, ie. Fx and Fy equal to or less than 10.48 N, Fz equal to or less than 7.67 N, and maximum continuous applicable torques equal to or less than 0.948 Nm. However, transient forces and torques must still be less than the peak values, ie. Fx and Fy equal to or less than 19.71 N, Fz equal to or less than 13.94 N, and peak applicable torques equal to or less than 1.72 Nm. Also, any system instability, due to continuous oscillations or large amplitude vibrations, must be avoided. In the summary sections, the results of a series of related tests according to the expectations of those tests are discussed.

5.2. Studying the Simulator Stability in the Position Control Mode - Experiment 1

As mentioned in section 3.1.2, the default values for the stiffness in the control mode are set to 1500 N/m for X, Y and Z and 2 Nm/rad for roll and pitch. In order to study the stability of the simulator, which is developed on the HD^2 haptic device, the stiffness is set to default values. Furthermore, the following tests are designed to observe the simulator behaviour in position control mode through the common implementing condition, which is drilling a prototyped physical model of temporal bone with a surgical drill. In each test, the system is moved to the desired 3D position and orientation (Figure 20) and the position controller is activated to hold the position of the system. Different conditions and disturbances are applied to the system to study the impact of those disturbances.

Figure 20: Simulator in the position control mode, Experiment 1. The controller holds the position of the handle, the attached gripper and the surgical drill at the desired 3D position and orientation.

Test 1-1: This is a standard test to measure the performance of the developed simulator in the general control mode. The controller holds the position of the handle, the attached gripper and the surgical drill at the desired 3D position and orientation. There should be little flexibility according to the chosen default stiffness values. The results for this test are shown in Figure 21. The system is held in its position between B and C.

In order to overcome the gravity effect of the paraller links, handle, gripper and the drill, a constant force is applied in the Z direction, and low forces and torques are applied in other directions including Fy, pitch-torque, and roll-torque, as seen in Figure 21.

In order to perform the tests in this section, the handle and the attached gripper-drill are moved from the home position to reach to the desired position. The operator performs this movement

using his hand and when the system reaches the desired position he activates the position controller. Afterwards, the position of the system is held by the desired flexibility based on the chosen stiffness, as in Figure 20. When the test is completed, operator turns off the position controller, gets the handle and brings it back to the home position. The sharp changes in the Y and Z values, in Figure 21 at A and D, show these movements at the beginning and termination of the test. When the position controller is turned on, it saves its first position as the desired position and tries to hold it. At the beginning, in the transient mode, the system experiemces some position errors and the PV controller causes some oscillations. Oscillations in the values of Fx and Fy at B, are due to the transient mode of the position controller.

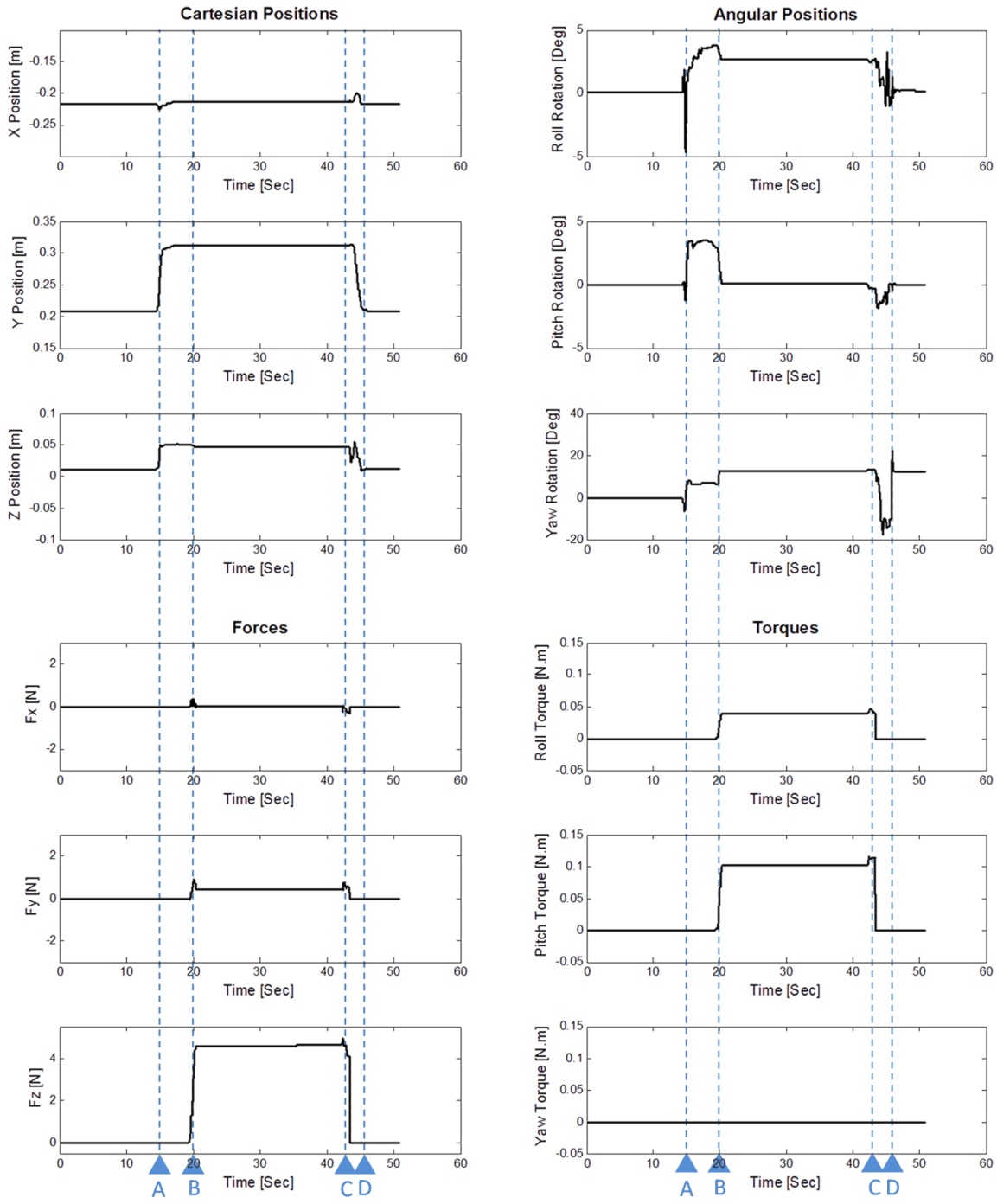

Figure 21: Results of Test 1-1. System is moved to the desired 3D position and orientation. The position controller is activated to hold the position of the system, between B and C. No disturbance is applied to the system. At A, operator moves the system from home position to the desired position. The reverse movement occurs at D.

Test 1-2: This test is similar to the Test 1-1. However, the conditions are changed to determine the capacities of the system in the control mode. Random disturbances are applied to the handle through the operator hand and mostly in the Z direction. These disturbances are created by shaking the whole system which consists of handle, gripper, and drill with the operator's hand. As shown in Figure 22, the position controller is activated between A and D, while the disturbances are applied between B and C.

Red rectangles in Figure 22 indicate sample parts of the disturbances, which are expanded in Figure 23. The controller applies oscillatory forces in X, Y, and Z directions; and oscillatory torques in pitch and roll (Figure 23). As shown in Figure 23 the maximum disturbances are applied in the Z direction, and the controller applies maximum oscillatory forces in the Z direction homogeneously around the Fz=5N, which is the necessary force in the Z direction in the standard test (Test 1-1) to keep the system in its position. According to section 3.1.2, the applied controller is a five degrees of freedom controller and cannot apply the yaw-torque; hence, the values of yaw-torque are constant.

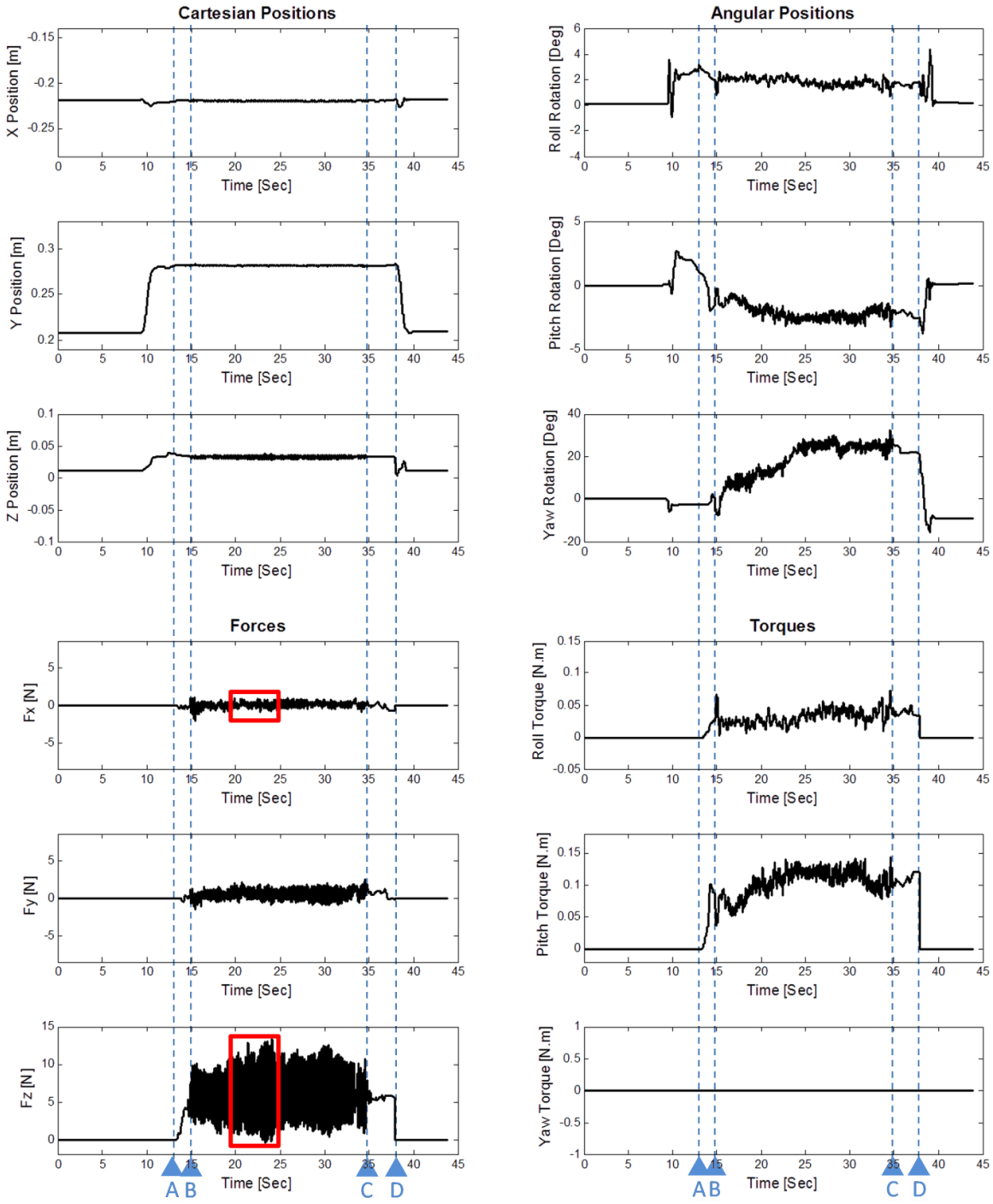

Figure 22: Results of Test 1-2. Random disturbances are applied to the handle through the operator's hand between B and C, while the position controller is activated to hold the position of the system, between A and D. Red rectangles indicate sample parts of the disturbances.

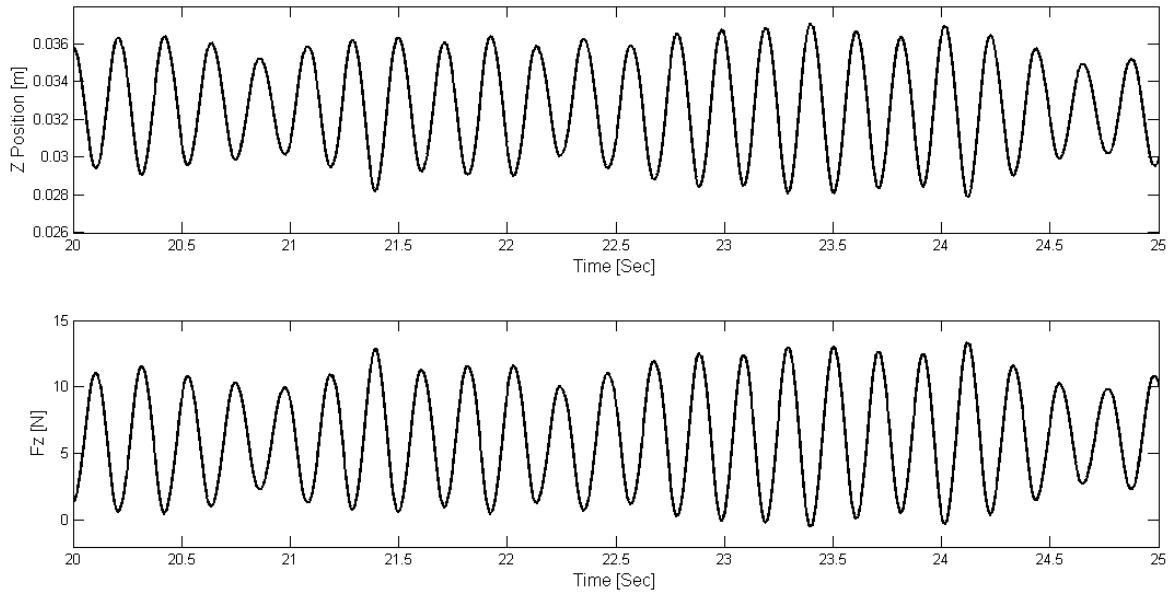

Figure 23: Sample parts of disturbances in the Z direction and Fz in Test 1-2. Random disturbances are applied to the handle through the operator's hand.

Test 1-3: This test is based on the standard test, Test 1-1, with some modifications. While the system holds its position, the surgical drill turns on and off with different rotational velocities. The objective of this test is to study the impacts of drill's vibration on the simulator in the control mode. Also, there is no operator's hand acting as an external damper holding the surgical drill.

While the system holds its position this test is performed in three steps:

1. The drill is turned on and drill tip rotates at the maximum velocity of 42000 RPM clockwise around B.
2. The condition changes and drill tip rotates at the maximum velocity counter clockwise around C.
3. In the last step of the test, drill tip rotates clockwise with variable velocities between D and E.

The results for this test are shown in Figure 24. The system is held in position between A and F. In the yaw-rotation part of Figure 24, step 1 as clockwise rotation around B, step 2 as counter clockwise rotation around C, and step 3 as clockwise rotation with variable velocity between D and E, are depicted. There is no yaw-torque applied by the controller in Test 1-3, so yaw-rotation is not controlled and it changes along with the drill vibrations. Comparing Figure 24 with the standard Test 1-1, the forces and torques values are the same, merely they have very a few oscillations related to three steps of the test.

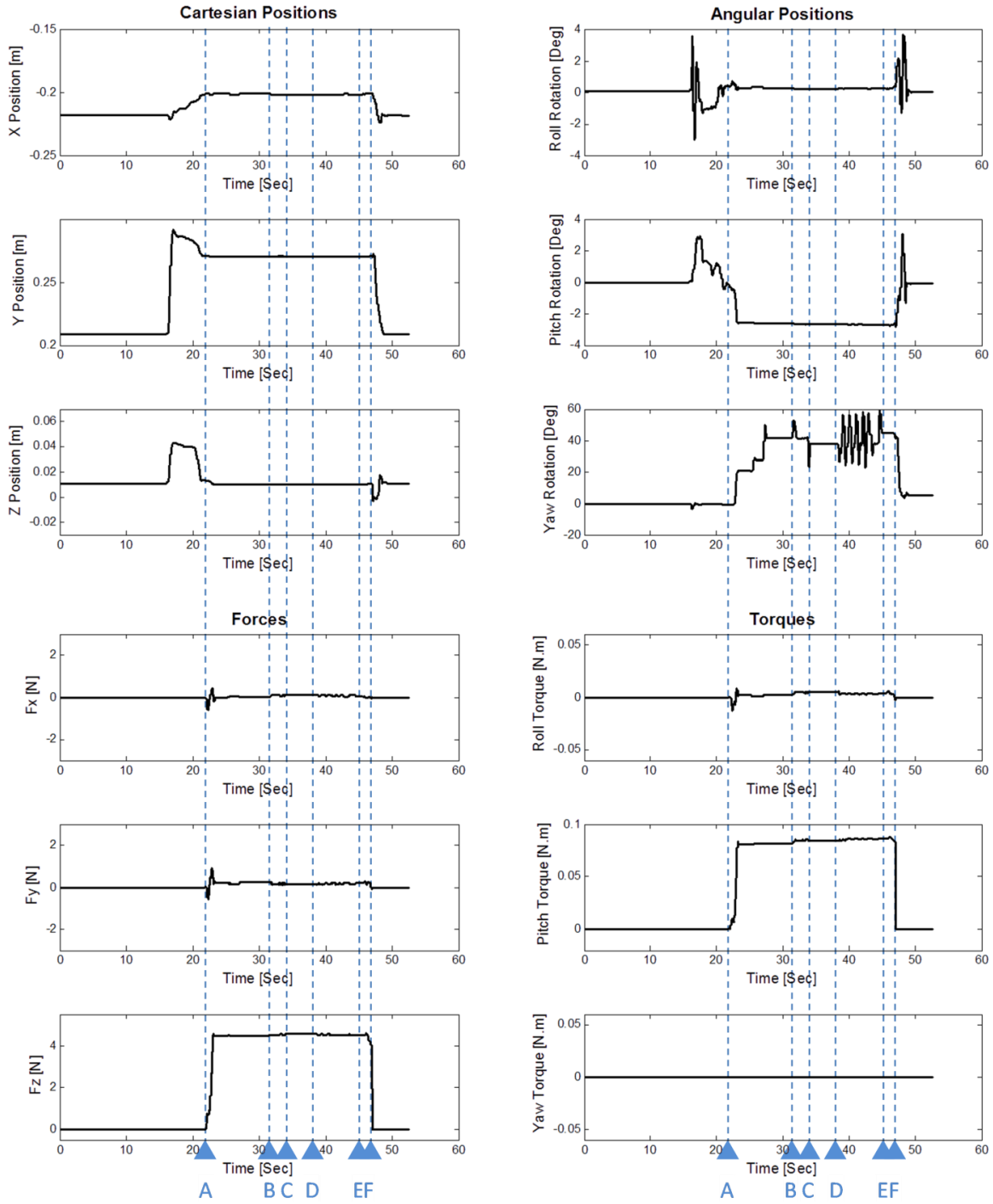

Figure 24: Results of Test 1-3. While the position controller is activated to hold the position of the system, between A and F, the surgical drill is turned on and off with different rotational velocities in three steps: 1) At B: drill tip rotates at the maximum velocity of 42000 RPM clockwise, 2) At C: drill tip rotates at the maximum velocity counter clockwise, 3) From D to E: drill tip rotates clockwise with variable velocities.

Test 1-4: Complete temporal bone drilling condition is simulated in this test. Like the standard test Test 1-1, the system is held in the desired position. A part of prototyped physical model of bony structures is placed beneath the drill tip and moved upward while the drill is on and drill tip rotates at maximum velocity of 42000 RPM. The drilling condition is therefore simulated and the impact of the contact forces on the system can be studied.

The results of this test are shown in Figure 25. The system is held in its position between A and D, and the physical model is drilled between B and C. Compared to the standard test, more oscillations occur in the angular position due to the impact of contact forces on the system. These oscillations are especially evident in the yaw-rotation which is not controlled by the position controller, Figure 25.

From Figure 25, an oscillation in the values of Fx, Fy and roll-toque can be observed at A, which is the transient mode of position control. There is a short period in the begining of the surface contact test that values of forces and torques are similar to the standard test. In this short period, drill tip slides slightly on the suface of the physical model before starting the drilling procedure in a fixed position. During drilling process, the bony structure, which is under the drill tip, resists the drilling and downward movement of the drill tip. This will cause resistant contact forces in the positive Z direction. Because the controller applies Fz in the positive Z direction to overcome the gravity of the drill, the resistant contact forces in the positive Z direction are added to the controller force. Hence, the necessary force in the Z direction decreases and the controller applies less forces, since a part of system's gravity is compensated by the contact forces. This condition is similar to a box placed on a spring or on a table, while a portion of the box's gravity is compensated by the spring or table surface contact forces; hence, the hand should apply less upward forces to keep the box in its position. In addition, contact forces are not only in the Z

direction. Due to the spherical shape of drill tip there are forces in other directions that cause oscillation in the applied forces and torques of the controller, Fx, Fy, Fz, pitch-torque and roll-torque. Yaw-torque does not have this oscillation; since, controller does not apply any yaw-torque. While drilling, the drill tip goes inside the drilled hole. Contacting with the internal walls of this hole, causes sharp changes in the values of forces and torques, especially in pitch-torque and roll-torque. Going up and down in the drilling process this causes sharp changes in the values of Fz and increase the chance of contact with the internal walls of the hole.

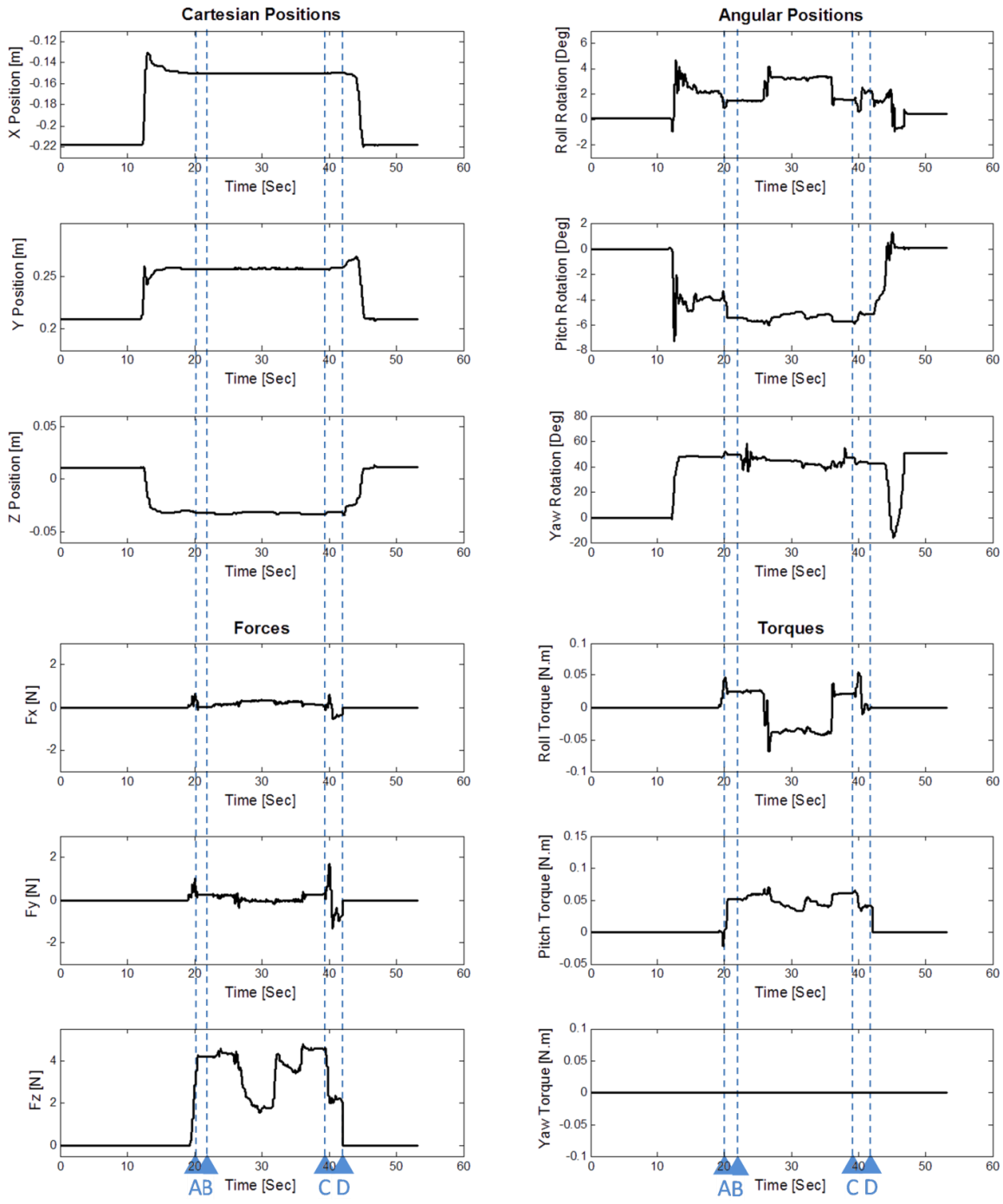

Figure 25: Results of Test 1-4. While the position controller is activated to hold the position of the system, between A and D, the physical model, which is placed beneath the drill tip, is moved upward and drilled, between B and C.

5.2.1. Summary

The results of four experimental tests of position control, especially the hand force test, show that the developed simulator is clearly stable in the anticipated temporal bone surgery simulated condition, and drill vibrations and physical model's drilling contact forces do not impact on the gross stability. According to Table 1, in the operating position:

- The maximum continuous applied Fx and Fy can be 10.48 N and the peak applied Fx and Fy can be 19.71 N. According to Figure 21, Figure 22, Figure 24, and Figure 25, the applied Fx and Fy by the controller are considerably less than the maximum applicable values. The maximum required Fx or Fy is less than 30% of the maximum continuous applicable values. The maximum continuous applied Fz can be 7.67 N and the peak applied Fz can be 13.94 N. According to Figure 21, Figure 22, Figure 24, and Figure 25, the applied Fz by the controller in all tests is less than 6 N. Especially in the fourth test, which closely resembles the desired simulator conditions, the maximum Fz is about 5 N. Only in the second test, which includes the random disturbances by the operator's hand movement, does the value of Fz rise to more than 7 N. Although, this is an unusual condition and the values of Fz oscillate highly; however, still they do not reach to the peak value, 13.94 N.
- The maximum continuous applied torques can be 0.948 Nm and the peak values can be 1.72 Nm. In all tests, as shown in Figure 21, Figure 22, Figure 24, and Figure 25, the system requires less than the maximum allowed values.

Consequently, all the applied forces and torques are less than the maximum continuous applicable forces and torques of the device, especially in the fourth test which closely resembles the desired simulator conditions. In addition, the forces and torques applied by the controller have sufficient safety margins to remain in the haptic device's operational range. Just in the

unusual condition of the second test, the system exceeds the maximum continuous capabilities; however, it still does not reach the peak capabilities and system appears stable and continues the procedure in all tests.

The most important situations are: changes in the rotational direction of the drill tip, contact force between the drill tip and the drilled hole's wall, sharp changes in the value of Fz due to sudden upward movements of operator's hand, and sudden changes in tissue density and related resistance forces.

5.3. Studying the Effect of the Gripper Gravity Compensation program

In order to prove the effect of the performed actions for compensating the gripper's gravity, two set of experiments are designed. In real surgery, surgeons just feel the weight of the drill and its attachments such as power and control cables and the irrigation tubing. The designed simulator should have the same conditions, so the gravity effects of the gripper, handle and other parts of the system excluding the drill, should be cancelled as much as possible. Therefore, the impact of the gravity of gripper, handle and links on the reality of the simulated surgery is compensated. Two set of tests are designed to show the efficiency of this process. In these tests, the surgical drill is separated from the gripper and removed from the system. In this condition, when significant external forces, such as operator's hand forces and not the system's gravity, moves the new system, which is simulator without the drill, to a new position and then releases it, system should hold its new position until another significant external force changes the gripper's position. The position control is not activated in these experiments. Required forces and torques are calculated by the gripper gravity compensation program and commanded to the motors through open loop force control scheme.

Test 2-1: This test consists of two parts, Figure 26. In the first part, A to D, the gripper is placed on top of a box, between A to B, and the box is moved upward, between B and C, in the positive Z direction until reaching to a desired point, Figure 27-a. At that point the box is stopped and then separated from the gripper. In other words, the box goes downwards while the gripper is held in its position. The simulator should hold the gripper in its position at the desired point, from C to D, Figure 27-b. Then gripper is moved and placed on top of the box again for the second part of the test.

In the second part of the test, from E to G, the box suddenly is removed from the bottom of the gripper, F, while the gripper is not moving. The gripper should not fall down and the simulator should hold the gripper's position between F and G.

The results for this test are shown in Figure 26. The procedure of the test and the constant forces and torques during the test, A to G, can be observed.

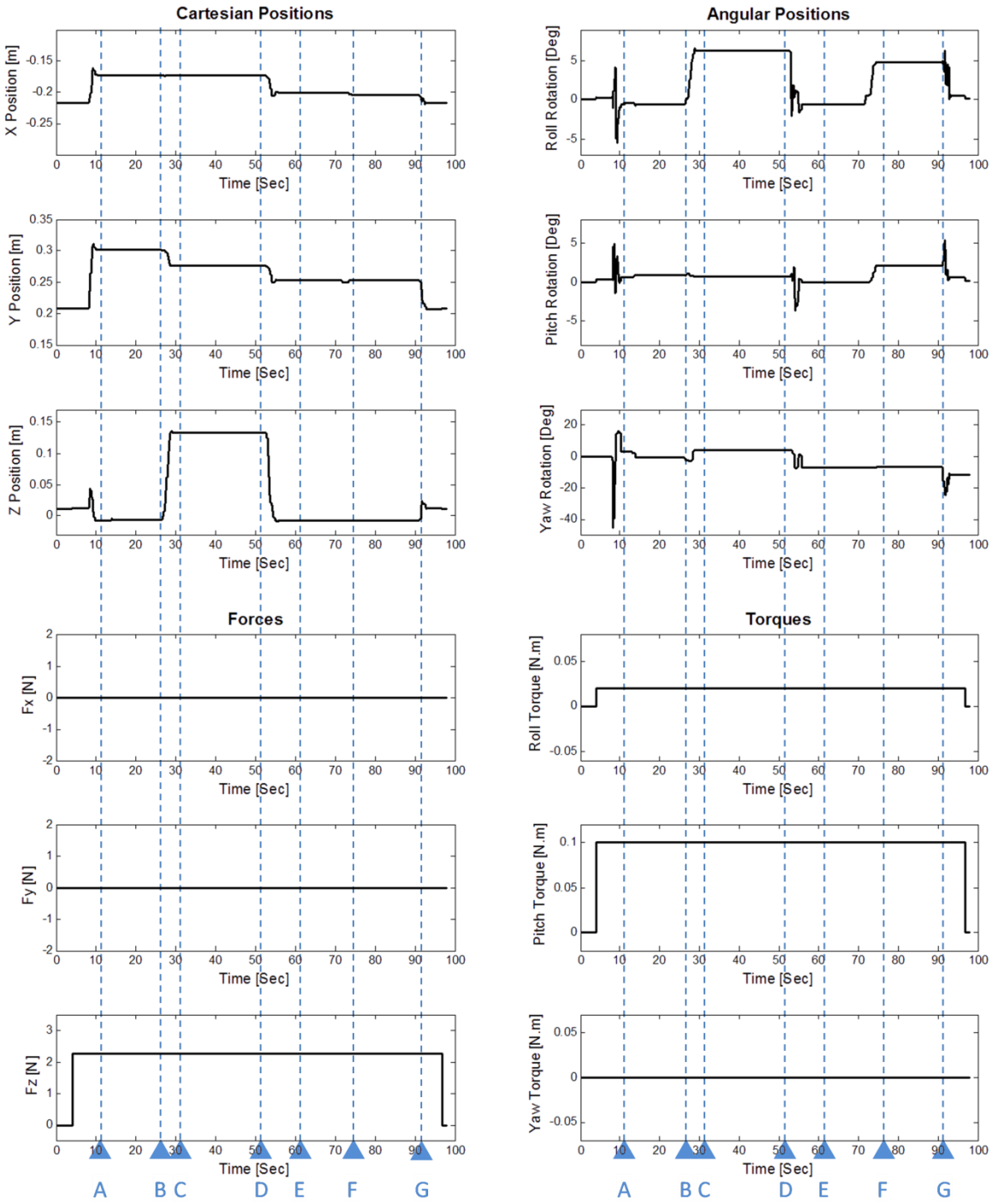

Figure 26: Results of Test 2-1. Test consists of two parts: 1) Gripper is placed on top of a box, from A to B. The box is moved upward, between B and C. At C, the box is stopped and removed. Simulator holds the gripper in that position from C to D. 2) Gripper is placed on top of the box, at E. At F, box is suddenly removed from the bottom of the gripper. The simulator holds the grippers position and the gripper does not fall down from F to G.

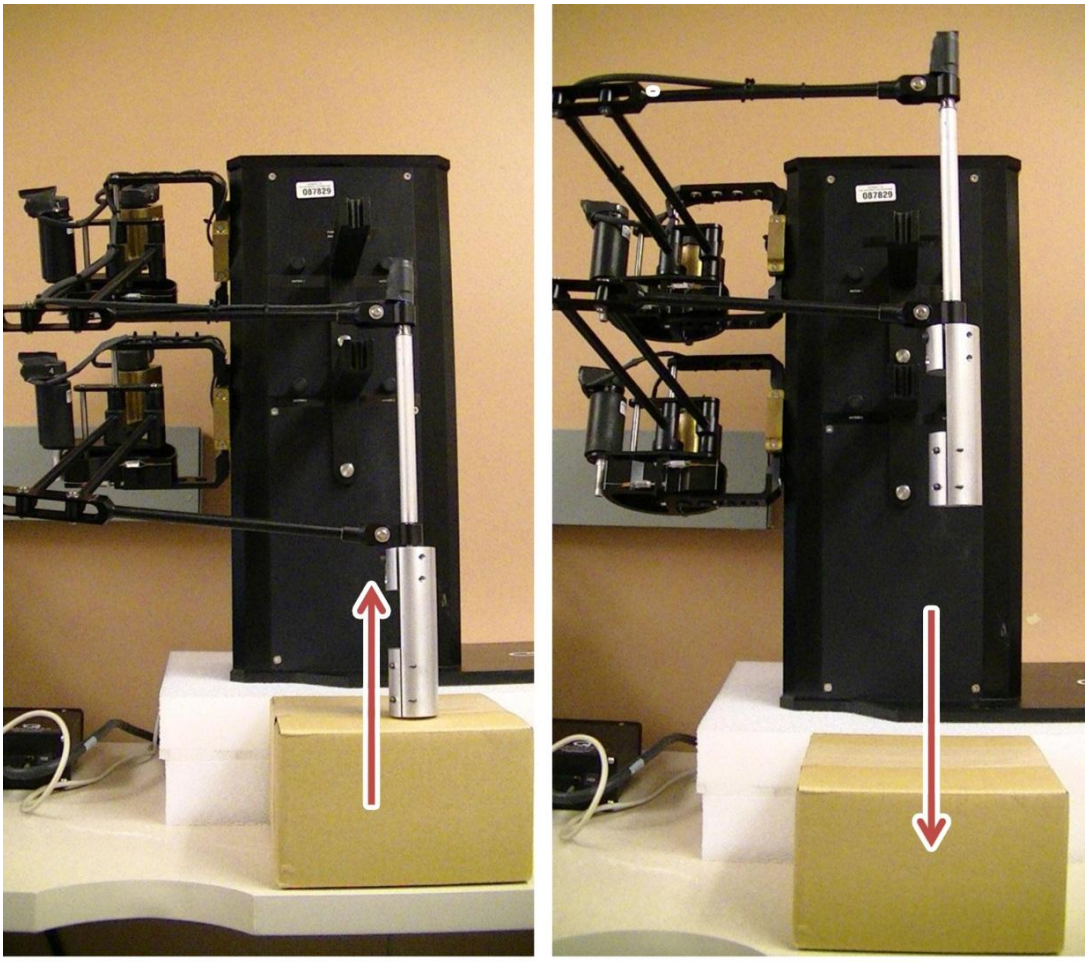

(a) (b)

Figure 27: Box movement in the first part of Test 2-1. a) The gripper is placed on top of a box and the box is moved upward in the positive Z direction until reaching to the desired position. b) At that position the box is stopped and then removed, goes down. The simulator should hold the gripper's in the desired position.

Test 2-2: In this test the operator moves the gripper to four different positions according to Figure 28, the first and fourth positions are close to each other and the operator releases the gripper to see if the system can hold its position in each of them or not. These points are chosen to represent the workspace. Next, when the gripper's position is held in the fourth desired point, gripper gravity compensation program is turned off and the system falls down quickly as long as near the border of the robot workspace operator catches the gripper.

Results of this test are shown in Figure 29. The gripper is held in four positions:

- Position one from A to B
- Position two from C to D
- Position three from E to F
- Position four from G to H

Then compensating gripper's gravity program is turned off at H, and the system falls down quickly. This sharp movement is clear in the Y position plot of Figure 29. Forces and torques are constant until the gripper gravity compensation program is activated, from A to H. Then forces and torques become zero when the gripper gravity compensation program is turned off.

Figure 28: Four different positions of Test 2-2, which represent the workspace: a) First and forth positions, they are close to each other. b) Second position. c) Third position.

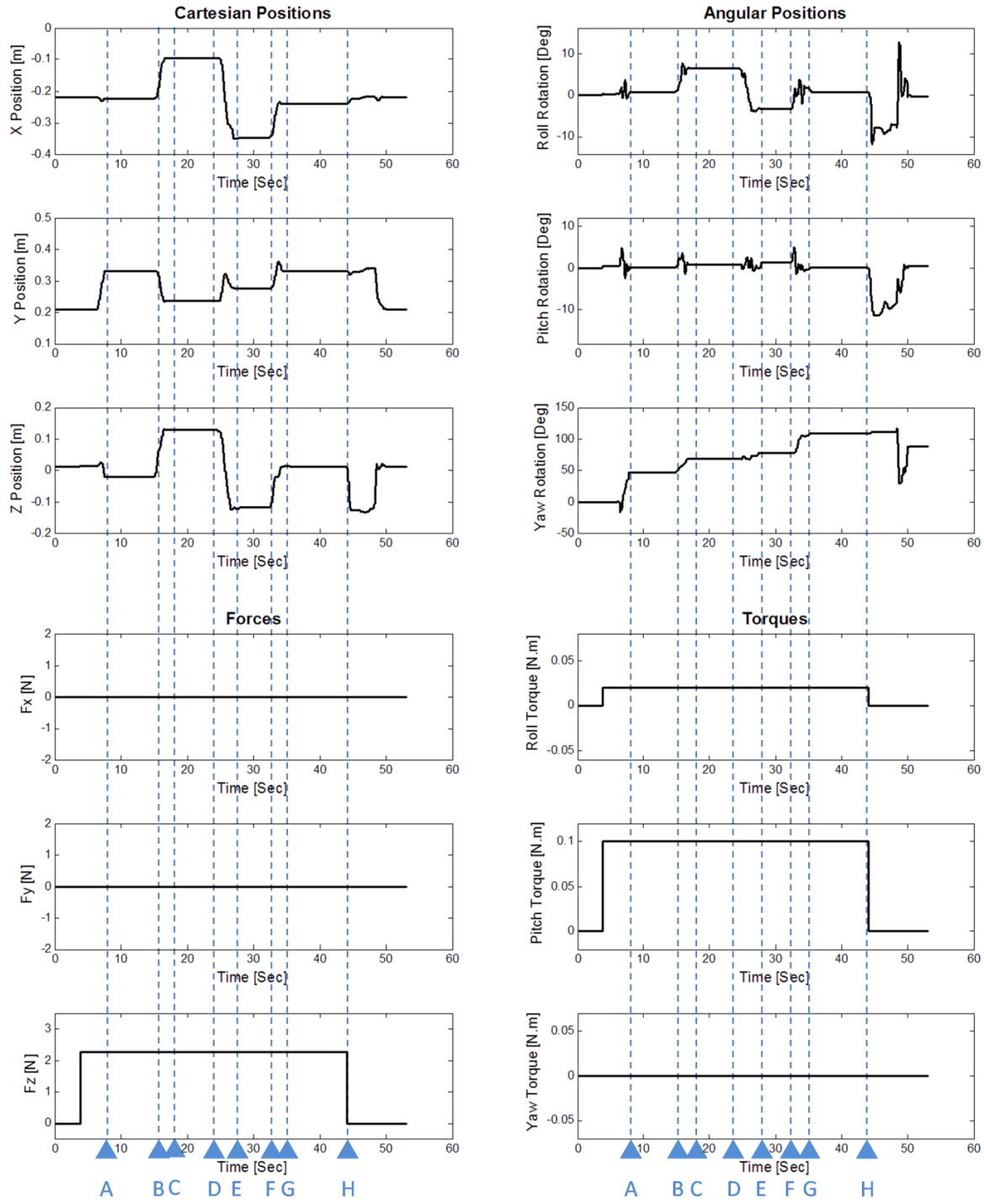

Figure 29: Results of Test 2-2. The gripper is moved to four different positions and released in each position for short period. In each of these periods the simulator should hold the gripper's position. These periods are: A to B at first position, C to D at second position, E to F at third position, from G to H at fourth position. From H, the gripper gravity compensation program is turned off, the system falls down quickly and the values of forces and torques go to zero.

5.3.1. Summary

According to Figure 26 and Figure 29, the gripper gravity compensation program holds the position of the simulator, when the drill is removed and there are no external forces. In both tests the values of the forces and torques are less than the maximum continuous applicable forces and torques of the device, and the applied forces and torques allow significant margins of error, remaining well within the device's limitations. Also, the system appears stable and continues its procedure.

5.4. Studying the Impact of the Gripper Gravity Compensation program on the Performance of the System in the Force Control Mode

After investigating the effectiveness of the gripper gravity compensation program, the impact of this program on the performance of the system in the simulation condition, which is temporal bone surgery, should be studied. In this section three tests are designed to evaluate the functionality of the system when the gripper's gravity effects are compensated and the drill is added to the system.

Test 3-1: In this test, the operator is asked to hold the surgical drill similarly to a real surgery condition and then move the drill around the area that is needed for a regular temporal bone surgery. According to the surgeon's recommendations for human temporal bone surgery, a workspace of 20×20×20cm is an ideal space; since most of the surgeon's hand movements can be considered as wrist related movements. During these movements the gripper gravity compensation program is activated and the haptic device applies the force and torques, which are commanded by the open loop controller.

The results of this test are shown in Figure 30. The operator's surgery simulated hand movement, wrist related movements, causes oscillations which are changes in position. These oscillations are clear in the Z position plot in Figure 30. Forces and torques are constant until the gripper gravity compensation program is activated between A and B.

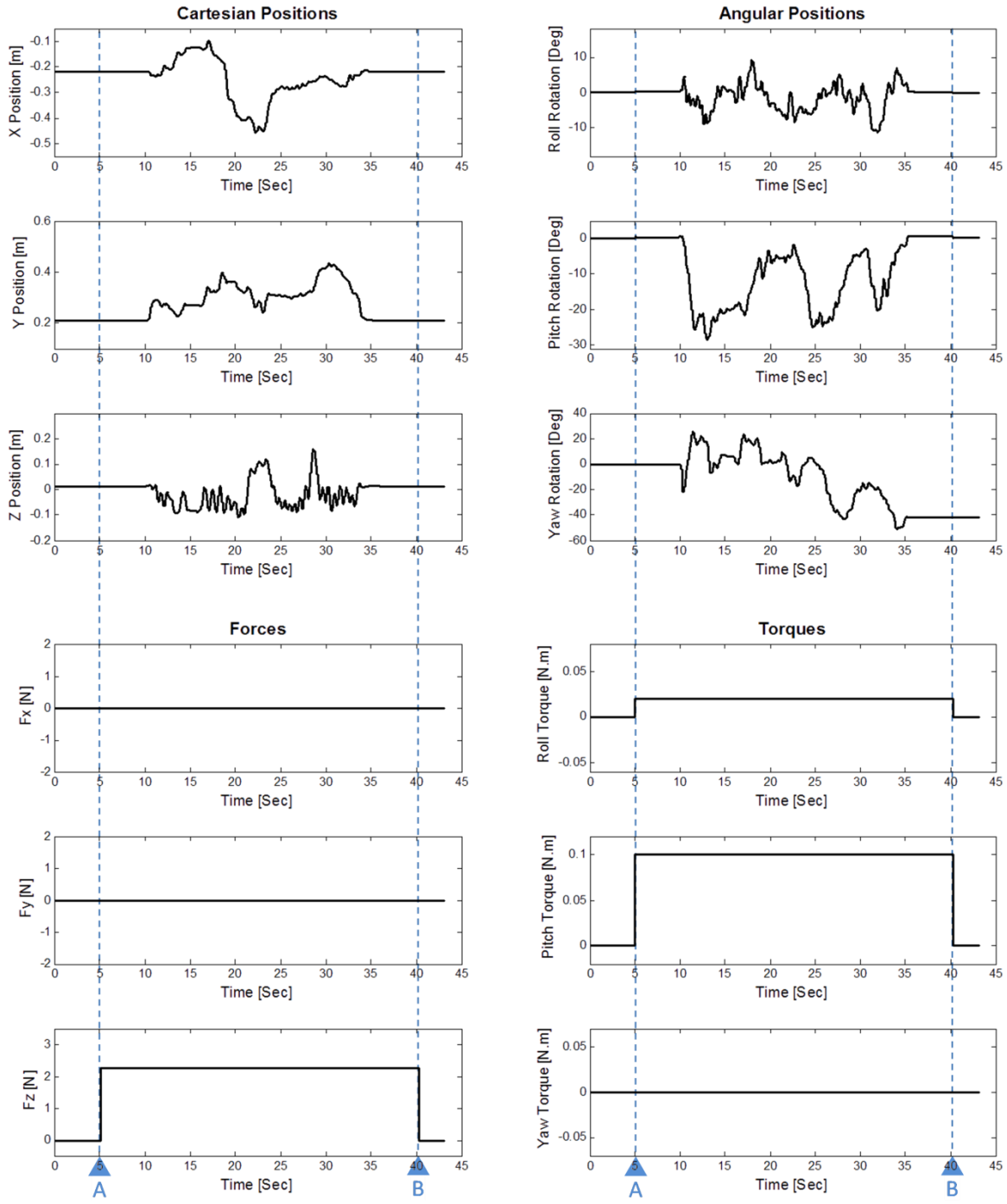

Figure 30: Results of Test 3-1. The drill is added to the haptic device. Operator is asked to hold the surgical drill and move it around the expected surgery workspace, while the gripper gravity compensation program is activated between A and B.

Test 3-2: In this test, in addition to previous test, while operator holds the surgical drill similar to a real surgery, the drill is turned on and drill tip rotates between B and C. The objective of this test is to study the impact of the drill's vibration on the simulator while the gripper gravity compensation program is activated and the haptic device applies the forces and torques which are commanded by the open loop controller.

The results of this test are shown in Figure 31. Very low amplitude oscillations in the values of the Cartesian and angular positions in Figure 31 are the result of the combination of drill vibration and the operator's hand movements; the drill vibration is the most significant contributor. Red rectangle in Figure 31 indicates sample parts of these very low amplitude oscillations, which are expanded in Figure 32. These oscillations are clear in the Z position and roll-rotation plots in Figure 31. Forces and torques are constant during the test, while the gripper gravity compensation program is activated, between A and D.

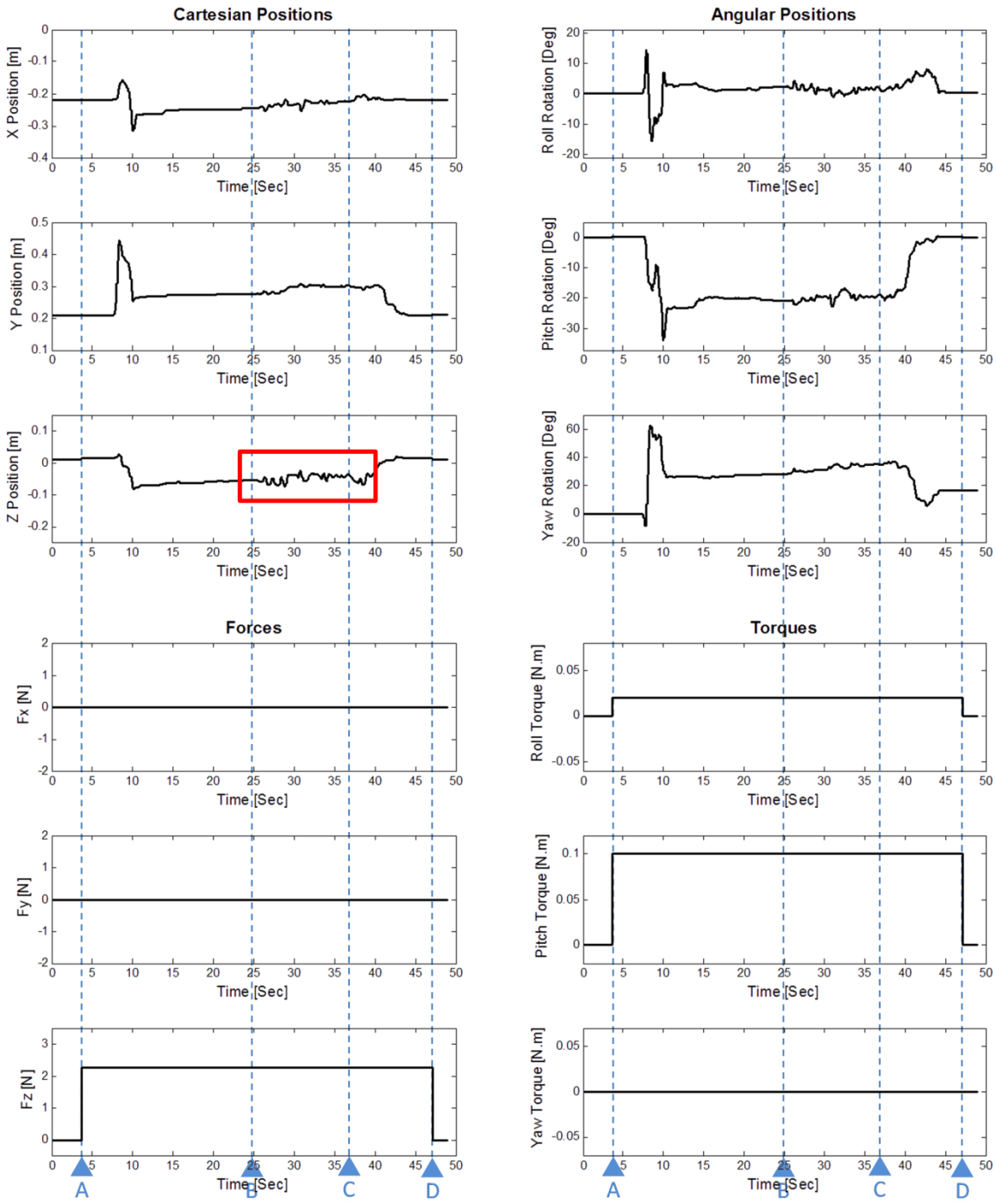

Figure 31: Results of Test 3-2. The drill is added to the haptic device. Operator holds the surgical drill, while the drill is turned on and drill tip rotates between B and C. Gripper gravity compensation program is activated between A and D. Red rectangle indicates sample parts of drilling vibration.

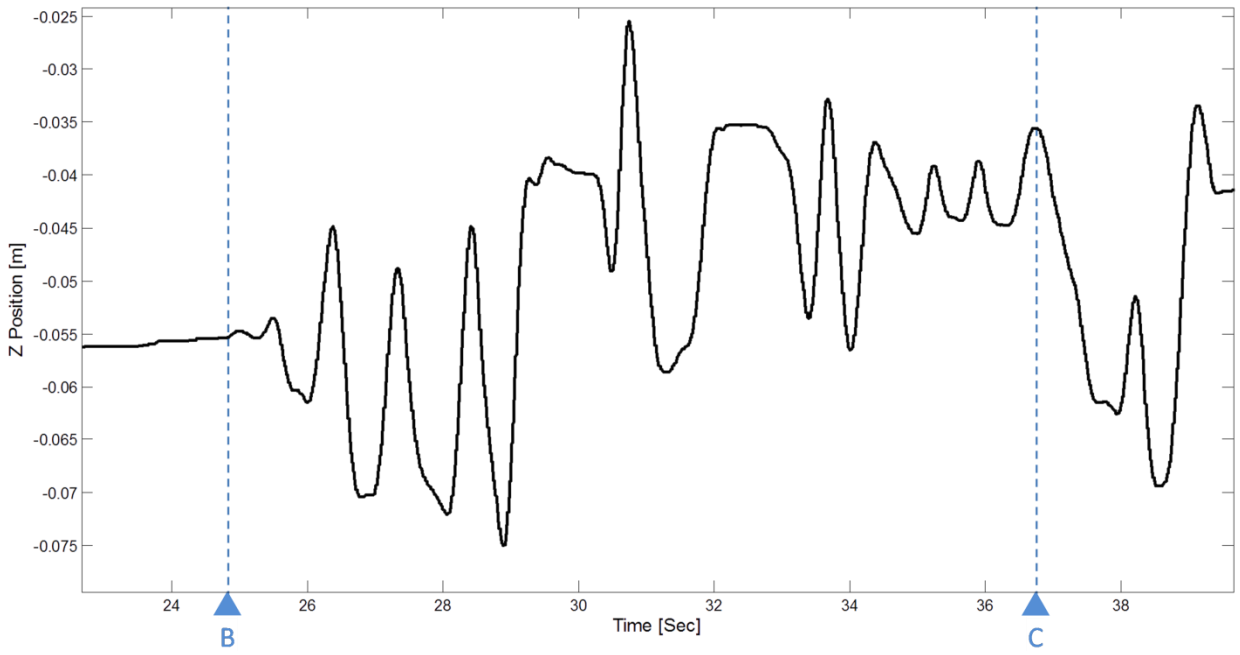

Figure 32: The Z direction position changes during the drilling vibration of Test 3-2, between B and C. The frequency of the measured data is equal to the frequency of the driver, which is 1 kHz.

Test 3-3: In this test the complete surgery condition is simulated. The operator holds the surgical drill similarly to a real surgery, the drill is turned on and the operator drills the prototyped physical model of the bony structures between C and E. The objective of this test is to study the effectiveness and impact of the gripper gravity compensation program when the complete surgery condition is simulated.

The results of this test are shown in Figure 33 and Figure 34. Red rectangle in Figure 33 indicates sample parts of the drilling process, which are expanded in Figure 34. Low amplitude oscillations can be seen in Figure 33 and Figure 34 due to the drilling contact forces. At D, the operator finishes the drilling of an area on the physical model and moves the drill to another area to continue the process. This movement, which consists of bringing up the drill shortly in the Z direction and moving along the X and Y directions, is distinct in Figure 33 and Figure 34. Also, moving the drill to the desired point for drilling causes sharp and short period changes in the

values of Cartesian and angular positions at the beginning of the test, at B. Forces and torques are constant during the test, while the gripper gravity compensation program is activated, between A and F.

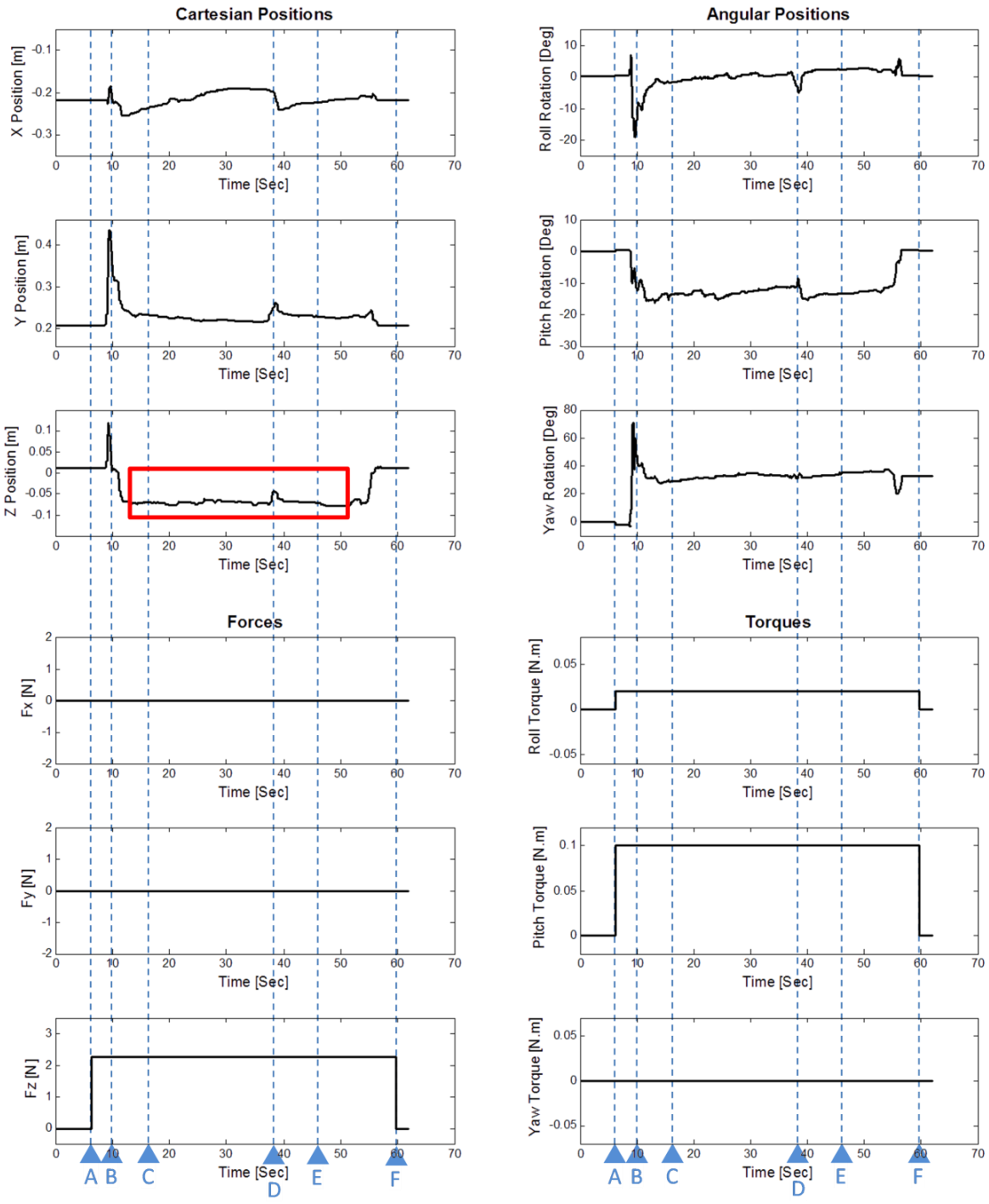

Figure 33: Results of Test 3-3. Drill is added to the haptic device. At B, operator moves the system from home position to the desired position. Operator holds the surgical drill, while drilling prototyped physical model of bony structures between C and E. At D, the operator finishes the drilling of an area of the physical model and moves the drill to another area to continue the process. The gripper gravity compensation program is activated between A and F. Red rectangle indicates sample parts of the drilling process.

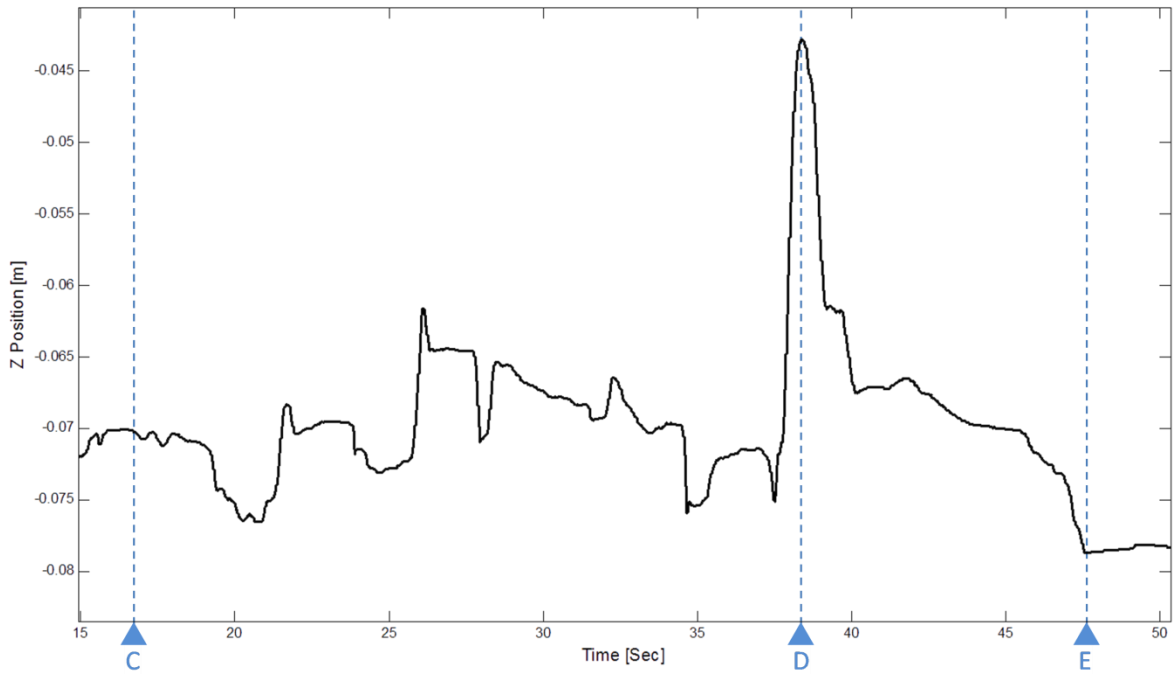

Figure 34: The Z direction position changes during the drilling process of Test 3-3, between C and E. At D, the operator finishes the drilling of an area of the physical model and moves the drill to another area to continue the process. The frequency of the measured data is equal to the frequency of the driver, which is 1 kHz.

5.4.1. Summary

As depicted in Figure 30, Figure 31, and Figure 33, the gripper gravity compensation program does not causes any instability in the operation of the developed simulator when simulator is equipped with the surgical drill and there are external forces such as operator's hand forces. The system appears stable and there is no system instability because of continuous oscillations or large amplitude vibrations. In all tests, the values of the forces and torques are less than the maximum continuous applicable forces and torques of the haptic device and the applied forces and torques have sufficient secure borders from devices' limitations. Because these tests are done in an open loop force control mode, the contact forces of drilling process in the third test do not change the applied forces by the haptic device.

5.5. Determination of Simulator Applicable Workspace

The objective of this experiment is to determine and study the simulator workspace where the gripper gravity compensation program can work properly. Four sets of experiments in two tests are designed. In the first test, the drill is moved around a 20×20×20cm area which is the expected area for the temporal bone surgery. In the second test, the next three experiments, the drill is moved along the X, Y, and Z directions, one direction in each experiment, to determine the maximum applicable workspace in each of these directions.

Test 4-1, Expected temporal bone surgery workspace: In this test, the operator holds the surgical drill similar to a real surgery and moves the drill around the area that is needed for a regular temporal bone surgery. Comparing to Test 3-1, in this test a more accurate workspace is chosen. In Figure 35, a box that has a volume similar to the expected temporal bone surgery, 20×20×20 cm, simulates the surgery workspace. The gripper gravity compensation program is activated between A and K, and the operator moves the drill to nine positions. Hence, the drill tip is placed at nine sample positions of the chosen workspace, eight vertexes and center of the cube box, B to J in Figure 36.

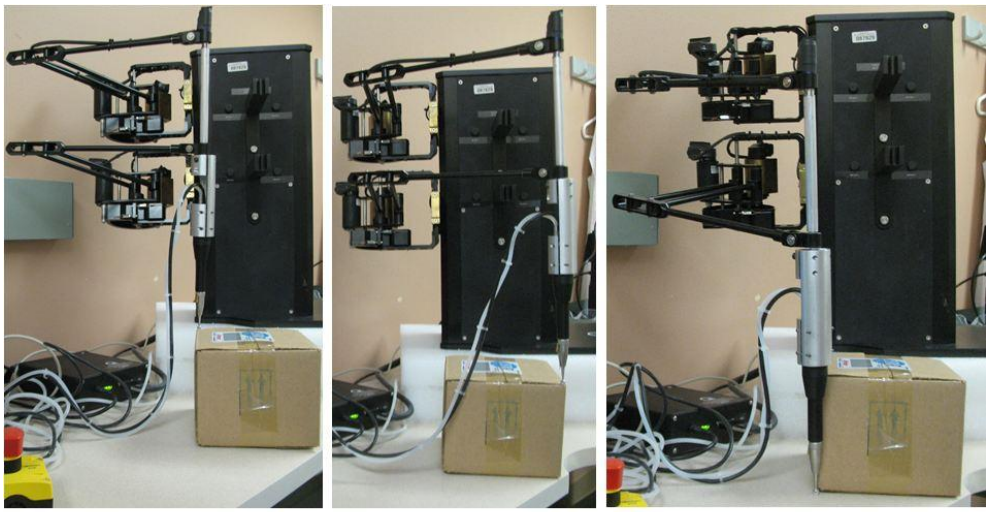

(a) (b) (c)

Figure 35: Simulated temporal bone surgery workspace in Test 4-1. A box which has a volume similar to the expected temporal bone surgery, 20×20×20 cm, simulates the surgery workspace. The drill tip is placed at nine sample positions of the chosen workspace, eight vertexes and center of the cube box. Three vertexes sample positions are shown.

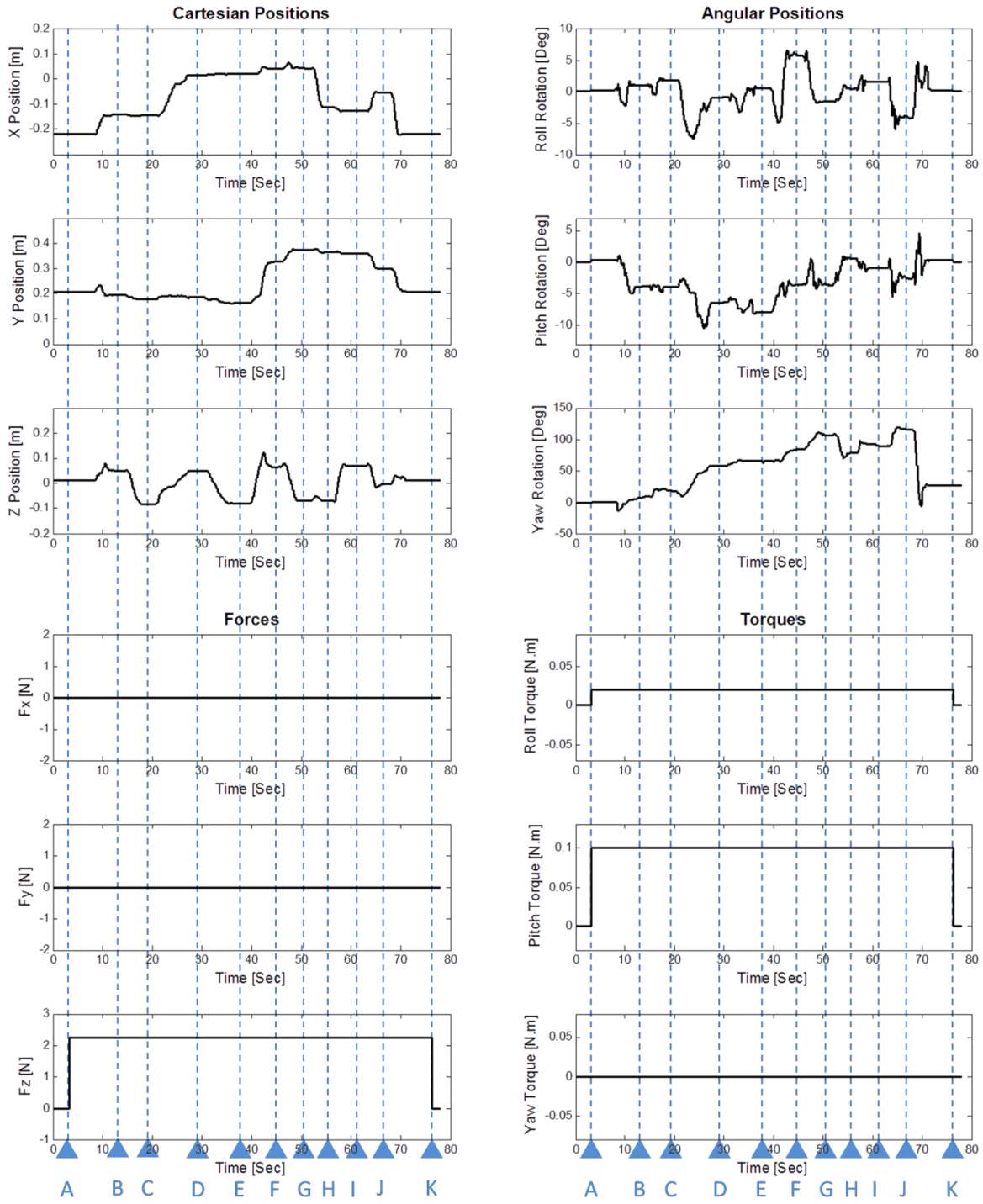

Figure 36: Results of Test 4-1. Operator holds the surgical drill and moves the drill around the workspace which is needed for a regular temporal bone surgery, 20×20×20 cm. This workspace is simulated by a cube box. Operator moves the drill to put the drill tip next to eight vertexes and center of the cube box, B to J. Gripper gravity compensation program is activated between A and K.

The results of this test are shown in Figure 36. In nine short period intervals, the Cartesian and angular positions are fixed, B to J. They are the periods that drill tip is place at the nine sample position of the chosen workspace, eight vertexes and center of the cube box. These nine short period intervals can be easily distinguished in plot Z and roll-rotation in Figure 36. Sharp changes in the values of the positions between each of these intervals are due to the drill movement to a new sample position by means of the operator.

Test 4-2, maximum applicable workspace: In addition to previous test, the objective of this test is to determine the maximum applicable workspace, which is larger than the surgical workspace, while the gripper gravity compensation program can still be activated without any problem.

In experiment1-Figure 37, maximum applicable workspace in the X direction is explored. The gripper gravity compensation program is activated between A and F in Figure 37. The operator holds the surgical drill and moves it along the X direction from B to E in Figure 37, with an almost constant velocity. The surgical drill reaches the lowest value of the X direction workspace, -43 cm at C, and reaches the highest end of the X direction workspace, 15 cm at D.

In experiment2-Figure 38, the maximum applicable workspace in the Y direction is explored. The gripper gravity compensation program is activated between A and F Figure 38. The operator holds the surgical drill and moves it along the Y direction from B to E in Figure 38, with an almost constant velocity. The surgical drill reaches the lowest end of the Y direction workspace, 18 cm at C, and reaches the highest end of the Y direction workspace, 51 cm at D.

In experiment3-Figure 39, the maximum applicable workspace in the Z direction is explored. The gripper gravity compensation program is activated between A and F in Figure 39, while the operator holds the surgical drill and moves it along the Z direction from B to E in Figure 39, with

an almost constant velocity. The surgical drill reaches the highest end of the Z direction workspace, 27 cm at C, and reaches the lowest end of the Z direction workspace, -24 cm at D. All these position values are in HD^2 space coordinates. In all of the three experiments of Test 4-2, oscillations in the values of roll-rotation and pitch-rotation are due to the operator's hand movements.

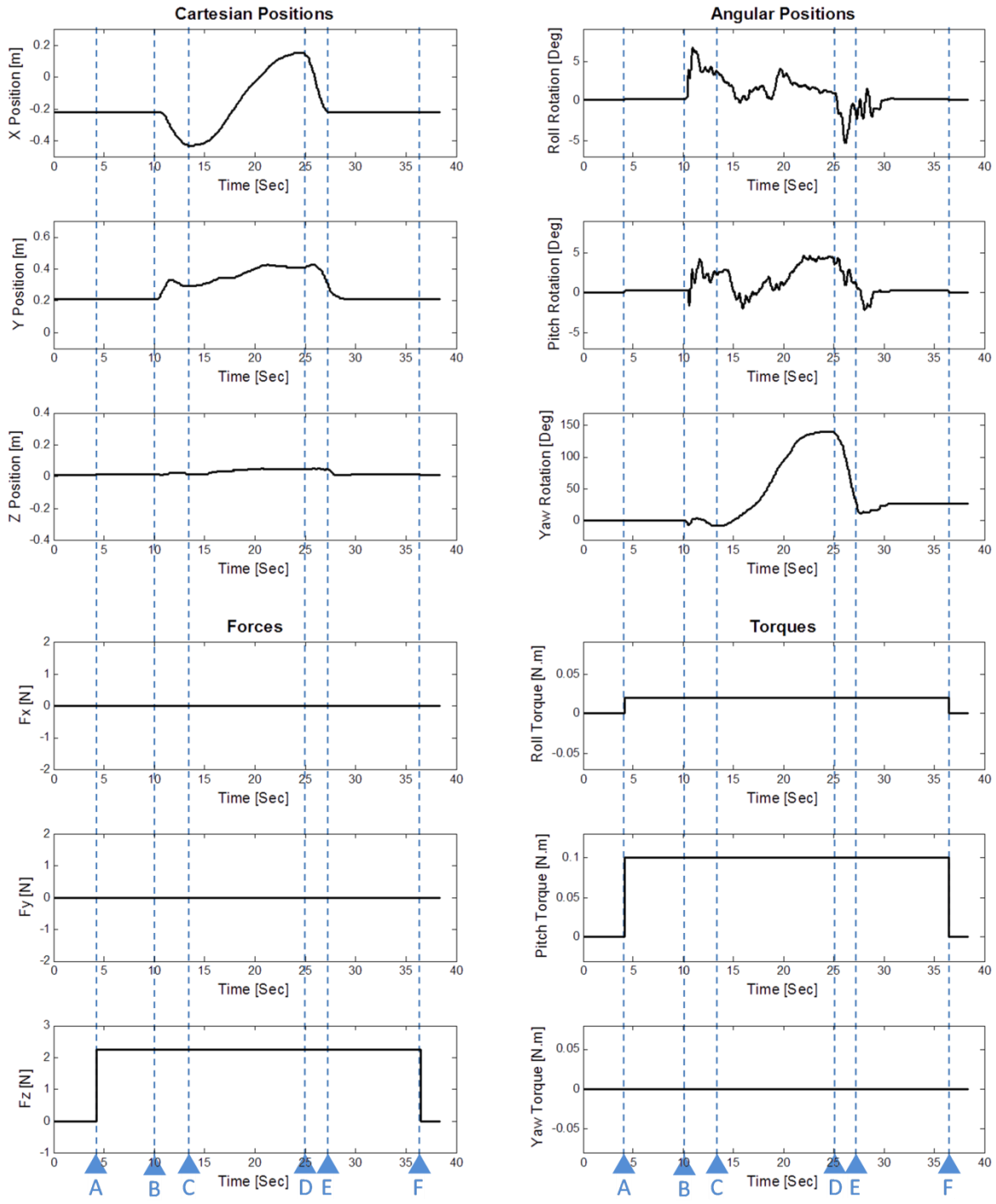

Figure 37: Results of test 4-2, experiment 1: Maximum applicable workspace in the X direction. The gripper gravity compensation program is activated between A and F. The operator holds the surgical drill and moves it along the X direction from B to E, with an almost constant velocity. Surgical drill reaches the lowest value end of the X direction workspace, -43 cm, at C, and reaches the highest value end of the X direction workspace, +15 cm, at D.

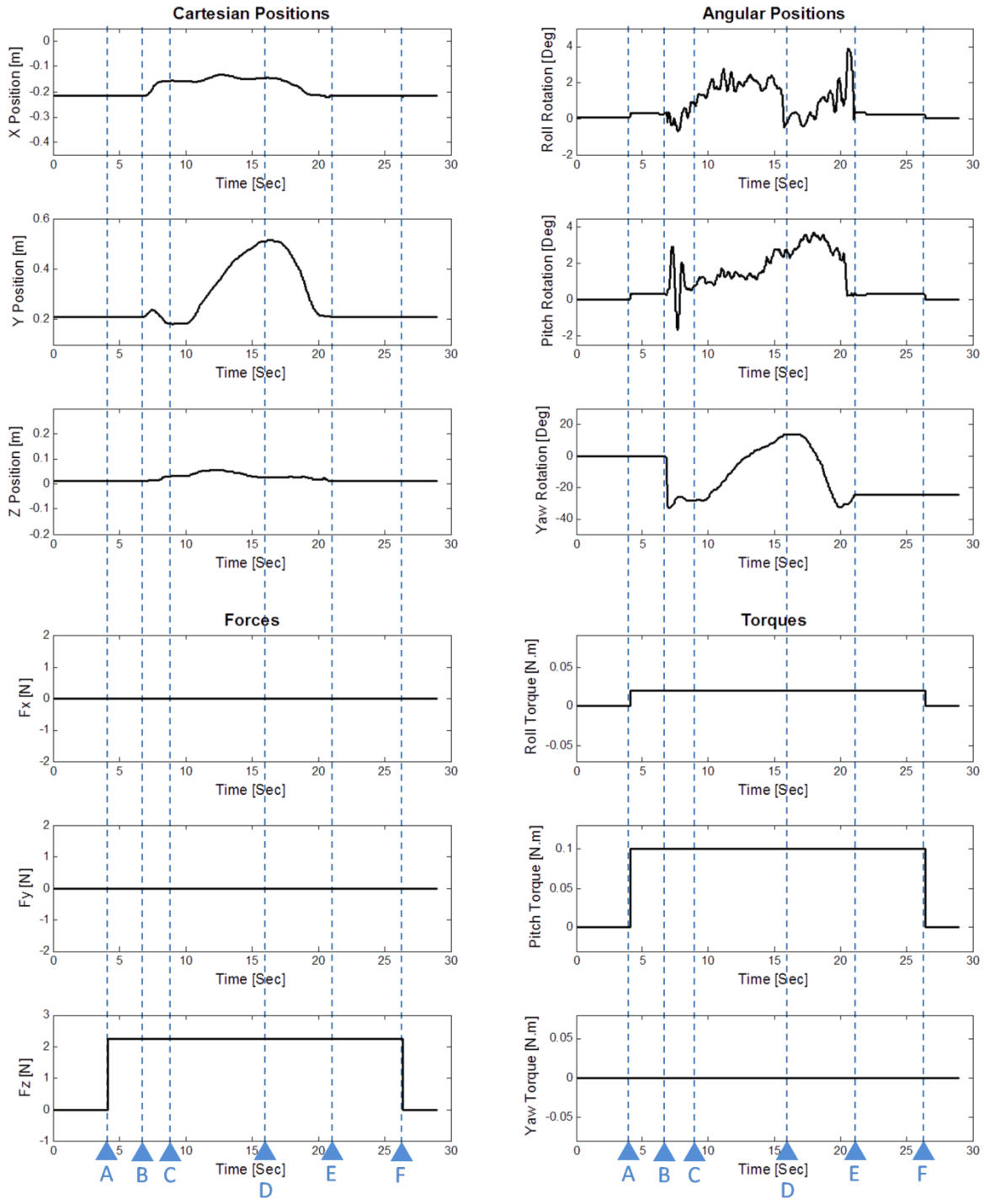

Figure 38: Results of Test 4-2, experiment 2. Maximum applicable workspace in the Y direction. The gripper gravity compensation program is activated between A and F. Operator holds the surgical drill and moves it along the Y direction from B to E, with an almost constant velocity. Surgical drill reaches the lowest value end of the Y direction workspace, 18 cm, at C, and reaches the highest value end of the Y direction workspace, 51 cm, at D.

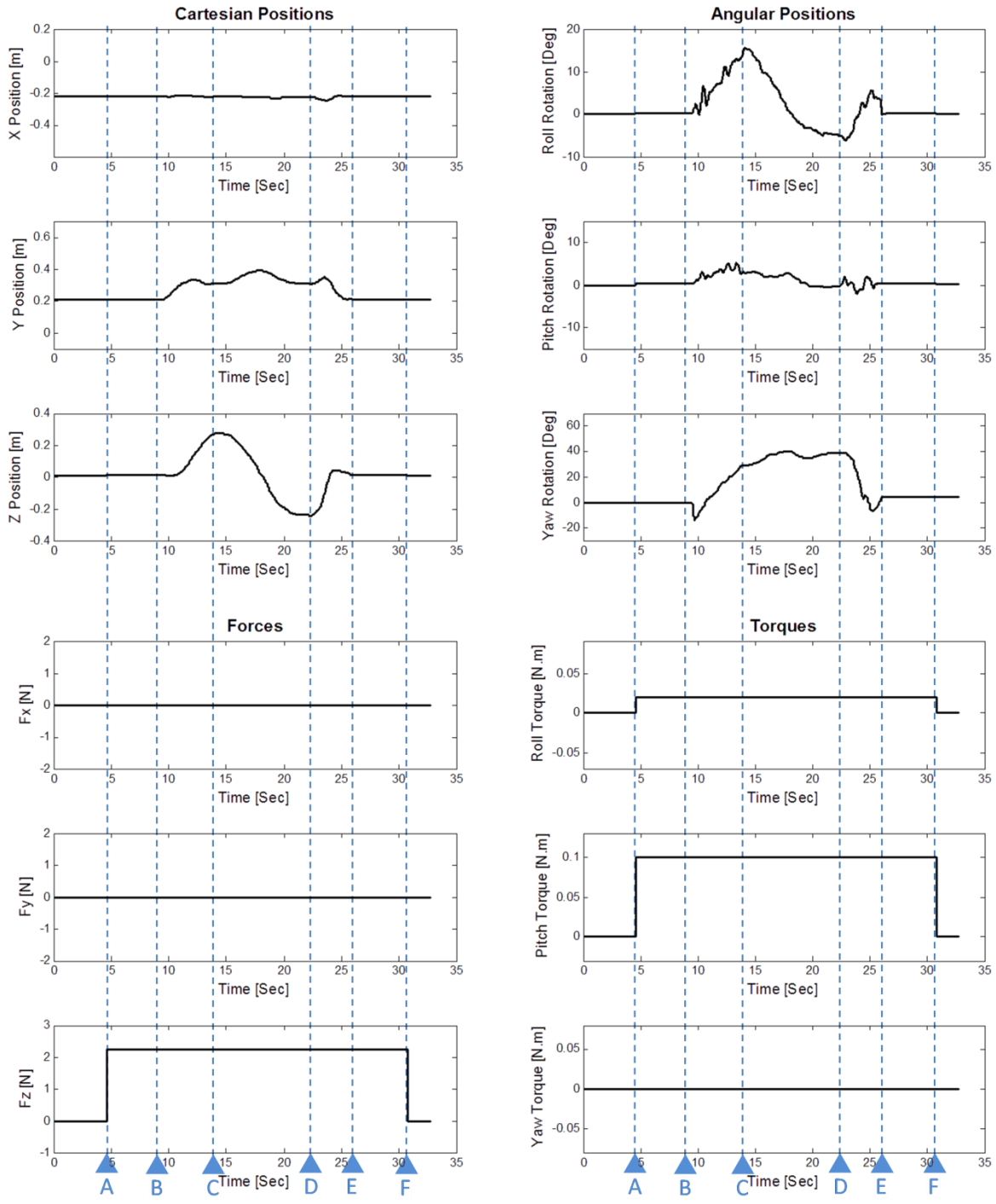

Figure 39: Results of Test 4-2, experiment 3. Maximum applicable workspace in the Z direction. The gripper gravity compensation program is activated between A and F. Operator holds the surgical drill and moves it along the Z direction from B to E, with an almost constant velocity. Surgical drill reaches the highest value end of the Z direction workspace, 27 cm, at C, and reaches the lowest value end of the Z direction workspace, -24 cm, at D.

5.5.1. Summary

Depicted in Figure 36, while the gripper gravity compensation program is activated, the system appears stable in the expected temporal bone surgery workspace, which can be considered as a $20 \times 20 \times 20$ cm area. Also, it is shown that gripper gravity compensation program can be effective in a larger workspace. In all these workspaces the system appears stable and there is no system instability because of continuous oscillations or large amplitude vibrations. The values of the forces and torques are less than the maximum continuous applicable forces and torques of the haptic device.

5.6. Implementing the Virtual Soft Tissue Model - Virtual Reality Experiment

In this experiment the presented virtual soft tissue model in the section 2.3.1, is implemented in the device workspace. Regarding Figure 40, the soft tissue is applied in the area between two planes, parallel to the X-Y plane and separated by 15 cm. When the virtual soft tissue is activated while the simulator's drill tip is inside this area (Figure 40) the operator can feel the forces and torques which he/she would feel during the real contact of drill tip with the modeled soft tissue. The soft tissues in real temporal bone surgeries are so much thinner than 15 cm. The objective of this test is to study the behaviour of the system in a much thicker virtual soft tissue area. Two sets of tests are designed to study the behavior and performance of the system when the gripper gravity compensation program and the virtual soft tissue model both are activated. The desired soft tissue model forces and torques are combined with the constant forces and torques of the gripper gravity compensation program; hence, the haptic device's applied forces and torques are not constant.

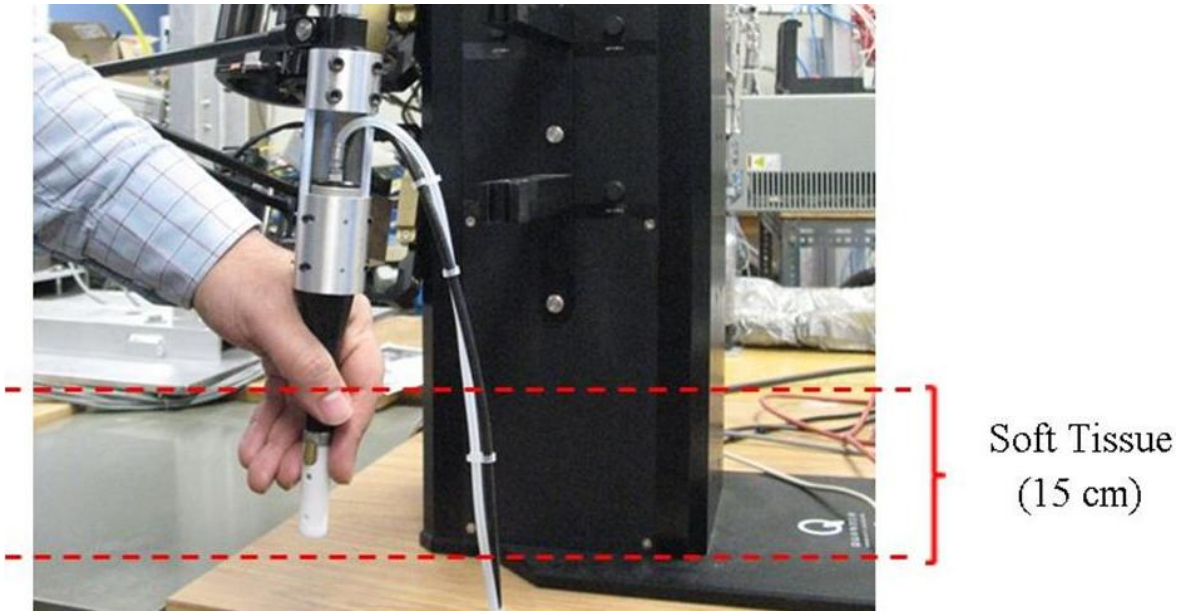

Figure 40: Virtual soft tissue Model Area: when the drill tip goes inside of this area, operator feels the tissue model forces.

Test 5-1: It is a standard test to determine the performance of the system while soft tissue model is applied. As shown in Figure 40, there is virtual soft tissue model rendered in the desired area. As seen in Figure 41, the operator starts from the top free area and brings down the drill. In the free area just the gripper gravity compensation program is activated. This downward movement continues until the drill tip reaches the top border of virtual soft tissue model area and goes inside the virtual soft tissue model area at B. At C, the drill tip passes the bottom border of virtual soft tissue model area. The operator moves the drill down a short distance and then starts the second movement. In the second movement, the drill is brought up in the same manner. The operator starts from the bottom free area and brings the drill up into the virtual soft tissue model area. At D, the drill tip passes the bottom border of virtual soft tissue model area. This upward movement continues until the drill tip passes the top border of virtual soft tissue model area and goes inside the top free area at E. This process is repeated three times in the standard test, which is clearly shown in the Z position plot in Figure 41.

The results of the test are shown in Figure 41. Red rectangles in Figure 41 indicate one process of insertion and retraction in the virtual soft tissue, which is expanded in Figure 23. The Z direction position changes and Fz values during the first process of Test 5-1, the red rectangle, are maximized in Figure 42. From the Fz plot of Figure 42, the changes in the forces, when the drill tip is inside the virtual soft tissue, can be observed. The gripper gravity compensation program is activated from A to F. Hence, in the periods that the drill tip is outside of the virtual soft tissue, for example from A to B, the values of forces and torques are constant at the values of the applied forces and torques for the gripper gravity compensation program, Fz= 2.25 N, pitch-torque= 0.1 Nm, and roll-torque= 0.02 Nm. In the remaining periods when the drill tip is inside virtual soft tissue model, the values of the forces and torques are changing. Low amplitude oscillations in the values of roll-rotation and pitch-rotation are due to the operator's hand movements.

According to the spring model part of the soft tissue model and the near constant velocity movement of the drill, while the drill tip is going down inside the virtual soft tissue for example from B to C, Fz has an almost linear increase until reaching the bottom border of the virtual soft tissue, Figure 42. According to section 4.1, the values of pitch-torque and roll-torque are changing along with the changes in the value of Fz. Reaching the bottom border of the virtual soft tissue; all these values have a sudden change to the constant values of the gripper gravity compensation program; since, the spring part's resistant force of the virtual soft tissue model is suddenly omitted.

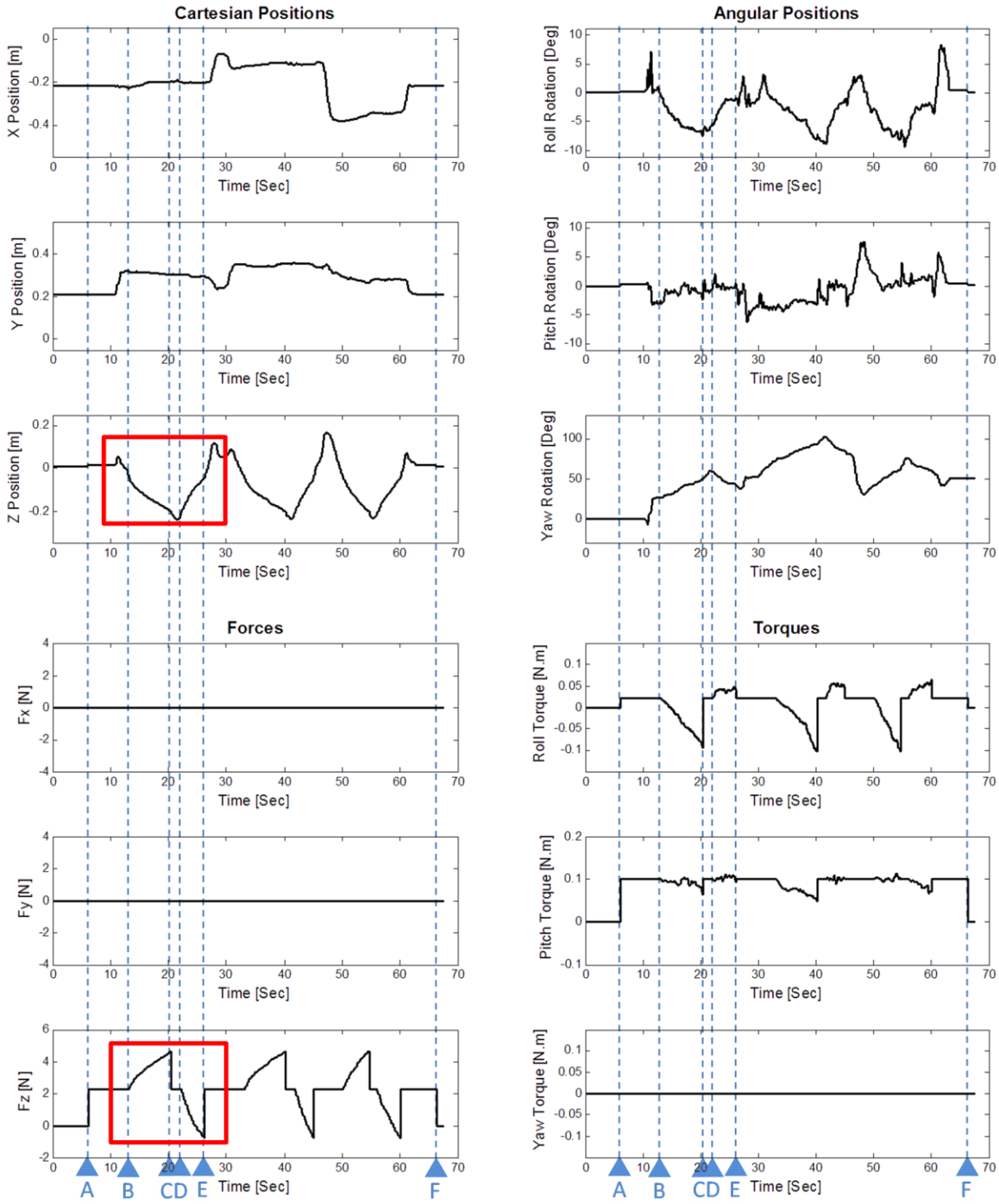

Figure 41: Results of Test 5-1. The gripper gravity compensation program is activated from A to F. In the first movement, operator holds the drill and starts from the top free area and brings down the drill. From B to C, the drill tip passes through virtual soft tissue and goes to the bottom free area at C. In the second movement, the drill is brought up. Drill tip passes through virtual soft tissue from D to E, and goes inside the top free area at E. This process is repeated three times. Red rectangles indicate one process of insertion and retraction in the virtual soft tissue.

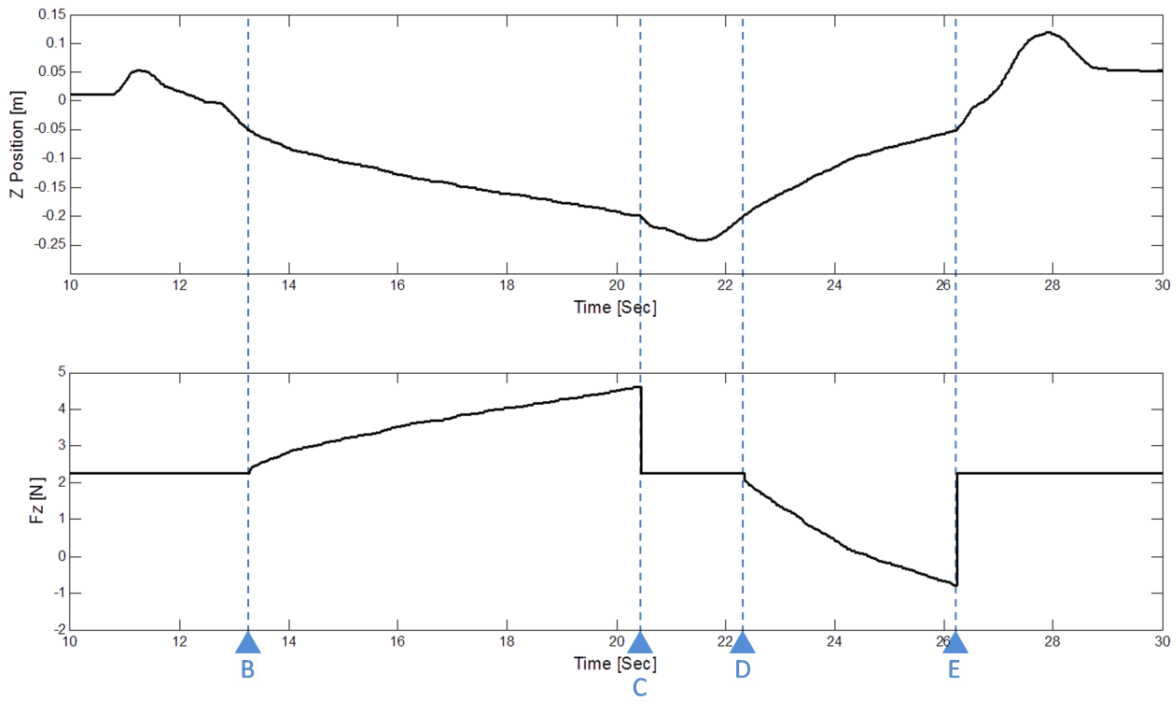

Figure 42: The Z direction position changes and Fz force values change during one process of insertion and retraction in the virtual soft tissue at Test 5-1. Insertion: From B to C, the drill tip passes through virtual soft tissue and goes to the bottom free area at C. Retraction: Drill tip moves up, passes through virtual soft tissue from D to E, and goes inside the top free area at E. Changes in the values of Fz based on the Z direction position, and sudden change in the value of Fz at C and E, are shown.

Conversely, while the drill tip is going up, as long as it is inside the virtual soft tissue for example from D to E; Fz has a near linear decrease till reaching the top border of the virtual soft tissue, Figure 42. According to section 2.3.1, in the applied virtual soft tissue model, the spring part is designed to resist against the downward movement of the drill tip after the drill tip passes the top border of the virtual soft tissue and goes down. Conversely, the spring part resists against the upward movement of the drill tip after the drill tip passes the bottom border of the virtual soft tissue and goes up. Hence, when the drill tip is going up, the spring's resistant force is negative, downward. This negative Fz is added to the constant gripper gravity compensation program force, Fz= 2.25 N; therefore, the values of Fz start decreasing from 2.25 N, until drill tip reaches to the top border of virtual soft tissue. This is because the soft tissue model forces are always

applied against the movement. Meanwhile, according to section 4.1, the values of pitch-torque and roll-torque are changing along with the changes in the value of Fz. Reaching the top border of the virtual soft tissue; all these values have a sudden change to the constant gripper gravity compensation program's values; since, the spring part's resistant force of the virtual soft tissue model is suddenly omitted.

In a real surgery, real soft tissues will have contact with the drill tip and apply the forces and torques to that point. A part of this research is to produce the modeled forces and torques of the soft tissue in the drill tip. These forces and torques are produced by the applied forces and torques of the haptic device in the HD^2 interaction point, which is in the center of the handle. Hence, according to section 4.1, the forces and torques, which should be felt in the drill tip, are applied in the center of the HD^2 handle and trasmitted to the drill tip. This force transmition needs certain torques to be applied by the haptic device, $\overrightarrow{T_t}$ in section 4.1. The applied soft tissue model is a one dimensional model which provides forces just in the Z direction, Fz. Certain torques, $\overrightarrow{T_t}$, should be applied by the haptic device to produce Fz in the drill tip. Consequently, while the drill tip is inside the virtual soft tissue, applied pitch-torque and roll-torque will be affected because of the trasmittion torques ,$\overrightarrow{T_t}$, Figure 43, although the soft tissue model is a one dimensional model in the Z direction.

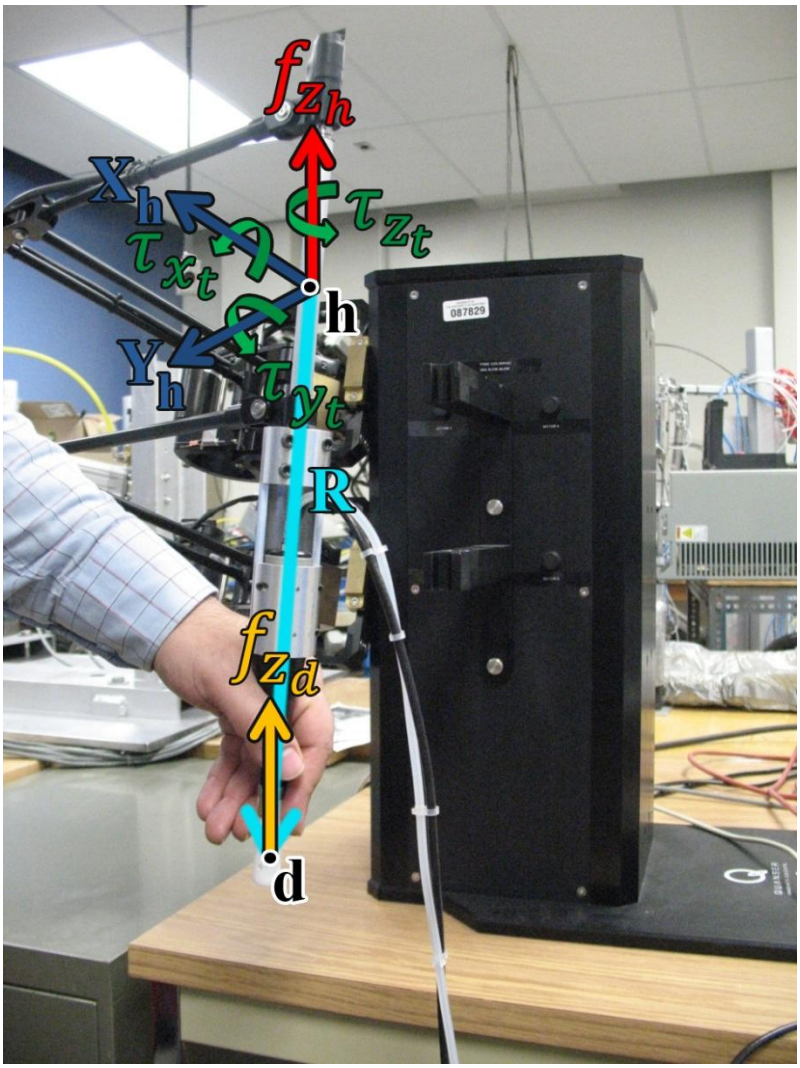

Figure 43: Force transmission of virtual soft tissue model's forces. Virtual soft tissue model is a one dimensional model in the Z direction, and its forces should be applied in the drill tip, point d, just in the Z direction. However, these forces are applied by the haptic device at the device interaction point, point h. In order to transmit the forces from point h to point d certain torques, $\vec{T_t}$, must be applied by the haptic device. Forces at point d and h and $\vec{T_t}$ terms along Cartesian coordinate frames are shown.

Test 5-2: This test is similar to Test 5-1. The operator starts the test in the top free area, moves the drill down through the virtual soft tissue until the bottom free area, and then brings the drill back to the top free area through the virtual soft tissue. This procedure is repeated three times as well, the Z position plot in Figure 44. In addition to the standard test, Test 5-1, the drill is turned

on and drill tip rotates. The objective of this test is to evaluate the impact of the drill vibrations on the performance of the virtual soft tissue program and the gripper gravity compensation program while both are activated.

The results of this test are shown in Figure 44. Red rectangles in Figure 44 indicate one process of insertion and retraction in the virtual soft tissue while drill is turned on. The Z direction position changes and Fz values during this process of Test 5-2, are shown in Figure 45. From the Fz plot the changes in the forces while the drill tip is inside the virtual soft tissue can be observed. Very low amplitude oscillations in the values of the Cartesian and angular positions in Figure 44 and Figure 45 are result of combination of drill vibration and the operator's hand movements, but the drill vibration is the most significant contributor. These oscillations are shown in the roll-rotation and pitch-rotation plots in Figure 44.

The gripper gravity compensation is activated from A to F. Hence, in the periods that the drill tip is out of the virtual soft tissue for example from A to B, the values of forces and torques are constant at the values of the applied forces and torques for the gripper gravity compensation program. The remaining time that the drill tip is inside the virtual soft tissue, the values of forces and torques are changing.

According to the spring model part of the virtual soft tissue model and the almost constant velocity movement of the drill, while the drill tip is going down inside the virtual soft tissue for example from B to C, Fz has an almost linear increase until reaching the bottom border of the virtual soft tissue. According to section 4.1, the values of pitch-torque and roll-torque are changing along with the changes in the value of Fz. Reaching the bottom border of the virtual soft tissue; all these values have a sudden change to the constant gripper gravity compensation

program values, since the spring part’s resistant force of the virtual soft tissue model is suddenly omitted.

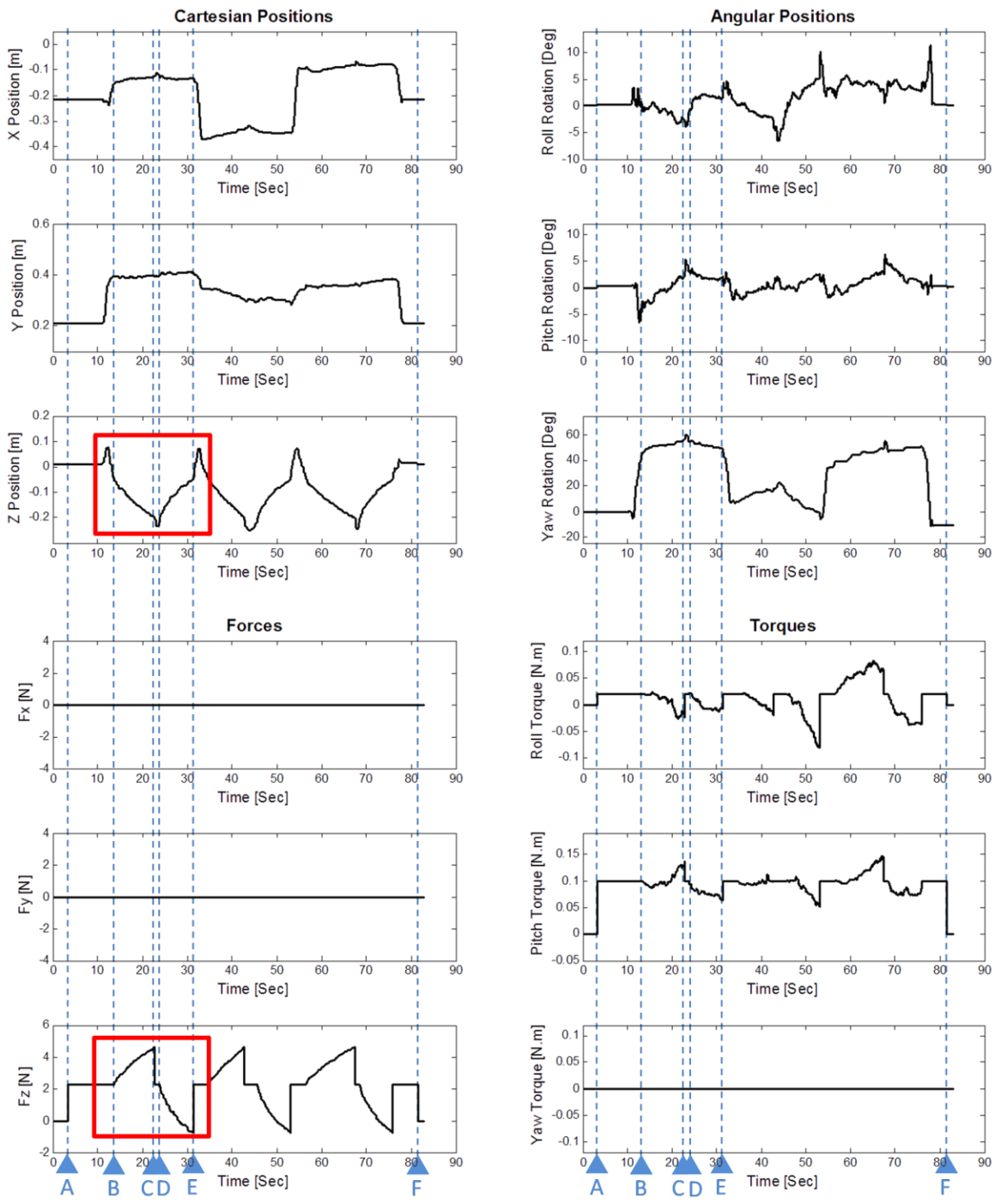

Figure 44: Results of Test 5-2. The gripper gravity compensation program is activated from A to F. Drill is turned on and drill tip rotates. Operator holds the drill and starts from the top free area and brings down the drill. From B to C, the drill tip passes through virtual soft tissue and goes to the bottom free area at C. In the second movement, the drill is brought up. Drill tip passes through virtual soft tissue from D to E, and goes inside the top free area at E. This process is repeated three times. Red rectangles indicate one process of insertion and retraction in the virtual soft tissue while drill is turned on.

Conversely, while the drill tip is going up, as long as it is inside the virtual soft tissue for example from D to E, Fz has an almost linear decrease until reaching the top border of the virtual soft tissue. According to section 2.3.1, the values of pitch-torque and roll-torque are changing along with the changes in the value of Fz. Reaching the top border of the virtual soft tissue; all these values have a sudden change to the gripper gravity compensation program values; since, the spring part's resistant force of the virtual soft tissue model is suddenly omitted.

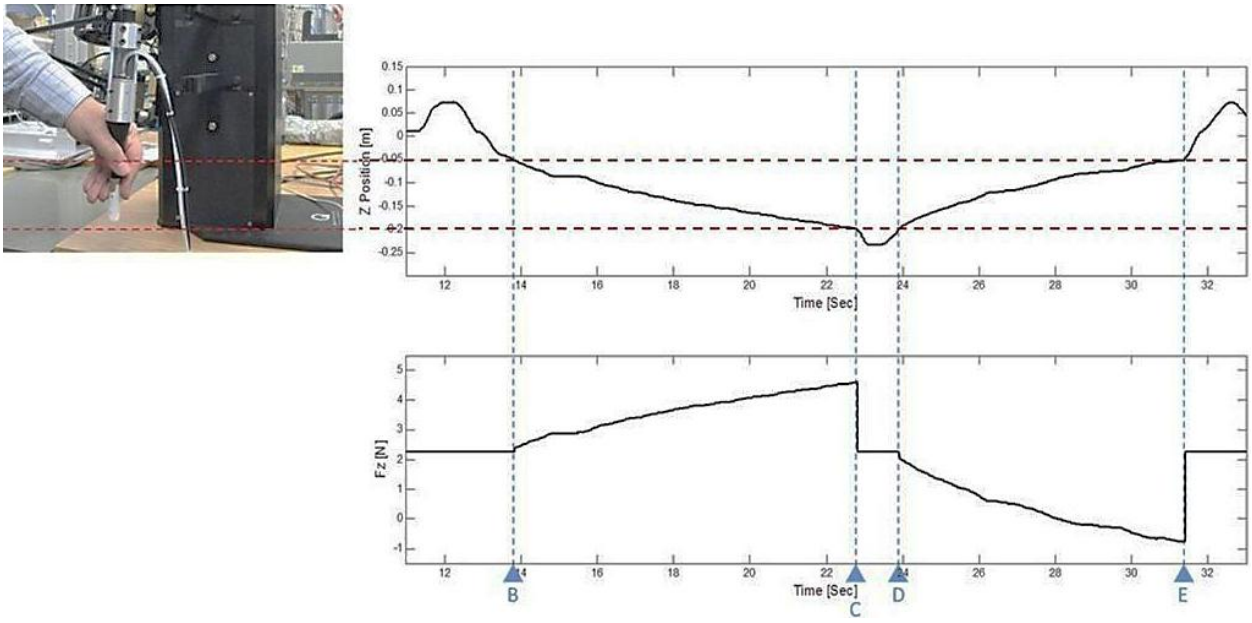

Figure 45: The Z direction position changes and Fz force values change during one process of insertion and retraction in the virtual soft tissue while drill is turned on, Test 5-2. Insertion: From B to C, the drill tip passes through virtual soft tissue and goes to the bottom free area at C. Retraction: Drill tip moves up, passes through virtual soft tissue from D to E, and goes inside the top free area at E. Changes in the values of Fz based on the Z direction position, and sudden change in the value of Fz at C and at E, are shown.

5.6.1. Summary

Figure 41 and Figure 44 show that that drill vibrations do not impact the simulator performance in implementing the virtual soft tissue model. A few low amplitude oscillations are added in results, toward Test 5-1. In addition according to section 5.2, the impact of drill vibration is negligible since in the virtual soft tissue model experiment, the operator's hand acts as an external damper while holding the surgical drill.

According to the results of these two tests, T5-1 and T5-2, for virtual soft tissue the soft tissue model is implementable by the developed haptic device. The system appears stable and continues to function within normal parameters. Comparing results of Tests 5-1 and 5-2 to the HD^2 operating conditions in Table 1, the applied Fx and Fy in both virtual soft tissue tests are zero. Also, the values of applied Fz are less than 6N and more than 2N, which are acceptable according to the maximum continuous applicable forces in Table 1. The applied yaw-torque in both virtual soft tissue tests are zero. Also, the applied pitch-torque is always positive and less than 0.2 Nm. The maximum pitch-torques value is slightly more than 0.15 Nm. The values of applied roll-torque is always less than 0.1 Nm and more than -0.2 Nm, the minimum pitch-torques value is a bit more than -0.1 Nm. These values are acceptable according to the maximum continuous applicable torques in Table 1.

As mentioned above, all the applied forces and torques are acceptable. The critical conditions occur at the borders of virtual soft tissue, especially when the system passes the virtual soft tissue and drill tip is about to enter the free area. Under these circumstances, the spring part of virtual soft tissue model has the maximum force value, and when the drill tip passes the border, this value rapidly changes to zero. Also, the movement of the drill should be in a regular manner

since the virtual soft tissue model has damper model parts as well. The forces of these damping model parts are in the form of $F(x, \dot{x}) = B(\dot{x})\dot{x}$. In this equation $B(\dot{x})$ presents the damping and viscosity effect and $\dot{x}$ is the velocity. Therefore, very fast movements, high values of $\dot{x}$, will cause high values of forces, $F(x, \dot{x})$, that cannot be generated by the haptic device based on the values in Table 1. Moreover, the device itself has certain velocity limitations, section 3.1.1, preventing the device from damage.

5.7. Implementing the Virtual Soft Tissue Model inside the Simple Prototyped Physical Model of Bony Structures - Mixed Reality Experiment

This experiment can be considered as the third part of the virtual soft tissue experiment. This experiment consists of two tests. Depicted in Figure 46, a simple rectangular cubic shape prototyped model of bony structures is designed for these tests. In the first test, the prototyped physical model of bony structures is drilled when there is no virtual soft tissue implemented in the empty space between two layers of prototyped physical model. In second test the virtual soft tissue model is implemented in the rectangular cuboid shape hole inside the designed model as the middle layer. Two layers of bony structures, top and bottom bony layers, are surrounding this soft tissue layer.

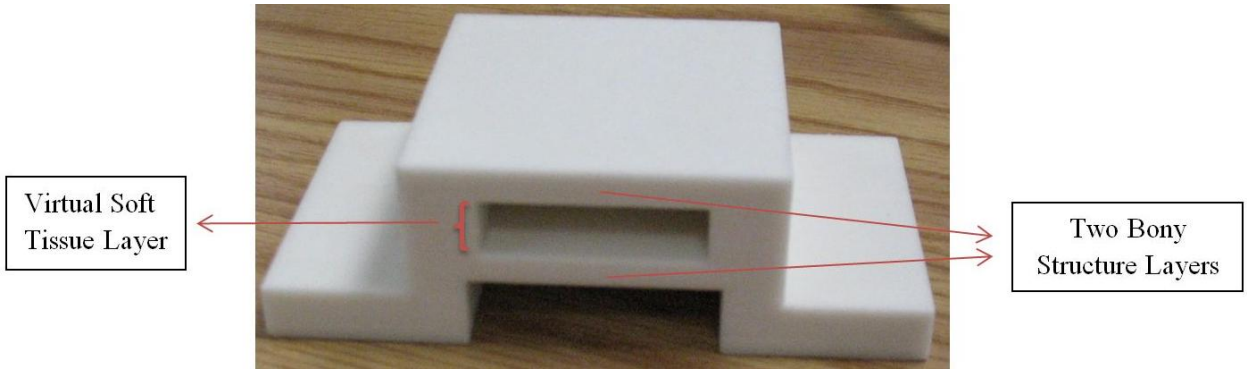

Figure 46: Designed simple rectangular cubic shape prototyped model of bony structures. The virtual soft tissue model is implemented in the rectangular cuboid shape hole inside the designed physical model as the middle layer.

Test 6-1: This test simulates a temporal bone surgery with physical models. The results of this test are shown in Figure 47. The plotted forces in Figure 47 are the gripper gravity compensation program forces applied by the haptic device. The gripper gravity compensation program is

activated between A and F. In the first movement between B and D, the operator starts drilling the top layer of bony structure, B. Then, the drill tip reaches the free area inside the hole, at C. At the boundary of the top bony structure area and free area inside the hole, the forces that can be felt by the operator's hand because of drilling contact forces, are omitted. Since there is not any resistance force, except constant forces of the gripper gravity compensation program, a fast downward movement of the drill tip, which is considered as kicking, happens at C. After passing the free area inside the hole, the drill tip reaches the bottom bony structure area. Passing the bottom bony structure area at D, the drill tip goes inside the free area, the area without physical or virtual model forces. Since, the resistance forces of the physical model suddenly are omitted the kicking behaviour happens again.

The second movement between D and E is the backwards movement. In this movement the drill tip comes up through the drilled hole inside the physical model. There is not any bony structure modeled materials in the hole; hence, the operator just feels the constant forces of the gripper gravity compensation program.

The Z direction position changes and Fz values during Test 6-1 are maximized in Figure 48. It can be seen that during drilling the top and bottom bony structure area, from B to C and from C to D, the plot has a low slope due to high resistance forces of the bony structure areas. Conversely, while reaching to the free area inside the hole at C, or bottom free area at D, sharp changes in the value of the Z position, occurs, due to the kicking behaviour. Red ellipsoids in Figure 48 indicate these kicking movements.

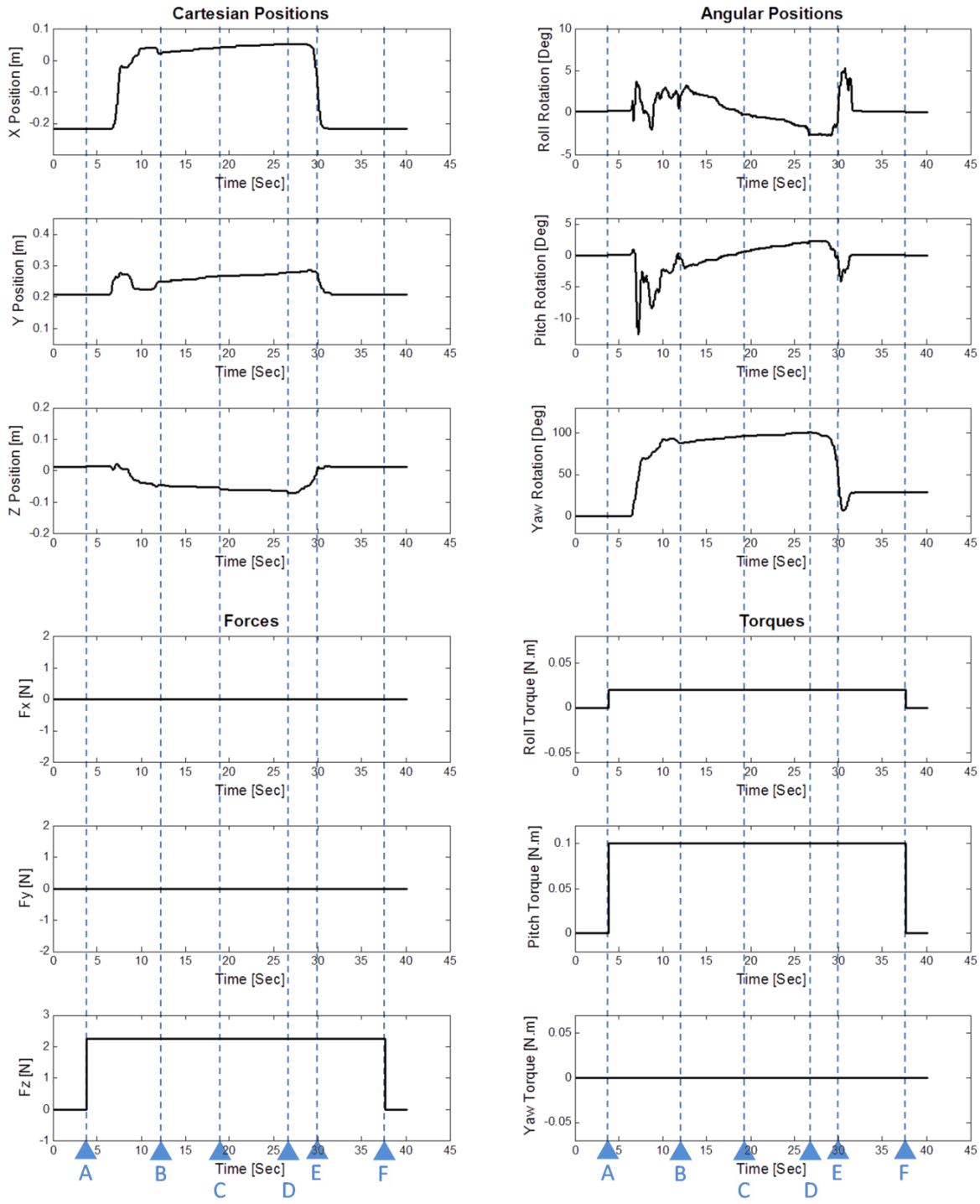

Figure 47: Results of Test 6-1. The gripper gravity compensation program is activated from A to F. Operator holds the drill and drills the top bony structure area between B and C. Drill tip reaches to the free area inside the hole at C. Bottom bony structure area is drilled between C and D, and then drill tip reaches to the bottom free area at D. Backward movement of drill happens between D and E.

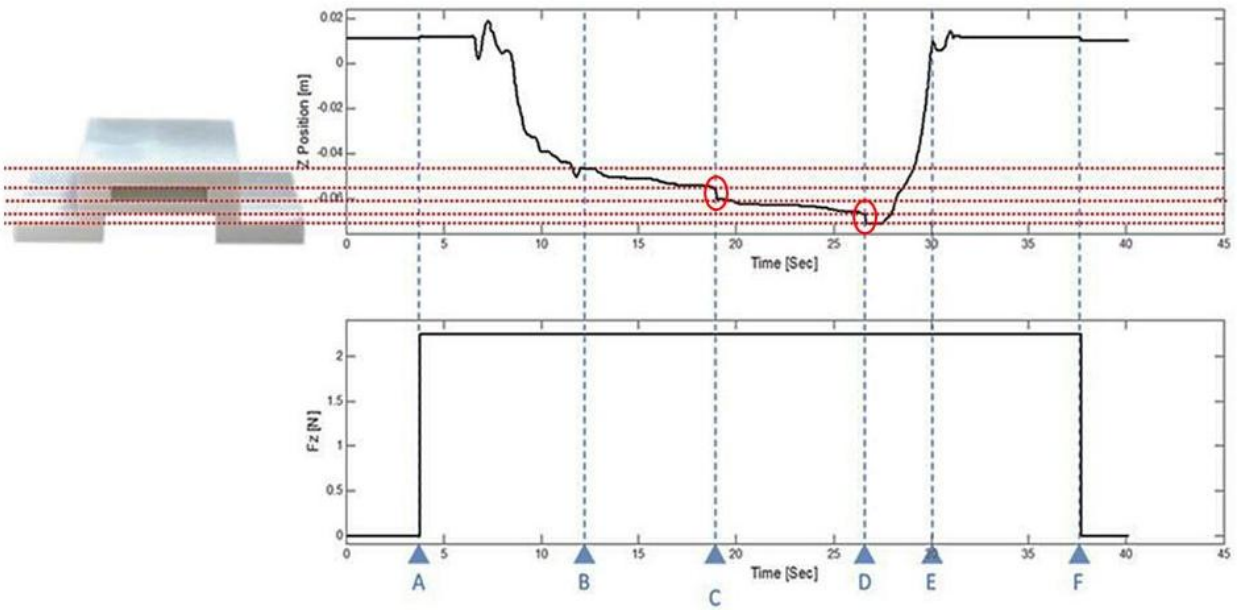

Figure 48: The Z direction position changes and Fz values during Test 6-1. Top bony structure area is drilled between B and C. Drill tip pass through the free area inside the hole, in a fast kicking movement at C. Bottom bony structure area is drilled between C and D, and then drill tip reaches to the bottom free area at D. Between D and E the drill is brought back upward. Red ellipsoids indicate kicking movements.

Test 6-2: This test has the complete conditions of the first step of simulation of temporal bone surgery which is the end goal of this research. In this step, the temporal bone surgery is simulated without considering the geometrical features of the bony parts. In addition, one model is considered for all the soft tissues. This experiment has the MR condition; since, the real model of the bony parts and virtual model of soft tissue co-exist simultaneously.

The results of this test are shown in Figure 49. The plotted forces in Figure 49 are the virtual soft tissue model forces and gripper gravity compensation program forces applied by the haptic device. According to the fact that the force control mode is an open loop control, just the applied forces by the haptic device are recorded and plotted. In this test, the operator practices the complete first step simulated surgery. The gripper gravity compensation program is activated between A and I.

In the first movement, between B and E, operator starts drilling the top layer of bony structure at B. Then the drill tip reaches to the hole at C, which is filled with simulated virtual soft tissue. The simulator adds the modeled forces and torques of the virtual soft tissue to the constant forces and torques of the gripper gravity compensation program and applies the resultant forces when the drill tip is inside this virtual soft tissue layer. At the boundary of the top bony structure area and virtual soft tissue area, the forces that can be felt by the operator's hand decrease significantly. Since, the soft tissue has less resistance compared to the bony structure this decrease in the resistance forces causes a fast downward movement of the drill tip which is considered as small kicking. In Test 6-2 the resistance forces of the virtual soft tissue model, damp this kicking behaviour and decrease its impacts. Conversely, according to Figure 49, at the boundary of the top bony structure area and virtual soft tissue area the applied forces by the device increases; since, virtual soft tissue model forces, which are always resistant to the movement of drill tip, are added to the gripper gravity compensation program forces.

After passing the virtual soft tissue area at the D, the drill tip reaches to the bottom bony structure area. The forces experienced by the operator's hand increase significantly in the merging of virtual soft tissue area and bottom bony structure area. Conversely, according to Figure 49, at the boundary of virtual soft tissue area and the bottom bony structure area the applied forces by the device decreases; since, virtual soft tissue model forces are omitted. Passing the bottom bony structure area at E, the drill tip goes inside the area without physical or virtual model forces. Since, the resistance forces of the physical model suddenly are omitted and there are no virtual soft tissue resistant forces, kicking behaviour similar to Test 6-1, without any soft tissue damping, happens.

The second movement, between E and H, is the backward movement. In this movement the drill tip comes up through the drilled hole inside the physical model. There are no bony structure model materials in the hole; hence, changes in the values of forces just can be feel by the operator when the drill tip passing through the virtual soft tissue area, between F and G. In the second movement, the force values decrease. Since the virtual soft tissue model forces resist the movement of the drill tip and subtract from the constant forces of the gripper gravity compensation program.

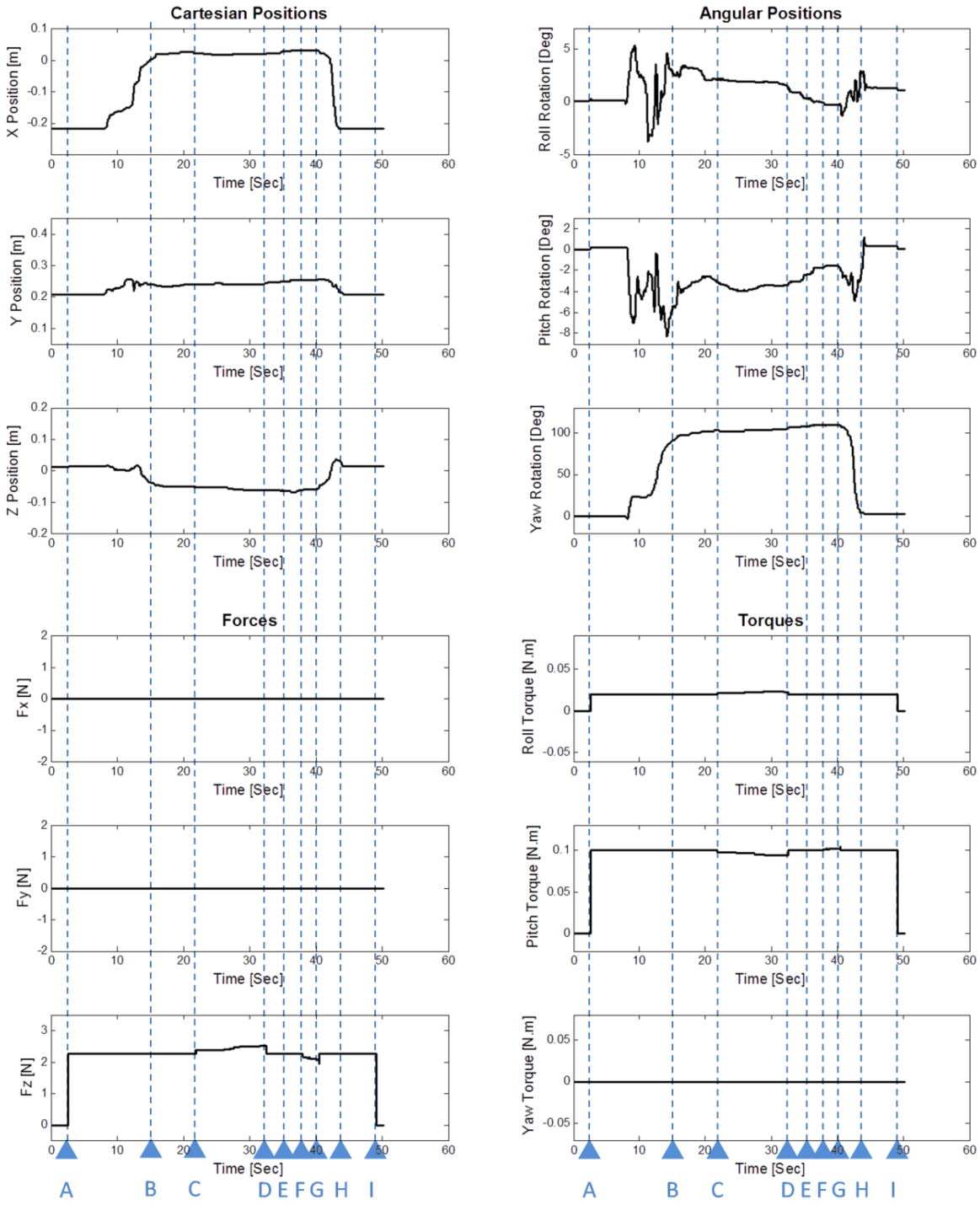

Figure 49: Results of Test 6-2. The gripper gravity compensation program is activated from A to I. Operator holds the drill and drills the top bony structure area between B and C. Drill tip passes through the virtual soft tissue inside the hole between C and D. Bottom bony structure area is drilled between D and E. Drill tip reaches to the bottom free area at E. Backward movement of drill happens between E and H, while from F to G, drill tip passes through the virtual soft tissue in the reverse direction, backward.

The Z direction position changes and Fz values during the Test 6-2, are extended in Figure 50. Red rectangles in Figure 50 show the Z direction position changes and Fz values during the first movement, insertion. These parts of the Figure 50 are maximized in Figure 51 to show the differences between the slope of the Z position plot during the bony structures drilling and virtual soft tissue insertion.

During drilling the top and bottom bony structure area, from B to C, and from D to E respectively, the plot has a low slope due to high resistance forces of the bony structures. Between C and D, while passing the virtual soft tissue area; the plot has a higher slope due to lower resistance forces of the virtual soft tissue. At E, when drill tip goes to the bottom free area sharp changes in the value of the Z position, due to the kicking, can be seen. Red ellipsoid in Figure 51 indicates this kicking movement. These differences between the slope of the Z position plot in the bony structure areas and virtual soft tissue area are clear in Figure 51.

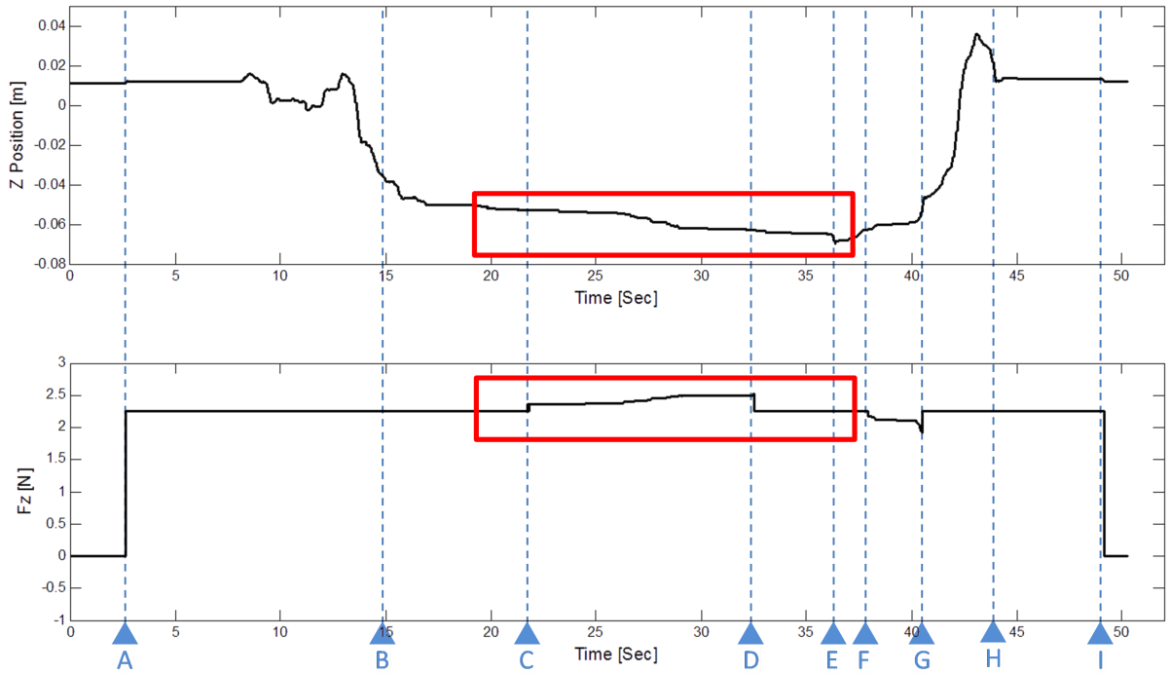

Figure 50: The Z direction position changes and Fz values during Test 6-2. Between B and C, and D and E the top and bottom bony structure area drilled respectively. Drill tip passes through the virtual soft tissue inside the hole between C and D. Kicking movement happened when drill tip entered to the bottom frea area at E. Backward movement of drill happens between E and H, while from F to G, drill tip passes through the virtual soft tissue in the reverse direction, backward. Red rectangles show the Z direction position changes and Fz values during the first movement, insertion.

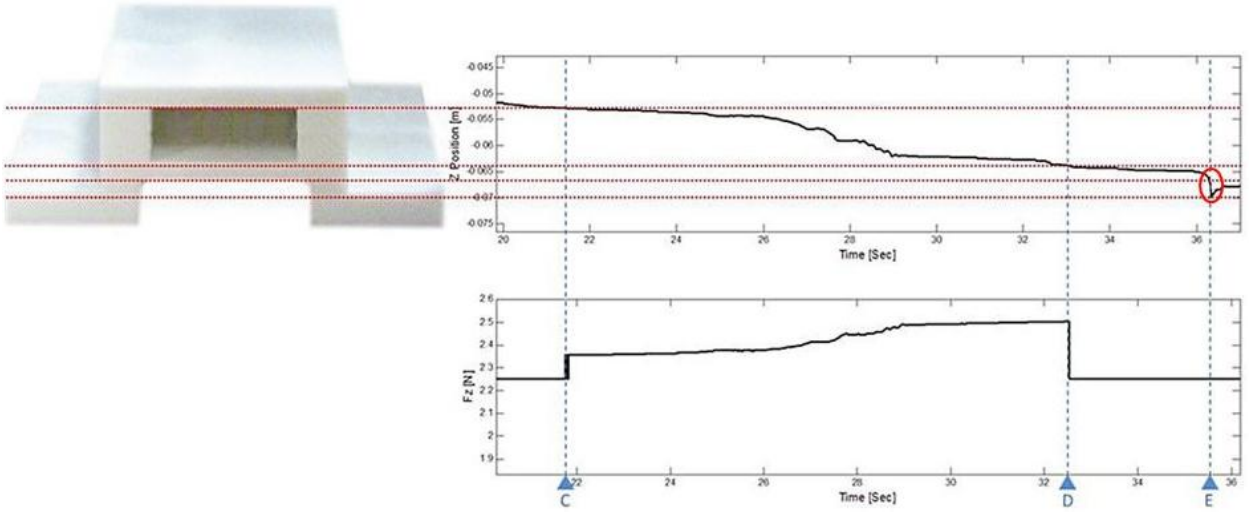

Figure 51: The Z direction position changes and Fz values during the first movement, insertion, of Test 6-2. Differences between the slope of the Z position plot during the bony structures drilling, between D and E, and virtual soft tissue insertion between C and D are clear. The kicking movement while entering the bottom free area is shown at D. Red ellipsoid indicates kicking movement.

5.7.1. Summary

Low amplitude oscillations in the values of roll-rotation and pitch-rotation in Tests 6-1 and 6-2 are due to the operator's hand movements and drills vibration. The drilling contact forces and drill vibrations do not impact on the gross stability of the system, and system appears stable and continues its performance. In the interaction between the real and virtual models, system appears stable as well. Comparing results of Tests 6-1 and 6-2 to the HD^2 operating conditions in Table 1, all the forces and torques are less than the maximum continuous applicable forces and torques of the haptic device. Also, these values have sufficient safety margins to remain in the haptic device' operational parameters.

Comparing Figure 48 and Figure 50 demonstrates that the MR systems and virtual soft tissues are applicable in temporal bone surgery training. Moreover, the resistance forces of the virtual soft tissue model, damp kicking behaviours and decrease their impacts.

The most significant problematic situations are interactions between different areas. Stable interaction in the boundary regions is an important issue. In this case critical factors can be assumed as: applied forces and torques by the simulator, robustness to the drill vibrations and drilling contact forces, kicking movements or any high velocity movement when the high resistant forces of bony structure is replaced with lower forces of virtual soft tissue.

Chapter 6

6. Concluding Remarks

6.1. Contributions of this Thesis

In this study, the Quanser HD^2 haptic device was retrofitted to be used as a MR medical simulator for temporal bone surgery training. HD^2 haptic device capabilities were studied, which demonstrated that this haptic device can be modified to work in a MR environment without exhibiting instability. A prototyped physical model of bone was overlaid with a virtual haptic model of soft tissue to create the MR environment. The advantages of each model were considered, while their individual limitations were overcome. Different tissue models were considered to determine the most appropriate one which is sufficiently simple to be implemented on the available haptic device, while satisfying the requirements for realistic temporal bone surgery simulation.

A gripper was developed to equip the HD^2 haptic device with real surgical drill. The weight of the gripper and its handle were cancelled in order to create a realistic training environment in which trainees merely feel the gravity effects of the surgical drill. Features of the haptic device were studied to transmit the haptic interaction point from the centre of the handle to the drill tip, where the forces and torques of the implemented soft tissue should be felt.

The performance of the developed system is examined regarding the temporal bone surgery conditions. The capabilities of the PV position controller implemented on the device were determined. The effectiveness of the "gripper gravity compensation" program within the anticipated surgical and haptic device workspaces, and its impact on the performance and gross stability of the haptic device were studied as well.

Moreover, the force profile of the implemented soft tissue model was determined experimentally. The chosen soft tissue model is sufficiently simple to be considered as a linear profile. In addition, a MR environment was designed consisting of a virtual deformable haptic model of soft tissue associated with a physical model of the bone.

Afterwards, the effectiveness of the soft tissue model was evaluated. In the simulated temporal bone surgery with haptic models of soft tissue, kicking movements of operator's hand after finishing drilling the bony parts procedure was reduced due to the resistance forces of the soft tissue model. Kicking movements are due to sudden changes in the density of drilling materials. The effect of the drill vibrations and contact forces, the physical model and the interactions between the real and virtual models on the stability and capabilities of the haptic device were studied as well. In the experiments, drill vibrations cause very low amplitude oscillations in the results, which do not affect the stability of the system. The physical model drill contact forces

change the value of the forces applied by the haptic device and the forces that are felt by the operator, but still new values of forces are acceptable according to the maximum continuous applicable forces of the haptic device. Interactions between the real and virtual models will cause kicking of the drill and sharp changes in the forces. However, the resistance forces of the real and virtual models prevent the system from becoming unstable. The simulator demonstrates gross stability while operating in normal temporal bone surgery conditions.

6.2. Future Works

In the MR system described in this thesis, force control operates in an open loop manner; while the controller sends the control signals to the motors in order to apply the desired torques computed by the running program. Future work will consider the development of calibration tests to verify the accuracy of applied forces.

Another issue which can be addressed for future work is to formulate the stability conditions of the system. Although gross stability of the system was observed during operation in normal temporal bone surgery conditions, this stability to large disturbances and conditions for safe operational use should be demonstrated more rigorously and proven mathematically.

In addition, in order to achieve a more realistic simulation, development of more complex soft tissue models, such as FEMs, is considered for future work. The implemented soft tissue model in this thesis was intentionally kept simple to minimize the model's effects on the performance of the simulator.

Derivation of the kinematics and modeling equations for the developed system and modifications in the control scheme can be considered as another future work. For instance, the position control of the haptic device does not have any integral control term; hence, the system always has a small position error in generating the required control forces.

Face validation of the developed prototype system by expert surgeons can be considered for future work as well. After trying the system out, their opinions on its feel and functionality would be valuable for future system development. Design of a stable MR system should prove a useful training tool for future students of temporal bone surgery.

Appendix A: "Force Trasmission" program.

This program is used to calculate the required forces and torques of the haptic device to produce the feeling of the soft tissue model's forces and torques in the drill tip.

```
t_double Tr = 0;//Roll
t_double Tp = 0;//Pitch
t_double R = 0.375;// Distance between HD2 interaction point and Drill tip in meter
//ForceH[3],TorqueH[2],Yaw_TorqueH; Forces and Torques at point H (HD2 interaction point)

t_double ForceH[3];//ForceH[0]=Fx;ForceH[1]=Fy;ForceH[2]=Fz;
t_double TorqueH[2];//TorqueH[0]=Roll-Torque; TorqueH[1]=Pitch-Torque;
t_double Yaw_TorqueH = 0;
for (int i = 0; i < 3; i++)
     ForceH[i] = 0;
for (int i = 0; i < 2; i++)
     TorqueH[i] = 0;

//ForceD[3],TorqueD[2],Yaw_TorqueD; Forces and Torques at point D (Drill tip)
t_double ForceD[3];//ForceD[0]=Fx;ForceD[1]=Fy;ForceD[2]=Fz;
t_double TorqueD[2];//TorqueD[0]=Roll-Torque; TorqueD[1]=Pitch-Torque;
t_double Yaw_TorqueD = 0;
for (int i = 0; i < 3; i++)
     ForceD[i] = 0;
for (int i = 0; i < 2; i++)
     TorqueD[i] = 0;

Tr= positions[3];//Roll
Tp= positions[4];//Pitch
for(int i = 0; i < 3; i++)
ForceH[i] = ForceD[i];// Generall force equation
//ForceD[i] = Calculated forces in point D (Drill tip);
//TorqueD[i] = Calculated Torques in point D (Drill tip);
//Generall Torque equation
TorqueH[0]=(R*cos(Tp)*sin(Tr))*ForceD[2]+(R*cos(Tp)*cos(Tr))*ForceD[1]+TorqueD[0];
TorqueH[1]=(R*sin(Tp))*ForceD[2]-(R*cos(Tp)*cos(Tr))*ForceD[0]+TorqueD[1];
Yaw_TorqueH=(R*sin(Tp))*ForceD[1]-(D*cos(Tp)*sin(Tr))*ForceH[0]+Yaw_TorqueD;
```

References

[1] R. A. Nelson, Temporal Bone Surgical Dissection Manual, Second ed., Los Angeles: House Ear Institute, 1991.

[2] Agus, M.; Brelstaff, G.J.; Giachetti, A.; Gobbetti, E.; Zanetti, G.; Zorcolo, A.; Picasso, B.; Franceschini, S.S., "Physics-based burr haptic simulation: tuning and evaluation," in *Proceedings of the 12th International Syrnposiurn on Haptic Interfaces for Virtual Environment and Teleoperator Systems*, 2004.

[3] Zirkle M, RobersonDW, Leuwer R, Dubrowski A., "Using a virtual reality temporal bone simulator to assess otolaryngology trainees," *Laryngoscope*, vol. 117, no. 2, p. 258–263, 2007.

[4] Barrs DM, Trahan CJ, Casey K, Brooks D., "The porcine model for intratemporal facial nerve trauma studies," *Otolaryngology - head and neck surgery* , vol. 105, no. 6, pp. 845-856, 1991.

[5] J. K. Salisbury and M. A. Srinivasan, "Phantom-based haptic interaction with virtual objects," *IEEE Computer Graphics and Applications,* vol. 17, pp. 6-10, 1997.

[6] P. Milgram and F. Kishino, "A Taxonomy of Mixed Reality Visual Displays," *IEICE Transactions on Information Systems,* Vols. E77-D, no. 12, pp. 1321-1329, 1994.

[7] P Milgram, H Colquhoun, "A Taxonomy of Real and Virtual World Display Integration," in *Mixed Reality – Merging Real and Virtual Worlds*, Y. O. a. H. Tamura, Ed., Springer, 1999.

[8] Markus Sareika, "Mixed Reality vs. Mixing Realities," [Online]. Available: http://www.mixingrealities.de/. [Accessed 02 07 2012].

[9] D.W.F. van Krevelen and R. Poelman, "A Survey of Augmented Reality Technologies,

Applications and Limitations," *The International Journal of Virtual Reality,* vol. 9, no. 2, pp. 1-20, 2010.

[10] R. Azuma, "A Survey of Augmented Reality," *Presence: Teleoperators and Virtual Environments*, vol. 6, no. 4, pp. 355-385, Aug 1997.

[11] R. Azuma, Y. Baillot, R. Behringer, S. Feiner, S. Julier, and B. MacIntyre, "Recent advances in augmented reality," *IEEE Computer Graphics and Application*, vol. 21, no. 6, p. 34 – 47, Nov/Dec 2001.

[12] Renaud Ott; Daniel Thalmann; Fr´ed´eric Vexo, "Haptic feedback in mixed-reality," *The Visual Computer,* p. 843–849, 2007.

[13] Zauner, J., Haller, M., Brandl, A., Hartman, W., "Authoring of a mixed reality assembly instructor for hierarchical structures," in *Proceedings of the Second IEEE and ACM International Symposium on Mixed and Augmented Reality*, 2003.

[14] Nojima, T., Sekiguchi, D., Inami, M., Tachi, S., "The smart tool: a system for augmented reality of haptics," in *Proceedings of the IEEE Virtual Reality Conference*, 2002.

[15] Walairacht, S., Yamada, K., Hasegawa, S., Koike, Y., Sato, M., "4+4 fingers manipulating virtual objects in mixed-reality environment," *Presence: Teleoperators and Virtual Environments*, vol. 11, no. 2, pp. 134-143, April 2002.

[16] A. Kotranza, J. Quarles, and B. Lok,, "Mixed Reality: Are Two Hands Better Than One?," in *Proceedings of the ACM Symposium on Virtual Reality Software and Technology (VRST2006)*, 2006.

[17] R. T. Azuma, H. Neely III, M. Daily, and J. Leonard, "Performance analysis of an outdoor augmented reality tracking system that relies upon a few mobile beacons," in *5th IEEE/ACM International Symposium on Mixed and Augmented Reality (ISMAR)*, 2006.

[18] T. Ohshima, K. Satoh, H. Yamamoto, and H. Tamura., "RV-Border Guards: A Multi-Player

Mixed Reality Entertainment," *Transactions of the Virtual Reality Society of Japan,* pp. 699-705, 1999.

[19] Tamura, H., Yamamoto, H., Katayama, A., "Mixed reality: future dreams seen at the border between real and virtual worlds," *Computer Graphics and Applications,* vol. 21, no. 6, pp. 64-70, Nov/Dec 2001.

[20] Gabriel Robles-De-La-Torre, "Virtual Reality: Touch / Haptics," in *SAGE Encyclopedia of Perception,* Sage Publications, 2009, pp. 1036-1038.

[21] M. Tavakoli, R. V. Patel and M. Moallem, "A force reflective master-slave system for minimally invasive surgery," in *IEEE/RSJ International Conference on Intelligent Robots and Systems,* 2003.

[22] A. J. Madhani, "The Black Falcon: a teleoperated surgical instrument for minimally invasive surgery," in *Proceedings of IEEE/RSJ International Conference on Intelligent Robots and Systems,* 1998.

[23] L. Sun, F. Van Meer, Y. Bailly and C. K. Yeung, "Design and development of a da Vinci surgical system simulator," in *IEEE International Conference on Mechatronics and Automation,* 2007.

[24] A. Baheti, "RoSS: virtual reality robotic surgical simulator for the da Vinci surgical system," in *Symposium on Haptic Interfaces for Virtual Environment and Teleoperator Systems,* 2008.

[25] Y. Matsumoto, "Dexterous manipulation in constrained bilateral teleoperation using controlled supporting point," *IEEE Transactions on Industrial Electronics,* vol. 54, pp. 1113-1121, 2007.

[26] F. Najafi and N. Sepehri, "A novel hand-controller for remote ultrasound imaging," *Mechatronics,* vol. 18, pp. 578-590, 2008.

[27] N. Diolaiti, "Teleoperation of a mobile robot through haptic feedback," in *IEEE International Workshop on Haptic Virtual Environments and their Applications*, 2002.

[28] Sun-Gi Hong ; Ju-Jang Lee ; Seungho Kim , "Generating artificial force for feedback control of teleoperated mobile robots," in *Proceedings of IEEE/RSJ International Conference on Intelligent Robots and Systems*, 1999.

[29] J. Lim, J. Ko and J. Lee, "Internet-based teleoperation of a mobile robot with force-reflection," in *Proceedings of IEEE Conference on Control Applications*, 2003.

[30] O. J. Rosch, K. Schilling and H. Roth, "Haptic interfaces for the remote control of mobile robots," *Control Engineering Practice,* vol. 10, pp. 1309-1313, 2002.

[31] G. Clement, "An overview of CAT control in nuclear services," in *Proceedings of IEEE International Conference on Robotics and Automation*, 1985.

[32] Kurosh Zarei-nia, "Haptic-Enabled Teleoperation of Hydraulic Manipulators: Theory and Application," PhD Thesis, University of Manitoba, 2011.

[33] Berkelman, P.J. and Hollis, R.L., "Dynamic performance of a hemispherical magnetic levitation haptic interface device," in *SPIE, International Symposium on Intelligent Systems and Intelligent*, Greensburg PA, 1997.

[34] Brooks, F.P., Ouh-Young, M., Batter, J.J., Jerome, P., "Project GROPE: Haptic displays for scientific visualization," in *Proceedings of the 17th annual conference on Computer graphics and interactive techniques*, 1990.

[35] Yokokohji, Y.; Hollis, R.L.; Kanade, T.;, "What you can see is what you can feel-development of a visual/haptic interface to virtual environment," in *Proceedings of the IEEE Virtual Reality Annual International Symposium*, 1996.

[36] William A. McNeely, Kevin D. Puterbaugh, James J. Troy, "Six Degree-of-Freedom Haptic Rendering Using Voxel Sampling," in *Proceedings of ACM Siggraph*, 1999.

[37] S. De and M. A. Srinivasan, "Thin walled models for haptic and graphical rendering of soft tissues in surgical simulations," *Studies in Health Technology and Informatics,* no. 62, pp. 94-99, 1999.

[38] G. Debunne, M. Desbrun, M. Cani and A. Barr, "Adaptive simulation of soft bodies in real-time," *Computer Animation 2000. Proceedings,* pp. 15-20, 2000.

[39] J.P. Gourret, N. Magnenat Thalmann, and D. Thalmann, "Simulation of object and human skin deformations in a grasping task," in *Proceedings of the 16th annual conference on Computer graphics and interactive techniques*, 1989.

[40] Demetri Terzopoulos, John Platt, Alan Barr, Kurt Fleischer, "Elastically deformable models," in *Proceedings of the 14th annual conference on Computer graphics and interactive techniques*, 1987.

[41] A. Pentland and J. Williams, "Good vibrations: modal dynamics for graphics and animation," in *Proceedings of the 16th annual conference on Computer graphics and interactive techniques*, 1989.

[42] Athanasios Dimopoulos, Evangelos Papadopoulos, Karl Iagnemma, "Experimental tissue parameter identification for use in endoscopic urological haptic simulation," in *17th Mediterranean Conference on Control & Automation*, Thessaloniki, Greece, 2009.

[43] A. P. George, R. De, "Review of temporal bone dissection teaching: how it was, is and will be," *The Journal of Laryngology & Otology,* vol. 124, no. 2, p. 119–125, 2010.

[44] Kuppersmith RB, Johnston R, Moreau D, Loftin RB,Jenkins H., "Building a virtual reality temporal bone dissection simulator," *Stud Health Technol Inform,* vol. 39, p. 180–186, 1997.

[45] T. Harada, S. Ishii, and N. Tayama, "Three-dimensional re-construction of the temporal bone from histological sections," *Arch Otolaryngol Head Neck Surgery,* 1988.

[46] J. Bryan, D. Stredney, G. Wiet, and D. Sessanna, "Virtual temporal bone dissection: A case study," in *IEEE Visualization*, 2001.

[47] Stredney D, Wiet GJ, Bryan J, Sessanna D, Murakami J, Schmalbrock P, Powell K, Welling B., "Temporal bone dissection simulation - an update," *Medicine Meets Virtual Reality*, pp. 507-513, 2002.

[48] G. Wiet, J. Bryan, D. Sessanna, D. Streadney, P. Schmalbrock, and B. Welling, "Virtual temporal bone dissection simulation," *Medicine Meets Virtual Reality*, pp. 378-384, 2000.

[49] B. Pflesser, A. Petersik, U. Tiede, K. H. Hohne, and R. Leuwer, "Volume based planning and rehearsal of surgical interventions," in *Computer As¬sisted Radiology and Surgery,Excerpta Medica International Congress*, Amsterdam, 2000.

[50] B. Pflesser, A. Petersik, U. Tiede, K. H. Hohne, and R. Leuwer, "Haptic volume interaction with anatomic models at sub-voxel resolution," in *10th International Symposium on Haptic Interfaces for Virtual Environment and Teleoperator Systems*, 2002.

[51] Marco Agus, Andrea Giachetti, Enrico Gobbetti, Gianluigi Zanetti, Antonio Zorcolo, "Real-time haptic and visual simulation of bone dissection," in *Proceedings of the IEEE Virtual Reality Conference*.

[52] Agus M, Giachetti A, Gobetti E, Zanetti G, Zorcolo A., "Tracking the movement of surgical tools in a virtual temporal bone dissection simulator," *Medical Image Computing and Computer assisted Intervention*, 2003.

[53] Matthew A. Hutchins, Duncan R. Stevenson,Chris Gunn , Alexander Krumpholz , Tony Adriaansen,Brian Pyman , Stephen O'Leary , "Communication in a networked haptic virtual environment for temporal bone surgery training," *Virtual reality*, vol. 9, p. 97–107, 2006.

[54] Quanser, "Quanser's High Definition Haptic Device (HD2) User Manual," Quanser.